Departamento de Física

FCTUC

Faculdade de Ciências e Tecnologia
da Universidade de Coimbra

Hemodynamic Parameters Assessment

Development and Characterization of an Acoustic Probe

Dissertação de Mestrado em Engenharia Biomédica

Maria Inês Belo Dias Graça Contente

Setembro de 2011

Hemodynamic Parameters Assessment

Development and Characterization of an Acoustic Probe

Cordinators:

Prof.Dr. Carlos Correia

Dr. João Cardoso

Supervisor:

Eng. Helena Catarina Pereira

Maria Inês Belo Dias Graça Contente

Setembro de 2011

Research Unit

Centro de instrumentação – Grupo de Electrónica e Instrumentação

(http://lei.fis.uc.pt)

Colaborators

ISA – Inteligent Sensing Anywhere

(www.ISA.pt)

Instituto Investigação & Formação Cardiovascular, S.A.

Abstract

The measurement of the Pulse Wave Velocity (PWV) is considered the standard method for the arterial stiffness assessment, pointed out as the major cardiovascular risk factor. However, the equipments available in the market are very expensive and have to be operated by trained persons.

In this context, this research project consisted on the development of a new double probe based on two acoustic sensors and its characterization. The main goal of the proposed equipment is the PWV estimation. Nevertheless, it also enables the estimation of the Left Ventricle Ejection Time (LVET), a very important parameter to assess ventricular function.

Several tests were performed in order to characterize the instrument, regarding the existence of cross-talk between the sensors, their repeatability, waveform analysis and the determination of the sensors' impulse response. The temporal resolution was also determined through some tests realized in a dedicated bench.

'Clinical' data acquisitions were also carried out in some volunteers for PWV and LVET estimation, yielding very interesting and promising results. Indeed, the obtained values for PWV and especially for LVET were, generally, very close to the expected for each individual.

Keywords

Cardiovascular Disease, Arterial Stiffness, Local Pulse Wave Velocity, Left Ventricle Ejection Time, Acoustic Sensor

Resumo

A medição da Velocidade de Onda de Pulso (VOP) é considerada a metodologia mais eficaz no diagnóstico da Rigidez Arterial, o maior factor de risco de doenças Cardiovasculares. No entanto, os equipamentos disponíveis hoje em dia no mercado são muito dispendiosos e exigem a manipulação por operadores treinados.

Neste sentido, este projecto de investigação centrou-se no desenvolvimento de uma nova sonda dupla, baseada em dois sensores acústicos e na sua caracterização. O principal objectivo da sonda proposta é a determinação da VOP. No entanto permite também a determinação do Tempo de Ejecção do Ventrículo Esquerdo, um parâmetro muito importante na avaliação da função do ventrículo esquerdo.

Para a caracterização da sonda, foram realizados vários testes de modo a avaliar o desempenho do equipamento ao nível da existência de cross-talk entre os dois sensores, o estudo da sua repetibilidade, a análise das formas de onda obtidas e a determinação resposta a impulso dos sensores. Também foi determinada a sua resolução temporal através de alguns testes realizados numa bancada de testes.

Foram também recolhidos dados 'clínicos' de um grupo de voluntários, para determinação da sua VOP e Tempo de Ejecção do Ventrículo Esquerdo, revelando resultados muito interessantes e promissores. De facto, os valores obtidos para as VOP e especialmente paras os tempos de ejecção foram, de forma geral, muito próximos do esperado para cada indivíduo.

Palavras-chave

Doenças Cardiovasculares, Rigidez Arterial, Velocidade de Onda de Pulso Local, Tempo de Ejecção do Ventrículo Esquerdo, Sensores Acústicos

Acknowledgements

This research project represented a great opportunity of learning and growth and I must address my thanks to everyone who have supported me along this year.

First of all I would like to thank my supervisors, Prof. Dr. Carlos Correia and Dr. João Cardoso, for their guidance and great ideas, which allowed overcoming some difficult practical problems.

A very special thanks goes to Eng. Helena Pereira for her constant guidance and help throughout all this year of work.

I must thank to all members of *Grupo de Electronica e Investigação* for their sympathy and especially to the volunteers that allowed me to collect the indispensable signals for 'clinical' tests. To them, a big thanks for their patience and availability.

I cannot forget my work colleague, Vânia Relvas, for her companionship and friendship along this year.

A huge thanks to my friends, who have helped me even when they didn't know they were, simply with their presence. A very specially thank to Pedro, for his patience and constant support.

Finally I thank my family, specially my parents, for their constant encouragement, aid and effort along my entire academic journey. To them I dedicate this work.

Maria Inês Belo Dias Graça Contente

September, 2011.

Contents

List of Figures

List of Tables

Acronyms

CVD	Cardiovascular Diseases
CV	Cardiovascular
PWV	Pulse Wave Velocity
LVET	Left Ventricle Ejection Time
HR	Heart Rate
PZ	Piezoelectric
PTT	Pulse Transit Time
ECG	Electrocardiogram
DAQ	Data Acquisition
DAP	Double Acoustic Probe
IR	Impulse Response
FFT	Fast Fourier Transform
IFFT	Inverse Fast Fourier Transform
RMSE	Root Mean Square Error

1. Introduction

1.2 - Motivation

According to INE (*Instituto Nacional de Estatística*) statistics, four people die every day in Portugal due to Cardiovascular Disease (CVD). Although decreasing in number in the previous years, CVD are still the leading cause of death in Portugal **[1]** and in all over the world **[2]** and according to World Health Organization, 'by 2030 almost 23.6 million people will die from CVDs, mainly from heart disease and stroke'.

Arterial Stiffness is nowadays considered an important risk factor in the development of CVD **[3]**, and for the past few years it has been demonstrated its importance as an independent marker for CV risk and as a predictor of all-cause mortality in hypertensive patients **[4]**. Its assessment is, indeed, of utmost importance.

On the other hand, Pulse Wave Velocity (PWV) has been considered as the most simple, reproducible and non-invasive indicator of arterial stiffness [4].

Nowadays the main equipments available on the market for non-invasive assessment of PWV are the Complior® (Colson), Sphygmocor® (AtCor Medical, Australia), PulsePen® (Diatecne, Italy) and Arteriograph® (TensioMed, Budapest, Hungary), [5][11]. All of these equipments are based on pressure sensors but their cost and the need of trained medical staff, constitute important obstructions for a general use in clinical environments, where the main used techniques rely on invasive methods.

In this context, for its simple base concept, low-cost, easily handling and the possibility of assessing other important hemodynamic parameters such as Heart Rate (HR) and Left Ventricle Ejection Time (LVET), the Acoustic Probe developed in this work could constitute an important alternative for the aforementioned techniques.

1.2 – Objectives

The main objectives of this project are the development and characterization of a new double probe based on acoustic sensors for hemodynamic parameters assessment and the algorithms required for the determination of those parameters.

Being a continuity project, this work attended to use a new technology and determine some new hemodynamic parameters to complement the information provided by those already used by this investigation group in the study of cardiovascular system.

1.3 – Hemodynamic Project Team

This project was developed in *Grupo de Electrónica e Instrumentação* (GEI) *da Universidade de Coimbra* in the framework of a partnership with *Instituto de Investigação e Formação Cardiovascular* (IIFC) and *Intelligent Sensing Anywhere* (ISA).

It is part of the major project research, *Hemodynamics Parameters – New Instrumentation and Methodologies*, which aims the development of new instrumentation and techniques related with hemodynamic parameters assessment.

In the followed table are summarized the main projects currently ongoing at GEI as well as the staff and students dedicated to them.

Table 1 - Project team members.

Team Members	Contribution	Main area of research	Institution
Prof. Dr. Carlos Correia Prof. Dr.Requicha Ferreira Dr. João Cardoso	Scientific and Technical Supervisors	Scientific and Technical Supervisors	GEI
Dr. Telmo Pereira	Clinical Supervisor	Clinical Research Trials/Prototypes validation	ESTeSC
Eng. Helena Pereira Eng. Vânia Almeida Eng. Tânia Pereira Eng. Edite Figueiras	PhD Students	PWV Assessment Blood Perfusion in Microcirculation	GEI
Eng. Elisabeth Borges		Bioimpedance	GEI
Maria Inês Contente Vânia Relvas Tatiana Oliveira João André Vieira		PWV Assessment	

1.4 – Contents by Chapter

This project can be divided in three main stages: the study of the theoretical background, the characterization of the proposed instrument, and the execution of some 'clinical' trials.

In Chapter 2, are discussed the main concepts concerning to this project work, from the importance of arterial stiffness and pulse wave velocity, to the role of the heart sounds and carotid artery auscultation as important methods for arterial pathologies assessment and also the measurement of some hemodynamic parameters including the PWV. In addition, it is also presented a discussion regarding the advantages and disadvantages of local and regional determination of PWV, which is the basis of a review article in development and to be published soon.

Chapter 3 describes, in a general way, the main methodologies as well as the system's architecture and the software platforms used along the project.

Chapters 4 and 5 correspond to the description of the methodologies performed for the probe's characterization.

Chapter 6 depicts the procedures used in the 'clinical' trials and the preliminary results of the instrument applied in human carotid arteries.

Finally, in Chapter 7 draws some conclusions about the work performed and in Chapter 8 some suggestions for future work are presented.

Table 2 - Gantt Diagram of project tasks.

ID	Task name	Start	Finish	Aug	Set	Out	Nov	Dec	Jan	Feb	Mar	Apr	May	Jun	Jul	Aug
1	Study of the State of Art.	5/9/2010	15/01/2010													
2	Probes Development	10/10/2010	15/01/2010													
3	Bibliographical research for the review article writing.	18/2/2011	18/3/2011													
4	Development of the first experimental setup and preliminary studies.	21/3/2011	6/5/2011													
5	Tests for probes characterization and data analysis.	9/5/2011	10/6/2011													
6	Tests on the bench test and data analysis.	20/6/2011	22/7/2011													
7	Project report.	22/7/2011	30/8/2011													

2. Theoretical Background

2.1– Heart Function and Pressure Wave Generation

The cardiovascular system enables the exchange of gases, fluid, large molecules and other substances, as well as heat, between cells and their surrounding environment, which is only possible with an appropriate blood flow through the organs. The heart, together with the vascular system, allows the pressure variations that keep a proper blood flow all over the body [6].

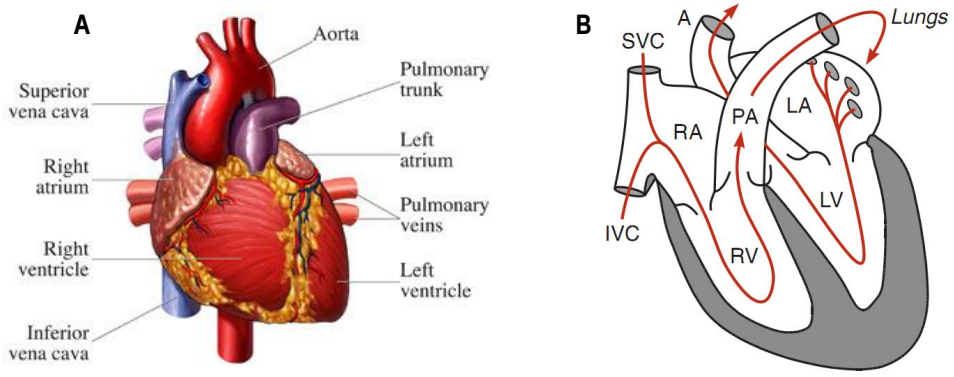

Figure 1 – General heart's anatomy. A-external view [7]; B- scheme of the blood flow in the heart: A-aorta, SVC – superior vena cava, IVC-inferior vena cava, RA-right atrium, RV-right ventricle, PA-pulmonary artery, LA-left atrium, LV-left ventricle [6].

Systemic venous blood, at very low pressures, enters in the right atrium. As atrial contraction occurs, blood is transferred to the right ventricle whose subsequent contraction ejects the blood to the pulmonary artery, to lungs. After the oxygenation process blood flows to the left atrium and then to the left ventricle which in turn contracts, ejecting the blood into the aorta, the major artery in the body, being distributed throughout the body by a complex arterial tree, of arteries, arterioles and capillaries [6].

The contraction period corresponds to the systole, while the relaxation period corresponds to diastole. The cyclic repetition of these phenomena leads to the needed pressure variations inside the aorta, generating a pulse pressure that propagates along the arterial tree.

Pulse pressure waveform varies along the arterial system due to alterations in elastic properties of the vessels but also caused by reflection phenomena in arterial branches. Figure

2A shows the aorta's pressure waveform and figure2B shows the pressure waveform detected on the carotid artery.

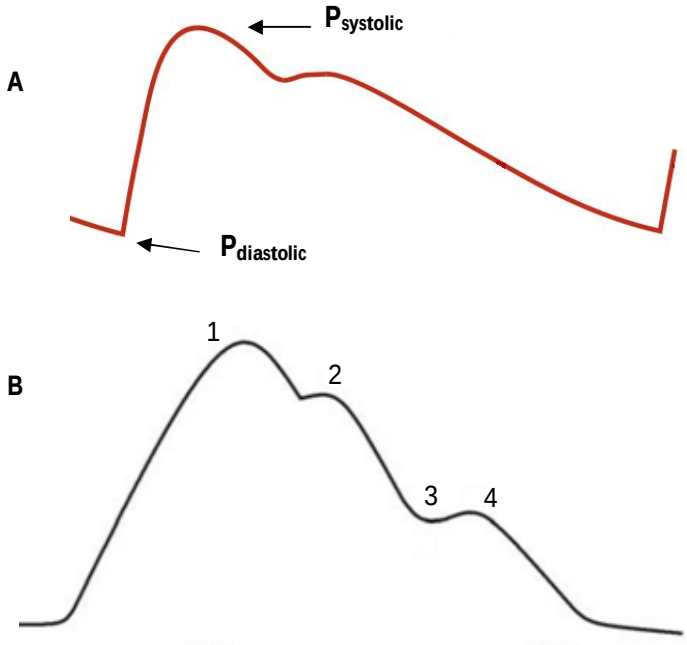

Figure 2 – Arterial pressure waves. A – aortic wave [6]; B- carotid wave. 1- systolic peak, 2- reflected wave, 3-dicrotic incisura, 4-dicrotic wave [8]

While aorta's pulse pressure presents just one discontinuity, after the maximum value corresponding to systolic pressure, carotid's pressure wave presents two discontinuities, the first one due to the blood reflection on aorta's branches, which summates with the forward wave (figure 3) and the third one corresponding to dicrotic wave consequent dicrotic incisura .

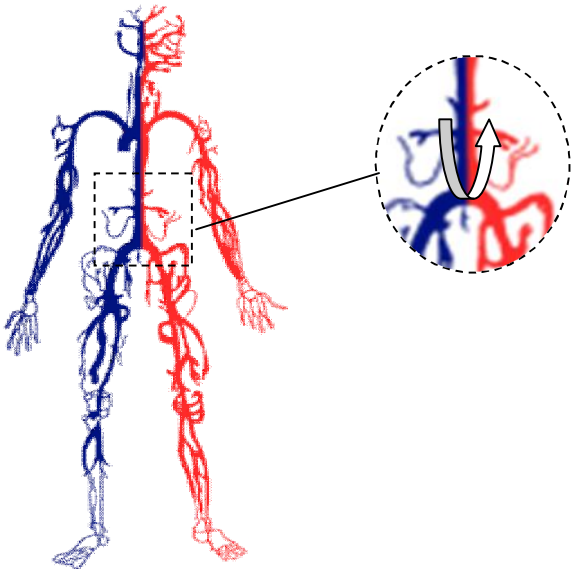

Figure 3 - Arterial tree. A-wave reflection on the aorta's branch (adapted from [9]).

In addition to the variations on the arterial wall properties along the arterial system, also ageing and some clinical conditions cause alterations on the pressure waveform, mainly by an increased arterial stiffness. Indeed, ageing as well as hypertension, cause a premature arrival of the reflected waves, in the early systole, while in young ages the reflected waves arrive in the late systole [10]. The analysis of the pressure waveform can provide important information regarding the patient's clinical condition, and the identification of some serious pathologies [11]. Figure 4 shows some examples of pressure waves detected in presence of some cardiovascular diseases.

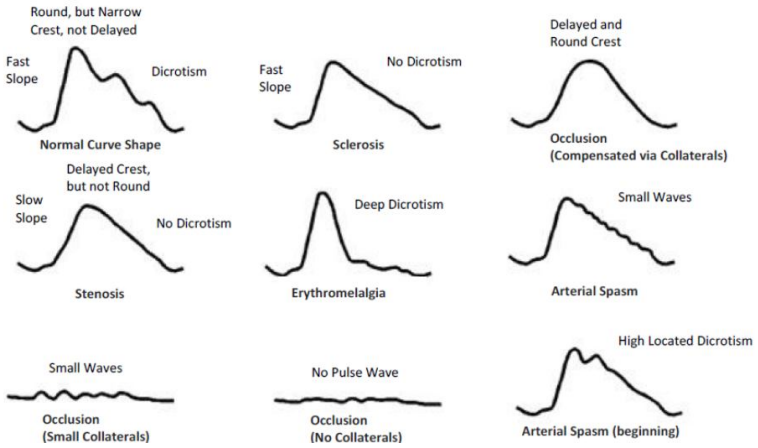

Figure 4 - Arterial waveforms caused by different diseases [11].

2.2 – Arterial Stiffness and Pulse Wave Velocity

As already mentioned, the elastic properties of the arteries are not homogeneous along the arterial system. The variations of those properties have important physiological consequences regarding not only the shape of pressure pulse, but also the pulse wave velocity (PWV) – the speed at which the pulse pressure, generated by the left ventricle contraction, propagates along the arterial tree.

In fact, distal arteries (brachial, radial, femoral, popliteal) are stiffer, while proximal arteries are more elastic (aorta, carotid, iliac) [12]. The increasing stiffness causes an increased PWV, as blood moves away from the heart. On the other hand, as pressure wave propagates along the arterial tree, suffers an amplification of its magnitude, caused by the approximation of reflection sites and consequent reflected waves. This phenomenon also contributes to the

increasing of the PWV [3].Thence, PWV is nowadays accepted as the simplest non-invasive, reproducible and robust method to access the arterial stiffness level [4].

In addition to the natural variations on arterial stiffness and PWV along the arterial system, pathological alterations on these hemodynamic parameters can lead to the development of several clinical conditions. Figure 5 resumes the main diseases associated with arterial stiffness, and indirectly, with PWV alterations.

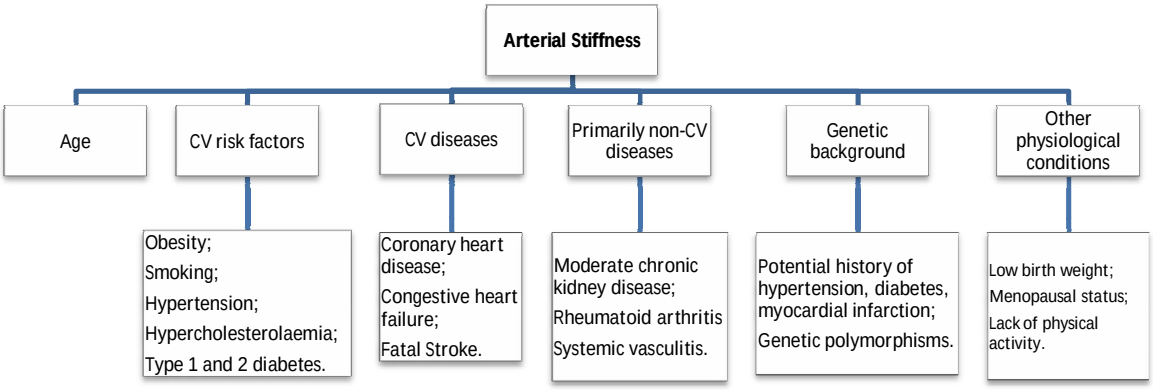

Figure 5 – Clinical conditions associated with increased arterial stiffness (adapted from [3]).

Due to its relation with the aforementioned diseases, the assessment of arterial stiffness is considered an important predictor of the development of cardiovascular diseases.

2.3 – Pulse Wave Velocity Assessment

Many studies have indicated PWV, and especially aortic PWV has an independent predictor factor of cardiovascular disease, due to its direct relation with arterial stiffness. This relation is described by the Moens-Korteweg equation [13]:

$$PWV = \sqrt{\frac{Eh}{d\rho}} \left(\frac{m}{s}\right) \qquad \text{(Eq. 1)}$$

where, E is the elastic modulus, h is the thickness of the wall d the lumen diameter and ρ the density of the blood.

Several methodologies have been developed to assess the PWV, mainly regionally, using the basic principle of velocity's determination (D – distance between recording sites; Δt - time delay between two pressure waves):

$$PWV = \frac{D}{\Delta t}\ (m/s) \qquad (Eq.2)$$

The standard method underlies on the estimation of time delay of arrival of pressure waves between the carotid artery and the femoral artery. However, given the increasing of PWV between these two regions, the estimated value corresponds to an average of the real PWV along the segment (table 3). Due to this and other disadvantages discussed below, the local assessment of this parameter has been increasingly studied.

Table 3 - Pulse wave velocity in different arteries [3].

Artery	PWV (m/s)
Ascending Aorta	4 - 5
Abdominal Aorta	5 – 6
Iliac and Femoral arteries	8-9

2.3.1 - Regional *vs* Local Pulse Wave Velocity

Despite of bigger distances between recording sites reduce the absolute error of the transit time determination **[3]**, regional assessment of PWV can include arteries with different elastic characteristics (elastic and muscular arteries) and the consequent alterations on the shape of the wave, leads to mistakes on the reference points identification and thus, to inaccurate values of transit time and PWV [14].

Another limitation of these techniques is the difficulty on the determination of the distance between the measurement sites. In fact, the lack of information about the arterial geometry doesn't allow a precise determination of the exact length of the segment under study, which will introduce errors on the absolute value of PWV [14][15].

Also the fact that regional PWV represents only an average value of the variations along the studied segment represents an important limitation, since it doesn't allow the identification of local alterations in PWV which can be an important indicator of early development of arterial disease, such as atherosclerosis [16 - 19].

Atherogenesis corresponds to the deposition of lipoprotein particles in arterial wall intima, following some chemical modifications that cause an inflammatory response, with cell migration and a consequent formation of a hard structure that affects the normal blood flow and causes vessel stenosis [20].

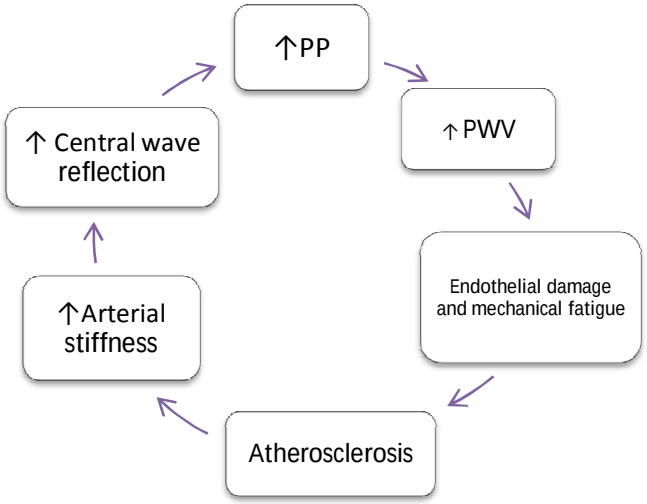

Figure 6 - Cyclic nature of Atherogenesis (adapted from [11])

Local assessment of PWV has as its main advantage, the possibility of an early diagnose of atherosclerosis, which in an early stage doesn't influence the regional value, being only detected in a dangerous advanced stage. Indeed, plaque development may not cause symptoms until 2/3 of the artery is occluded [19] so an early diagnosis is of utmost importance in order to prevent some serious symptoms which can ultimately cause heart attacks and strokes.

2.3.2 – State of the Art

2.3.2.1 – Measurement Methods and Techniques

For non-invasive regional PWV usually two pressure waves are recorded, at two measurement sites, and then systolic foot (the most frequently used) or systolic peak are identified and used as reference for transit time estimation. Several arterial segments have been used such as radial-tibial, brachial-ankle, carotid-radial, brachial-radial and femoral-tibia, but the most commonly used is carotid-femoral segment [3][5].

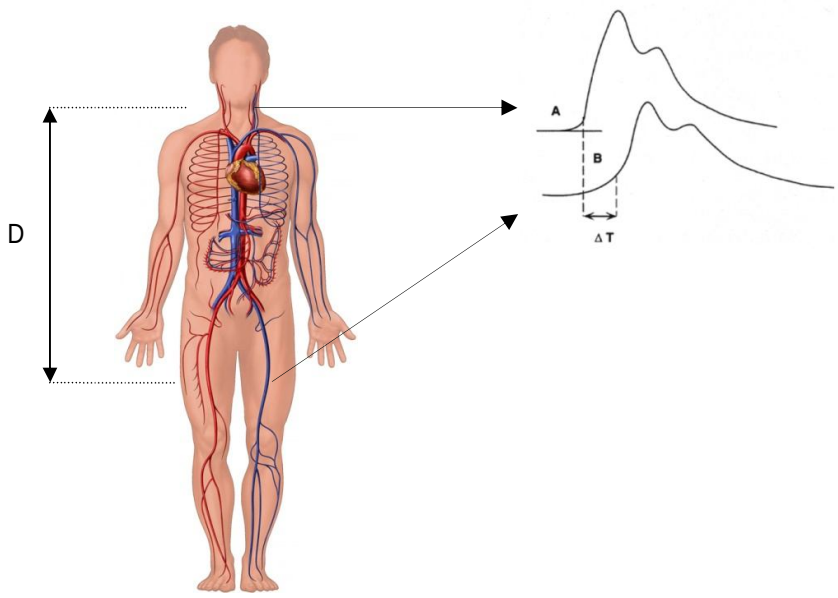

Figure 7 - Measurement of transit time through two waves recorded in carotid and femoral arteries (adapted from [21] and [22]).

Another approach, estimates the transit time through the determination of the cross-correlation between the two recorded pulses [23] and another method estimates the transit time of the reflected wave, by the determination of the instant of occurrence of the reflected wave on a single arterial pulse [24].

Regarding local PWV assessment, the most widely studied techniques are based on ultra-sounds (US), and echo-tracking of arterial wall movements, during pressure wave propagation. Echo-Doppler techniques have also been used to record arterial wall vibrations, being the transit time estimated by the detection of US reflections at two sites along the arterial segment, and the distance determined at B-mode image [16] [17]. Meinders *et al* have also suggested a methodology based on the simultaneous assessment of arterial diameter variations and pressure waveform in the carotid artery by means of US, being the PWV estimated as a function of pressure variation [25]. Hermeling *et al.* developed a method to measure the local PWV using an M-mode ultrasound identifying the systolic foot or the dicrotic notch from of distension waveforms and corresponding acceleration waveform and using them as reference for time-delay estimation [26].

Usually, the artery used for these measurements was carotid artery, since it has similar elastic properties to aorta, it's close to the heart and, on the other hand, can be easily assessed.

Also at GEI, researches has been devoted to the development and characterization of new sensors for local PWV assessment. A double probe (DP) piezoelectric has been proposed and characterized (impulse response determination, cross-talk analysis and temporal resolution determination). Two sensors separated by a known distance record (non-invasively) the pulse pressure in the carotid artery and transit time is then estimated as the time delay the pulses of arrival between the two sensors [27]. Two optical probes were also developed for the same propose, based on planar and avalanche photodiodes [28]. A programmable test bench capable of mimicking the main characteristics of the cardiovascular system was also developed, with which the previously mentioned probes and also the probe proposed in this work have been characterized [29].

2.3.2.2 – Commercialized devices

Devices available on the market perform regional measurements. Although an increasingly studied approach, there is not any commercialized device for local assessment of PWV yet.

The most commonly used in clinical environment are the Complior® (Colson, France), the Sphygmocor® (AtCor Medical, Australia) and the PulsePen® (Diatecne, Italy), all based on pressure sensors [5] and the Arteriograph® (TensioMed, Budapest, Hungary) based on the time to reflection determination, on brachial artery [12].

Complior® - allows a simultaneous detection of the pressure waves on two recording sites (carotid and femoral arteries) with two piezo-electric sensors, to determine the transit time and the PWV. In addition it also determines the central arterial pulse pressure and the augmentation index [5].

Figure 8- the Complior® system [30].

Sphygmocor® - includes several equipments that provide information about various hemodynamic parameters such as arterial pressure wave, central blood pressure, augmentation index (Sphygmocor CP® system), pulse wave velocity (Sphygmocor CPV® system) and heart rate variability (Sphygmocor CPVH® system) [31]. The underlying technology is the applanation tonometry for pressure pulse detection, associated with electrocardiogram (ECG) by sequential recording on the two measurement sites. Transit time is calculated in relation to R wave of ECG, by subtraction of delays to both pulses [5].

Figure 9 - The Sphygmocor® system [31].

PulsePen® - this equipment is based on a technology similar to Sphygmocor, with a tonometer and an integrated ECG unit. Two sequential measurements are performed at two recording sites (carotid and femoral arteries) and transit time is determined in relation to ECG [12].

A **B**

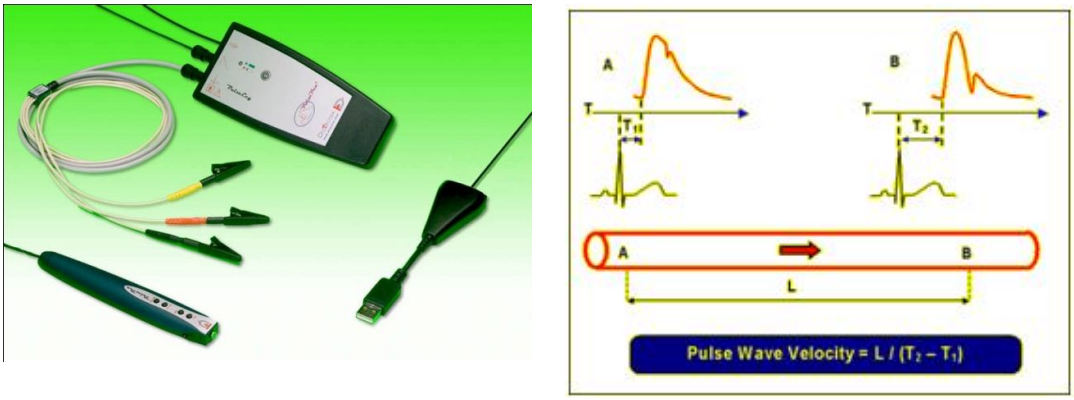

Figure 10 – A. PulsePen System; B – Scheme of the methodology used for transit time estimation [32].

Arteriograph®- this system measures the pulse transit time through the determination of the time to reflection of the recorded brachial pulse pressure. Similarly to the previous equipments, distance between measurement sites is estimated through superficial morphologic measurements [12].

Figure 11 - Arteriograph system [33].

2.4 - Heart Sounds

2.4.1 - Normal heart sounds

During the cardiac cycle, valves closure in association with the blood oscillation, generate sounds that can be heard auscultation techniques [6]. The analysis of these sounds can provide important information that allows the identification of pathological alterations on the normal functioning of the heart. In fact, heart sound auscultation is considered one of the most reliable tools for early diagnosis of some serious heart disease such as heart valve dysfunction or heart failure [34].

First Heart Sound

The first heart sound of the cardiac cycle (**S1**) corresponds to the closure of mitral and tricuspid valves, as a consequence of the atria contraction and the increased pressure that drives blood from atria, across the valves, to the ventricles (figure 1) [6].

Second Heart Sound

The second sound to be heard (**S2**) corresponds to the closure of pulmonary and aortic valves and since the blood flow from the ventricles is more forceful, S2 is usually louder and of shorter duration than S1 [35]. The closure of these valves coincides with a notch in aortic pressure wave, as illustrated in figure 12.

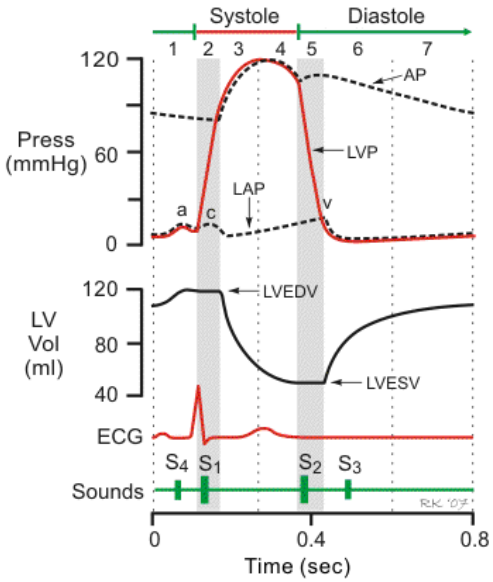

Figure 12 - The cardiac cycle. [36]

2.4.2-Abnormal heart sounds

Normal sounds correspond to valves closure [35]. However, due to some pathological alterations such as valve dysfunction, other sounds can be heard.

Third Heart Sound

Immediately succeeding S2, a third sound (**S3**) is normally heard in children, during early diastole. However, in adults, an audible S3 is considered pathological, indicating ventricle dilation [6]. In addition to ventricle dysfunction it is also associated with several types of heart valve disease, being commonly detected in patients with mitral regurgitation, for example [37].

Nevertheless, its physics characteristics such as low loudness, short duration and low frequency make it difficult to hear with traditional auscultation equipments, so automated systems are need for S3 identification and analysis from phonocardiograms [37].

Fourth Heart Sound

A fourth sound can be heard during atrial contraction due to vibration of the ventricular wall, as a consequence of a higher wall stiffness level, indicating ventricular hypertrophy.

2.4.4 - State of the Art

Heart auscultation is a widely used non-invasive tool and considered a fundamental technique in heart diseases assessment, mostly related to heart valve dysfunction, ventricle failure and arterial pathologies [38]. However, an accurate analysis of the heart sounds highly depends on the experience of the technician and on the other hand, some changes that could provide important information about heart disorders could not be heard by human ear [39].

In this context, phonocardiography and phonocardiogram analysis are widely used and many research groups have been dedicated their attention to the development of automatic systems for phonocardiogram analysis, allowing the detection of heart sounds and murmurs that would not be detected otherwise.

An automatic analysis cannot be done until pre-processing routines are performed, mainly related to heart sounds segmentation into meaningful lobes such as S1 and S2 [40][41].

The first methods applied in heart sounds segmentation were based on frequency domain analysis, but since heart sounds are nonstationary, the Wavelet Transform started to be also applied, allowing the representation of the signal's spectrum in time [42]. Other methodologies have been applied based on Hidden Markov models, decimation models, linear and high order statistical methods [43].

Most algorithms referred in the literature associates the phonocardiogram and the ECG signal or/and carotid pulse as reference for the sounds segmentation [40]. However some research groups have been working in new methods that dispense synchronization with those techniques. In 1997, H Liang *et al* proposed a new method based on heart sound envelogram determination, using normalized average Shannon energy [40]. In 2006, D. Kumar *et al* also applied the Shannon energy in the heart sounds main components segmentation, following their classification into S1 and S2 by a developed algorithm based on Mel-frequency cepstral

coefficients [41]. These investigators have been publishing several papers describing new and improved methods, not only for signal segmentation, but also for automatic classification of the heart sounds and murmurs [37] [39] [44].

2.4.4.1 - Carotid Auscultation

Although heart sounds auscultation is more commonly performed in heart area, the auscultation of the carotid artery can also provide important information about arterial problems such as stenosis or occlusion [45].

As early as the 1970s, vascular auscultation had been used in blood flow monitoring and in 1980, E. Wintermantel *et al* performed invasive carotid artery auscultation on Wister rats, and proved that blood flow alterations in a small vessel, caused by different degrees of stenosis, were detected by alterations in the sound waves [45].

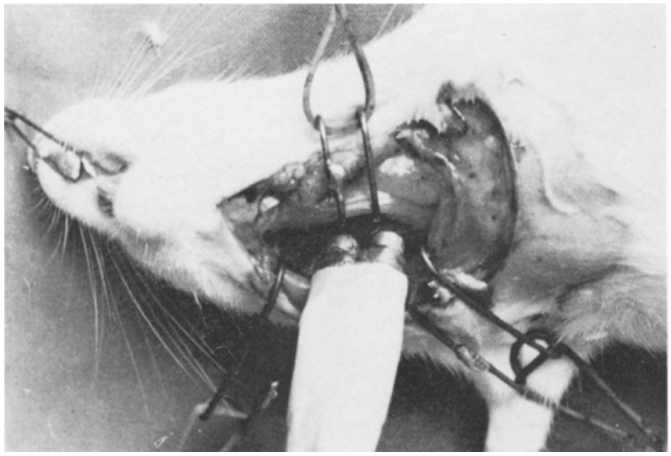

Figure 13 - Carotid auscultation on a Wister rat [45].

Also the relative analysis of the carotid pulse pressure and sounds can be performed. In fact, as well as heart sounds can be associated to some characteristic point references in aortic pressure waves, also carotid artery (ca) sounds correspond to characteristic points of its pressure waves. Figure 14 depicts that relation. As can be seen, the first carotid sound (CaS1) corresponds to the onset of the pressure wave and the second sound (CaS2) corresponds to the dicrotic notch.

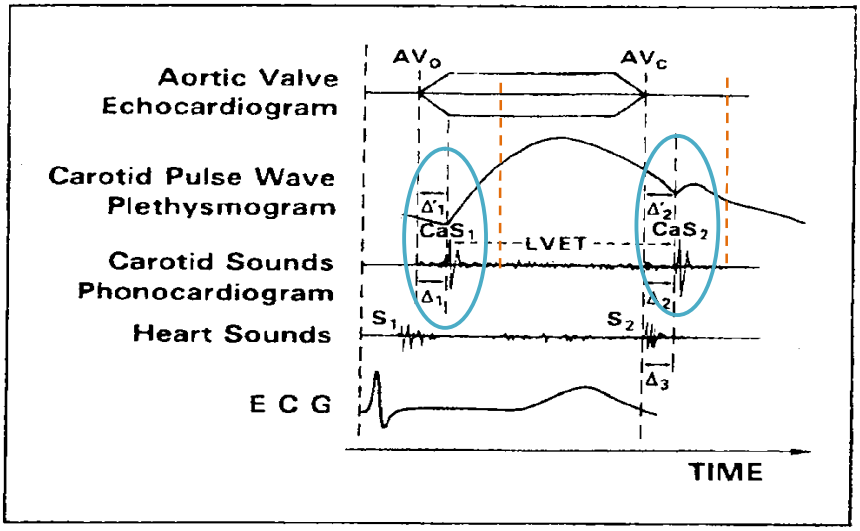

Figure 14 - Carotid pulse wave and sounds [adapted from 46].

On the other hand, the audible sounds at the carotid artery are obviously related to the heart sounds. Figure 15 illustrates both signals, from a phonocardiogram and from carotid artery auscultation where can be observed the delay between them.

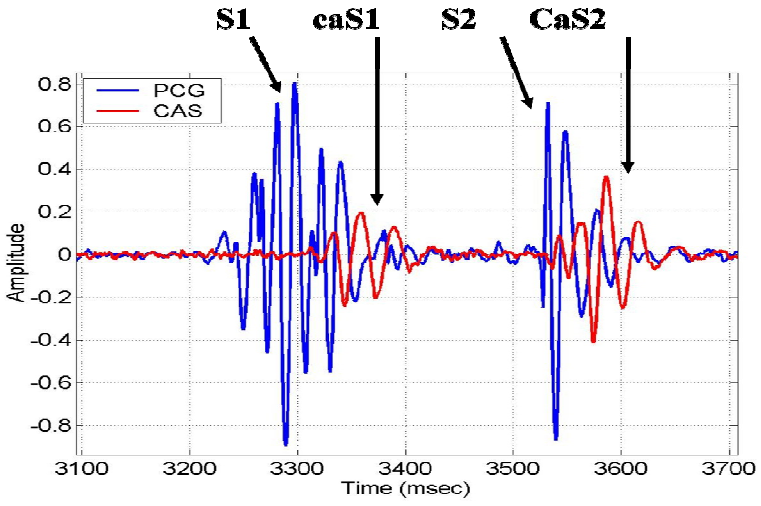

Figure 15 - Heart and carotid sounds [46].

In this context, Hasegawa *et al*. have proposed a new method for PWV determination based on the estimation of the time delay between heart and carotid artery sounds [46], and in 2003 Jelinek M *et al* also determined PWV between cardiac and carotid wave sounds in five volunteers, through a cross-correlation function between those signals, for time delay estimation, while distance was measured directly on their body's surface [23].

In the present work the new technique proposed is also based in carotid auscultation, but time delay will be estimated between two carotid pulses.

2.4.4.2 – Heart sounds and Left Ventricle Ejection Time

The Left Ventricle Ejection Time (LVET) corresponds to the time interval between the opening and closure of aortic valve for blood ejection from left ventricle to aorta. Its clinical significance, mainly related to the assessment of myocardial contractility and cardiac output, has been reported by several studies [47][48].

The analysis of its values is based on the relation between this parameter and heart rate. In fact, LVET values vary inversely with the heart rate [49], as demonstrated in the following figure:

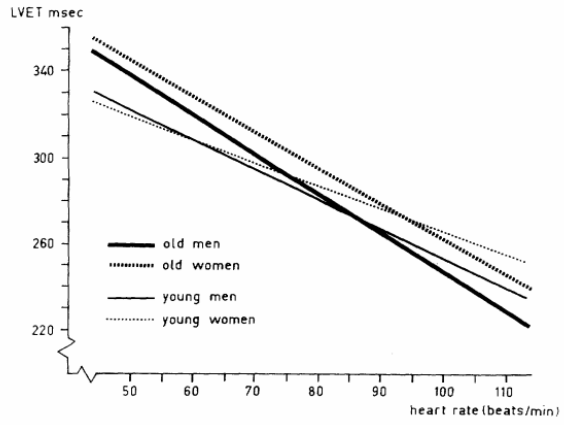

Figure 16 - Linear regression lines relating LVET to heart rate in young and old subjects (taken from [49])

The traditional methods for LVET assessment consisted in simultaneous recordings of ECG, the carotid pulse waveform and a phonocardiogram for recording of aortic closure sounds (see figure 17) [47].

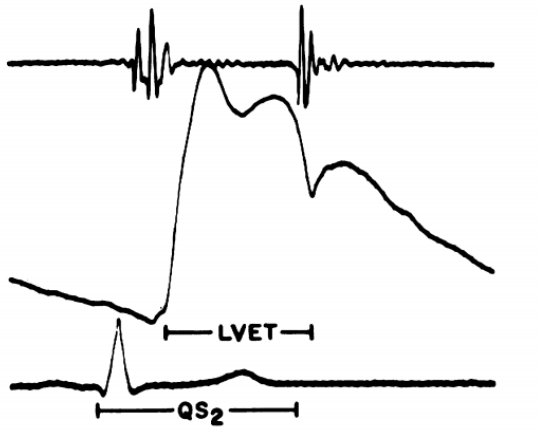

Figure 17 - LVET determination through a phonocardiogram, the carotd puse wave and ECG [47].

However, over the years, other methods have been developed based on M-mode echocardiography and Doppler echocardiography [50], and more recently, the relation between LEVT and heart sounds has been proved, and other methods have emerged. Indeed, Carvalho P. *et al* performed a feasibility study which concluded that opening and closure of aortic valve can be extracted from S1 and S2, respectively [51]. Later, the same work group has proposed algorithms for the determination of the systolic time intervals (pre-ejection period and LVET) from heart sounds and ECG [49].

On the other hand, also Hasegawa *et al*. used the relation of the time delay between S1 and S2 to the LVET determination, but for carotid sounds, as can be seen in figure 14.

The same idea will be used in this work for the LVET estimation through the carotid artery auscultation, with the proposed double acoustic probe (DAP).

3. Process Methodology

3.1 – Acquisition System

3.1.1 – Double Acoustic Probe

The Acoustic Probe consists of two independent sensors able to detect the main cardiac sounds in the carotid artery, in a totally non-invasive way, in order to determine the P-PWV, HR and LVET.

Figure 18- General measurement system.

For the testes realized for its characterization, however, was sometimes necessary the use of a Data Acquisition Module - NI-USB 6009© - for the simultaneous acquisition and recording of the signals from wave generator and the acoustic sensors.

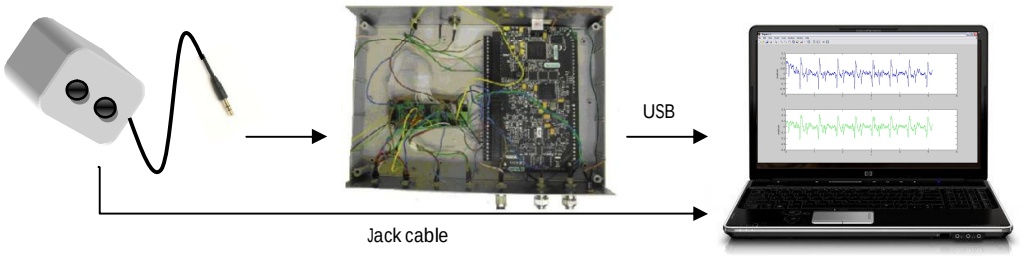

Figure 19 - Measurement system using the data acquisition unit NI6009©.

3.1.2 – Acquisition Unit and DAQ Module

The used acquisition unit allows the connection of a Double PZ Probe, by a RJ45 connector, and two pressure sensors, as well as a wave generator, through BNC connectors.

The acoustic sensors were directly connected to the DAQ Module which was the NI USB-6209©, with height analog inputs channels, two analog output channels and twelve digital input/output channels (datasheet at http://www.ni.com/pdf/manuals/371303l.pdf).

Figure 20 - DAQ Module NI 6009; normal view (a) and internal view (b) of the device; [52]

3.2 - Software Platforms for data logging and data processing

During the execution of the various tests performed in this project work, several software platforms were used, for signals acquisition, visualization and analysis, depending on the studies and their goals.

Thus, for simple waveform visualization were used both, the free software Audacity 1.2.6® and MatLab R2009a®; in order to compare input signals and sensors response it was necessary to use the Data Acquisition Module NI-USB 6009©, and consequently, LabView Signal Express 2009© for signal visualization; signal processing routines were performed on MatLab R2009a®.

3.3– Clinical Trials

In order to acquire and analyze the signals obtained in human carotids, were performed some data acquisitions on six young and healthy volunteers, for three weeks.

In each session the subjects were sited and relaxed, while an operator placed a probe on the left or right carotid starting the acquisition, using Audacity®. The data acquisition didn't stop until a good signal, during at least eight to ten cardiac cycles, wasn't acquired.

The criterion used to decide whether or not the signal was good, was the similarity between the acquired signals from the two sensors, as well as a good definition of the two expected peaks, correspondent to the two main cardiac sounds.

The procedure has been repeated for both, left and right carotids, once a week, for three weeks, and always for two different operators.

4. Probe's Characterization

4.1 – Experimental Setup and Methodologies

In order to carry out the probe's characterization, several studies were performed using the experimental setup schematized in Figure 21.

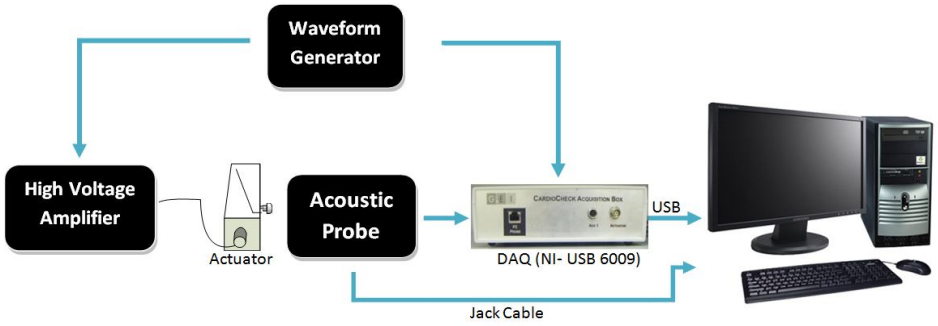

Figure 21- Schematic drawing of the setup used in Acoustic Probe characterization studies.

Five main studies were performed in this setup: the first one aimed the evaluation of the sensors response to four different waveforms; the second one had as the main goal a better understanding of the response waveforms of Acoustic sensors, using the response of PZ sensors as a reference; the third one consists on the evaluation of the existence of cross-talk between both sensors of double probe; the fourth study performed, aimed the analysis of the sensors repeatability regarding the waveforms; the last one corresponded to the determination of impulse response of both sensors in the double AP.

In a later phase, a sixth study was performed in order to evaluate the probes Time Resolution. The used methodologies will be described in the next Chapter of this report.

Some preliminary studies were also performed before the main studies already mentioned, in order to understand which were the best conditions for the acquisitions execution, mainly referring to the use of an interface material, between the actuator and the sensor's surface.

In all tests the inputs were generated by an Agilent 33220A Arbitrary Waveform Generator and a 700µm actuator (Physik Instrumente GmbH, P-287), driven by a High-Voltage linear amplifier (HV) (Physik Instrumente GmbH, E-508). A mushroom-shaped piece was used to excite the sensors with the movements of the actuator. As already mentioned, to register simultaneously the inputs used in each acquisition and the sensors response, both sensors and the actuator were connected to the Data Acquisition System NI-USB 6009©. The visualization of the signals was performed in LabVIEW Signal Express 2009©.

Several input signals were used in these studies including three cardiac-like waveforms previously synthesized and programmed in the Wave Generator [53]. Those waveforms can be observed in Figure 22.

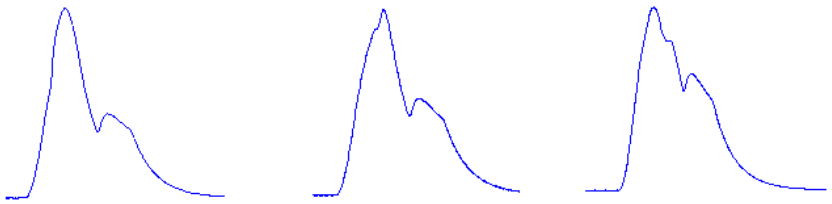

Figure 22 - Synthesized cardiac-like waveforms used in the probe's characterization studies – Type A, Type B, Type C, respectively.

4.2– Preliminary studies

Firstly, some tests, regarding the amplitudes and widths of the inputs to use, were performed, leading to the conclusion that the best signals are obtained for widths lower than 10Hz (T=100ms) and amplitudes between 2V and 3V. These conclusions are justified by the noise produced by the actuators motion which is lower for lower frequencies.

Also the need of using an interface between the sensor and the actuator was evaluated, intending to obtain better defined waveforms, with a lower noise level. For this purpose, several materials were used such as adhesive, Styrofoam and sponge. However, because they didn't allow the acquisition of good signals, they were immediately discarded.

Another interface method was, then, implemented, using a stethoscope, in order to amplify the signal, overlapping the noise level. The acoustic sensors were fixed to the rubber tubes of the stethoscope and connected to the computer and to NI-USB 6009 DAS, while the ACT excited the stethoscope's diaphragm. The method of coupling the three instruments is schematized in Figure 23.

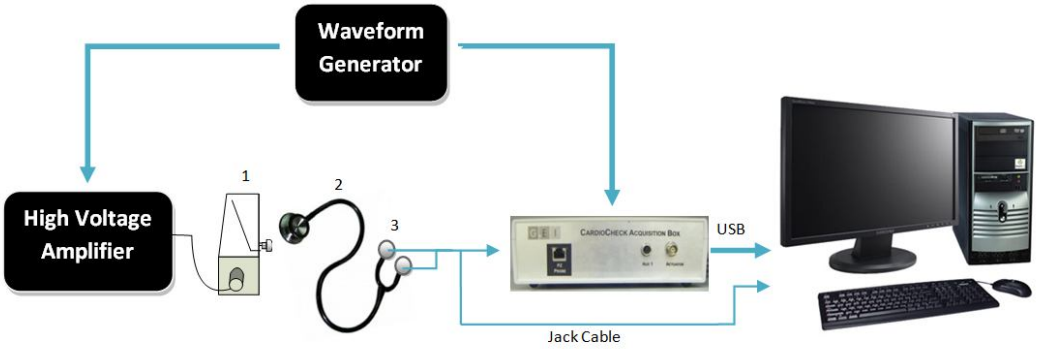

Figure 23 - Schematic drawing of the used setup for the evaluation of need of using an interface between ACT and the sensor being excited. 1- actuator; 2- stethoscope; 3 – acoustic sensors.

In Figure 24 is represented an example of the acquired signals, using this interface method as well as the results correspondent to the direct excitation, to the same inputs.

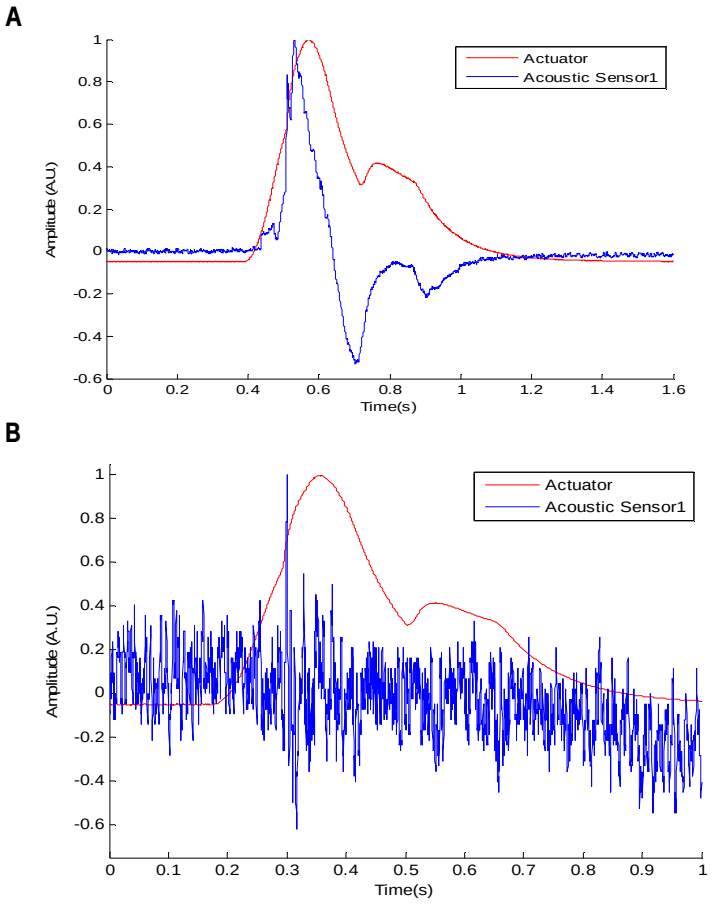

Figure 24 - Acoustic sensor response to a 500ms width type A - waveform with A- direct excitation and B - excitation of a stethoscope's diaphragm connected to the acoustic sensor.

Both signals were submitted to the same signal filtration, a 15 sample moving average filter. However, as can be seen, there weren't any improvements on signals quality with this method when compared with the direct sensors excitation. Indeed, the signals obtained with the stethoscope between ACT and the sensors surface presented neither reduced noise, nor better defined waveforms. Unlike the expected, the signals amplification wasn't enough to overlap to the noise level.

Thus, all the following studies were performed with direct excitation of the actuator in the sensors**.**

4.3- Waveform Analysis

This study aimed the analysis of sensors' response to a set of inputs generated by Agilent 33220A and exerted by the actuator, using the three cardiac-like waveforms depicted in Figure 22 as well as Gaussian waves.

For each input signal were selected the best amplitude and frequency in order to obtain the best response of the sensors.

4.3.1 – Signal Integration

Since the obtained waveforms correspond to the differentiation of the original signals, it was performed their integration through the application of the Matlab function *cumsum*, in order to compare them to the actuator signal, also recorded.

All sensors output signals (represented in blue) presented in the following figures were submitted to a 15 sample moving average filter, in order to reduce the high-frequency noise.

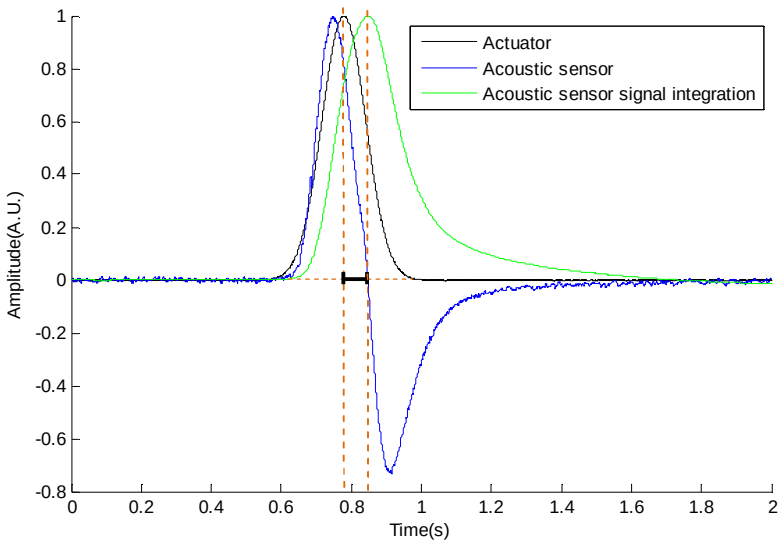

Figure 25 - Acoustic sensor response to a Gaussian impulse with amplitude=3.5V and 500ms width (2Hz); the sensors signal integration and the input signal (Actuator) are also represented; the orange dashed lines emphasize the delay between the signals.

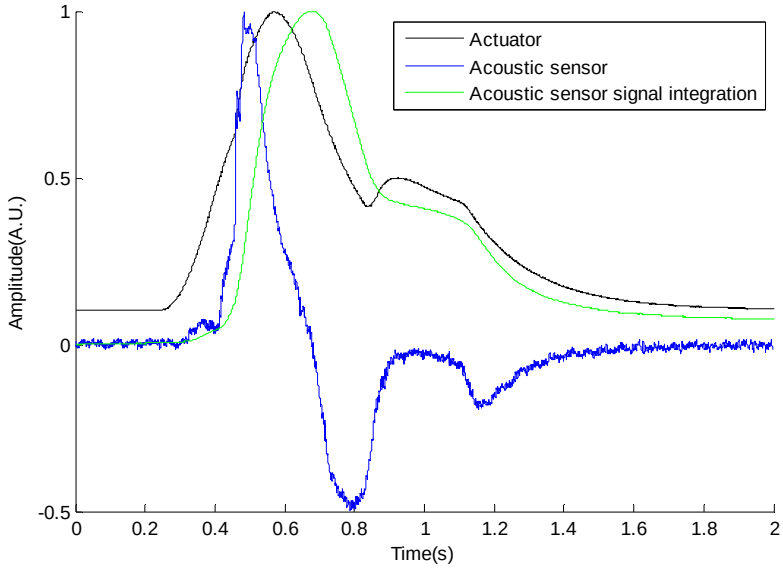

Figure 26 – Acoustic sensor response to a Type A cardiac-like impulse with amplitude=3.5V and 900ms width (1.11Hz); the sensors signal integration and the input signal (Actuator) are also represented

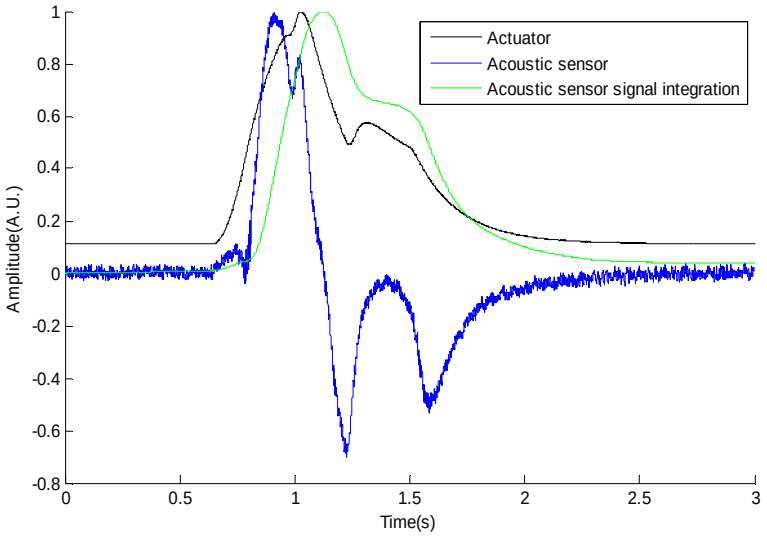

Figure 27 - Acoustic sensor response to a Type B cardiac-like impulse with amplitude=3.5V and 500ms width (2Hz); the sensors signal integration and the input signal (Actuator) are also represented.

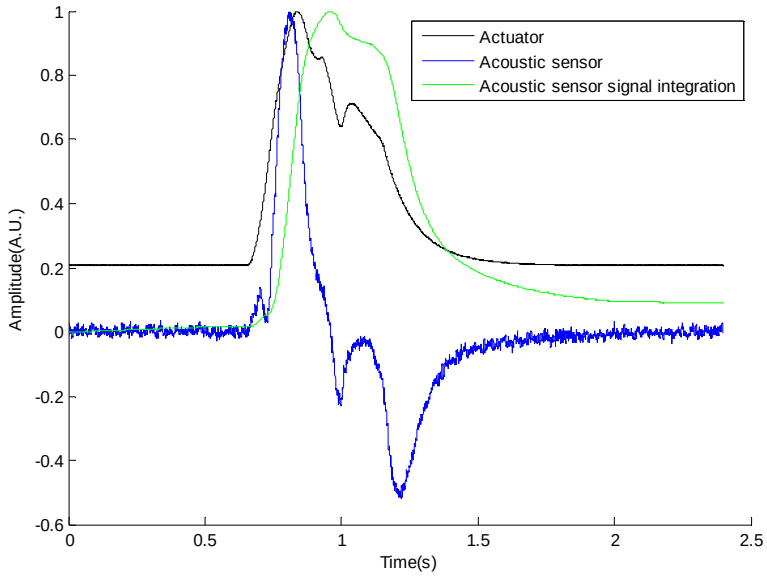

Figure 28 - Acoustic sensor response to a Type C cardiac-like impulse with amplitude=3V 500ms width (2Hz); the sensors signal integration and the input signal (Actuator) are also represented.

Observing the previous figures we can conclude that the simple integration of the acoustic sensors' response is not enough to obtain accurately the input waveform. In fact, as previously mentioned, the sensors proceed to a signal filtration which leads to a loss of potentially important information that hinders the regeneration of the original signal. Therefore, the accurate recovery of the waveform will be always compromised.

Indeed, despite of originating generally similar waveforms to the actuator's signal, they don´t enable the identification of important discontinuities and differences, between the three cardiac-like waveforms presented. For a more accurate analysis, were determined the Root Mean Square Errors (RMSE) between the sensors signals integration and the input signals, and all waveforms presented RMSE grater then 16% (table 4).

Table 4 - RMS errors of the waveforms obtained from the integration of the acoustic sensors output.

Input Signal	RMSE (%)
Gaussian wave	18.51
Type A cardiac-like waveform	16.74
Type B cardiac-like waveform	16.57
Type C cardiac-like waveform	19.75

Another detail to take in consideration is related to the delay between the ACT and the sensor's signal, in figure 25. The orange dashed lines emphasize the delay between the maximum amplitude point of the Gaussian wave and the zero-crossing point of the sensor's signal.

However, regarding the other signals, it is also visible that some of the most prominent discontinuities of the original sensors' signals correspond to the main notable points of the input waveforms, for example the type B cardiac-like waveform:

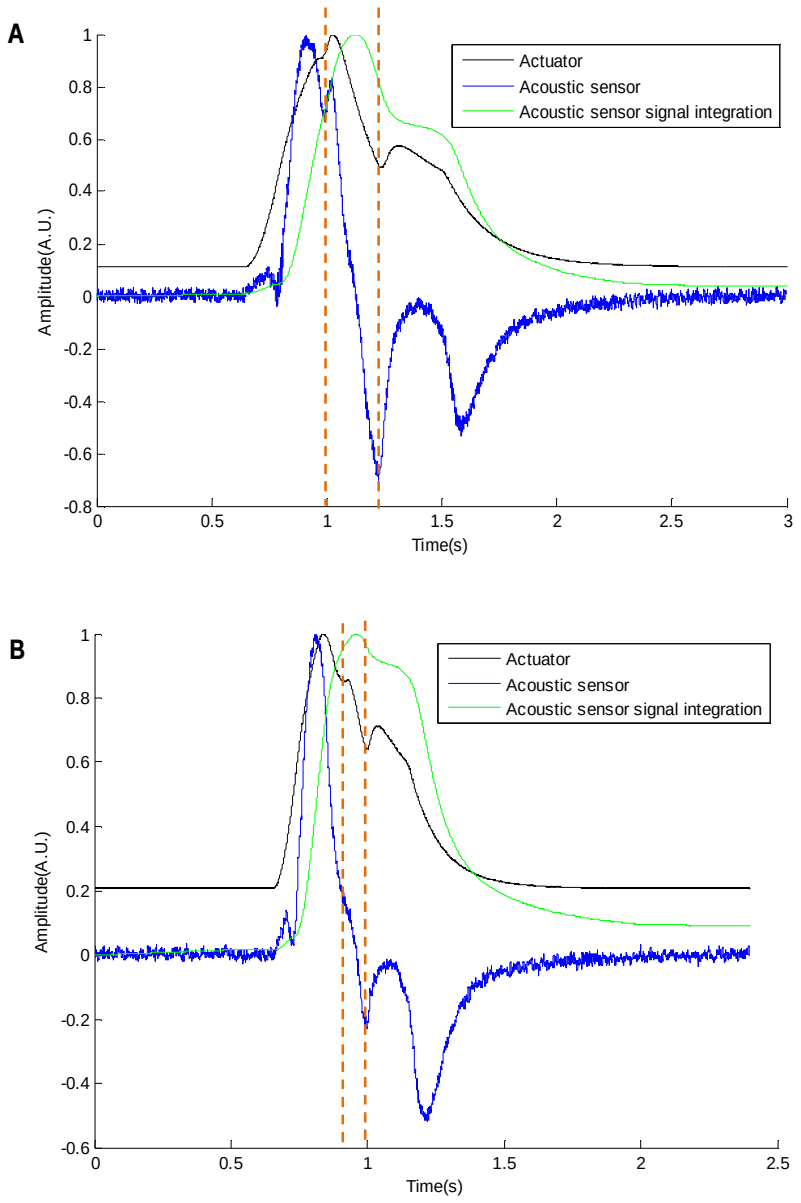

Figure 29 - Acoustic sensor response to a type B (A) and type C (B) cardiac-like impulses; the dashed lines enhance the correspondence between the discontinuities of the response and input signals.

In this context, another study was carried out, aiming the clarification and a better interpretation of these results.

4.4- Waveform comparison between Acoustic and Piezoelectric Probes

In order to compare the waveforms detected by the acoustic and the PZ sensors, when excited by the actuator, an Acoustic Probe and a Double Probe PZ were simultaneously actuated and their detected signals recorded, being both probes connected to NI-USB 6009©, in a setup similar to the one depicted in Figure 21, except the setup that allowed the contact between the actuator and both sensors:

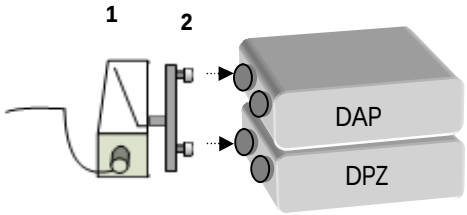

Figure 30- Accommodation of DAP and DPZ for simultaneous assessment. Two mushroom-shaped pieces were used to excite one of the sensors of each probe.1-piezo actuator; 2- support that connects the actuator to the mushroom-shaped pieces.

As can be seen in the previous figure, the original signals are considerably noisy, especially the acoustic sensor signal, so it was applied a moving average filter (15 samples). The followed figures show the sensors response to the three cardiac-like waveforms.

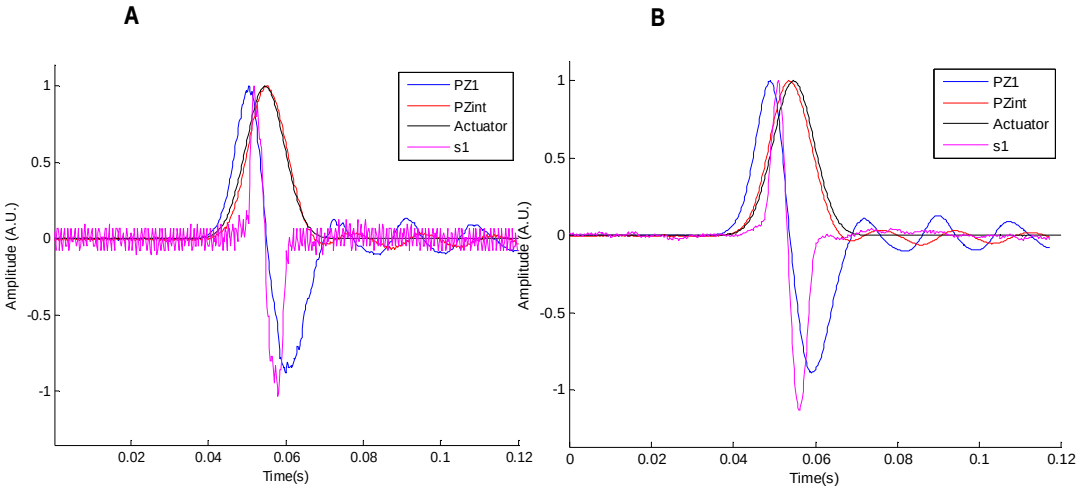

Figure 31 - Simultaneous acquisition with a DAP and a DPZ. A - original signals; B -filtered signals.

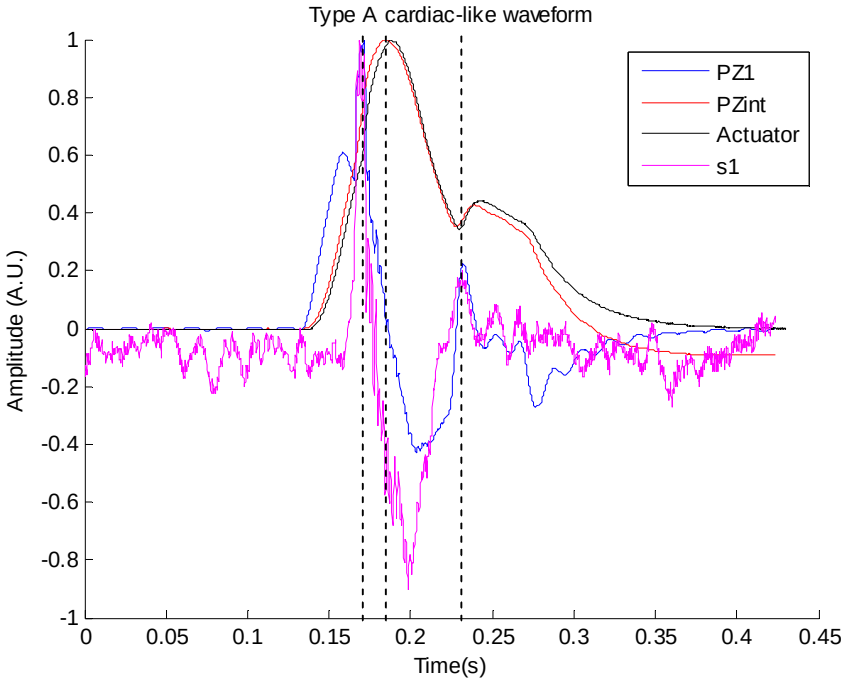

Figure 32- Sensors' response to a 350ms width type A cardiac-like waveform.

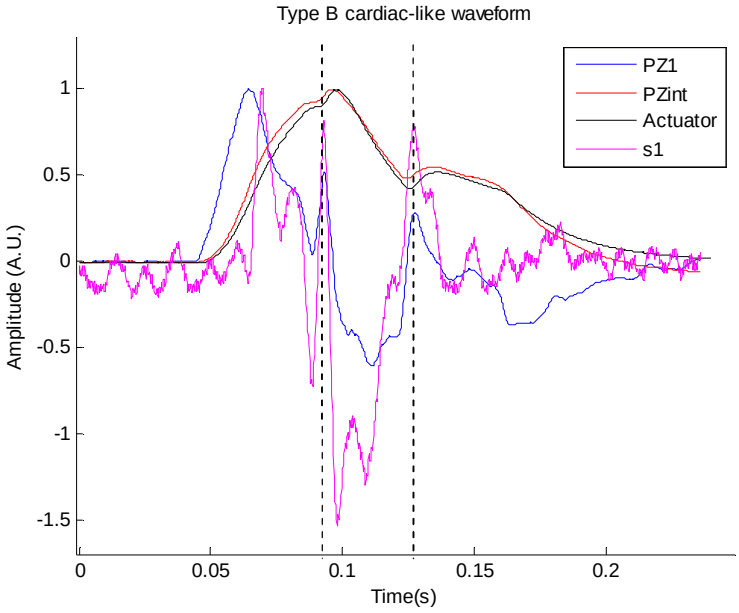

Figure 33 – Sensors' response to a 300ms width type B cardiac-like waveform.

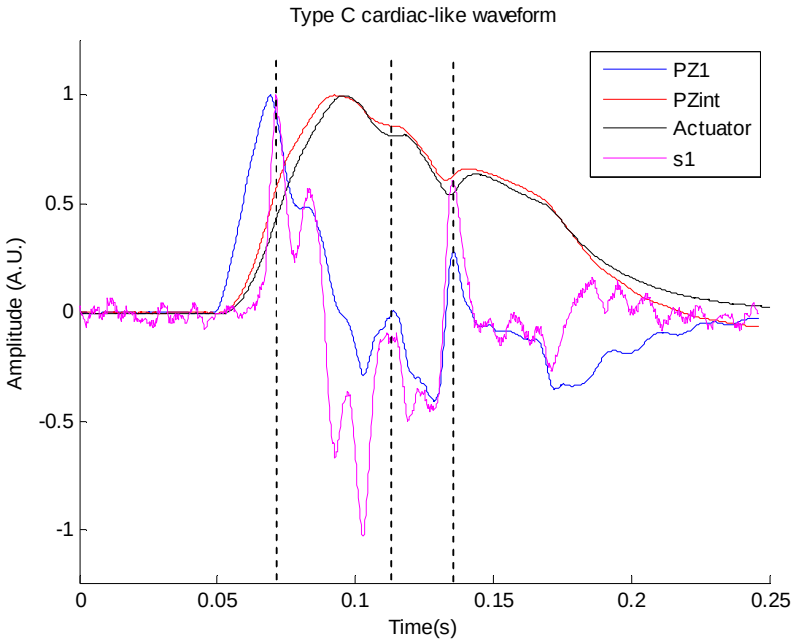

Figure 34 – Sensors' response to a 300ms width type C cardiac-like waveform.

By the analysis of the response signals of both probes we can see that the signals of the acoustic sensor differ from the presented in section 4.3.1, possibly due to the differences in the methods used for its excitation. Despite all the efforts to ensure the best conditions for the acquisitions execution, since both probes were being excited at the same time, the contact between the 'mushroom' and the acoustic sensor may had suffer alterations from the previous acquisitions, when only the DAP was being studied.

On the other hand, the delay between the signals is also verified, as in the previous section.

Nevertheless, we can still match some discontinuity points to specific and correspondent peaks of the acoustic and PZ probes, as depicted by the dashed lines in figures 28, 29 and 30. Thus we may conclude that signals of both probes are correlated and that acoustic probe has no kind of disadvantage, regarding the information provided, when compared with PZ probe. Although, other studies must be carried out in the future, in order to quantify and prove the relation of both signals as well as the identification of important discontinuities of the waveforms.

4.5 – Cross-Talk Analysis

In order to analyse the existence of cross-talk between both sensors of DAP, several acquisitions were performed, recording the signals from both sensors but with just one being excited. Indeed, since the two sensors share the plastic box of the double probe, it is very important to understand if some kind of interaction, between them, occurs.

Since the recording of actuator's signal was no longer necessary, this study was performed with Audacity1.2.6®. This software has the advantage of performing signal filtration, which allowed a better detection of cross-talk that would be *hidden by noise* using other software such as LabVIEW Signal Express 2009© or MatLab®.

Several input signals with different amplitudes and frequencies were used in this study, leading to the conclusion that the presence of cross-talk is dependent of the frequency of the input signals, as schematized in Figure 35.

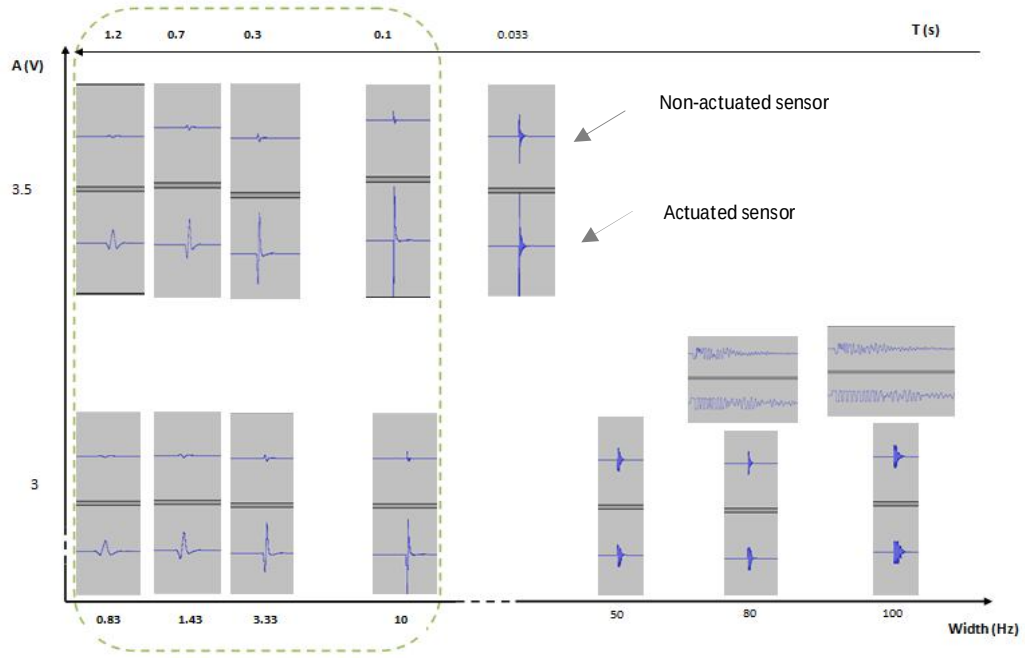

Figure 35 – Cross-talk analysis and its dependency to the signals input widths. Dashed rectangle delimits the widths values that allowed better signals.

Although the results suggest the existence of cross-talk between the two sensors of the double probe, this phenomenon may be due to the noise resulting from the actuators movements. Indeed, for higher frequencies the noise produced by the actuator is higher, as well as the noise caused by the contact between the mushroom-shaped piece and the excited sensor. The following figure depicts the signal obtained only for the noise produced by the actuator, for a 50Hz input Gaussian wave (with 0.02ms width), without any contact between the mushroom and the sensor:

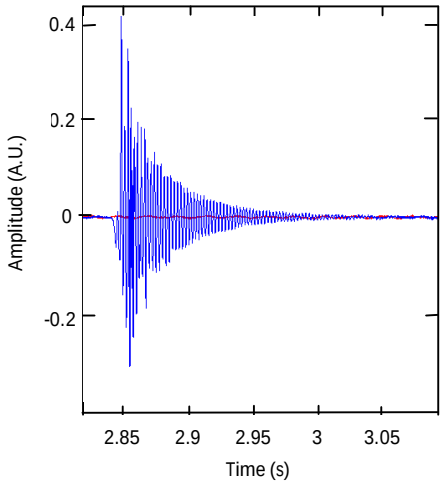

Figure 36 - Noise caused by the actuators movements, recorded by the acoustic sensor (no contact between the 'mushroom' and the sensor).

As demonstrated in the previous figure, the actuator may generate very high frequency signals with considerably high amplitude (depending on the input signal used) which will cause a response of the non-excited sensor. Regarding acquisitions realized in human carotids this source of noise does not exists and thus, the recorded signals will not be influenced by cross-talk effect. However, the reproduction of the mentioned procedure must be carried out in human carotids or in a bench model, in order to confirm these suppositions.

4.6– Repeatability

For this study, each sensor was excited with fifty independent impulses (Gaussian waves), with the same amplitude and width.

With those fifty signals, it was determined the average signal which was used as reference to determine the Root Mean Square Error (RMSE), for each one.

Figures 37 and 38 show the obtained results from sensor1.

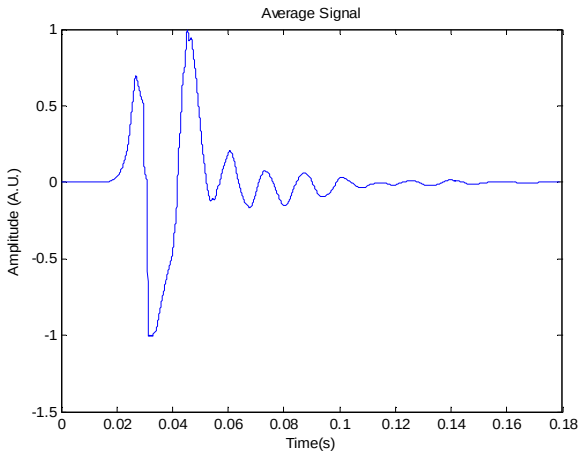

Figure 37 - Average signal from all the 50 signals acquired at the same conditions, with sensor 1.

The RMSE was then computed to each signal, and the results are depicted in the followed graphic.

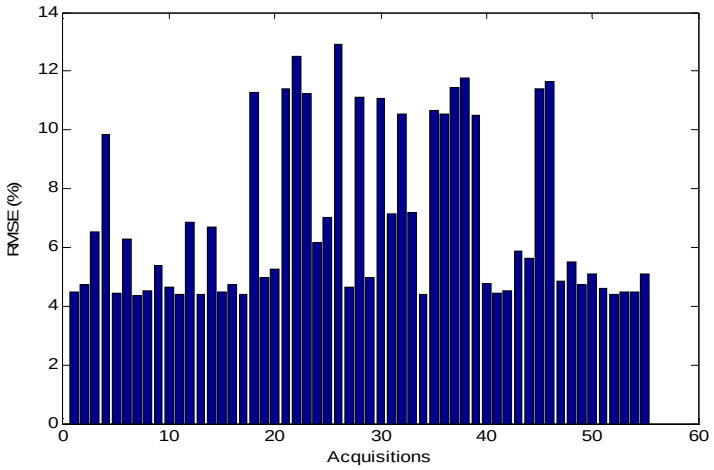

Figure 38 - Graphic representation of the RMSE distribution from each signal to the average waveform.

The mean value of RMSE is 6.94%, and the standard deviation 2.91%, which reveals some dispersion of the values (Figure 38).

Regarding the sensor 2, the RMSE distribution is represented in figure 39 (the average signal was similar to the depicted in figure 37).

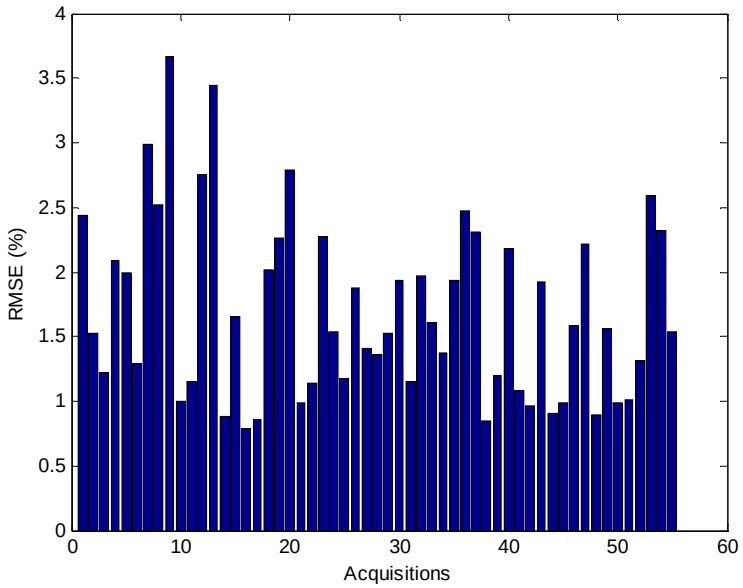

Figure 39 - Graphic representation of the RMSE distribution from each signal to the average waveform.

For the sensor 2 the average RMSE was 1.70% and the standard deviation 0.69%. As can be verified, the results from the two sensors vary and sensor 2 revealed better performance in this test.

This difference between the average relative errors of both sensors is significant and unexpected since the two sensors are identical in all their characteristics. However both obtained values are considered low and do not compromise the probes performance.

4.7-Impulse Response

To determine the Impulse Response of both acoustic sensors of DAP, they were directly excited with a linear sweep from approximately DC frequencies (500mHz) to 2kHz, generated by Agilent 33220A. This is indeed, the most effective approach to determine the impulse response [27].

Computing the Fourier Transform of both, input signal and sensors output signal (*X(jw)* and *Y(jw)*, respectively) the impulse response (IR) of each sensor can be determined taking into account that

$$H(jw) = \frac{Y(jw)}{X(jw)} \quad \textit{(Eq. 3)}$$

and in the time domain

$$IR = h(t) = IFFT(H(jw)) \quad \textit{(Eq. 4)}$$

Figure 40 schematizes the method.

Applying the deconvolution principle, the original input signal of an acquisition can be determined using spectra of the previously calculated IR (*H(jw)*) and of the sensor's output, with

$$X(jw) = \frac{Y(jw)}{H(jw)} \quad \textit{(Eq.5)}$$

and similarly with Eq.4,

$$x(t) = IFFT(X(jw)) \quad \textit{(Eq.6)}$$

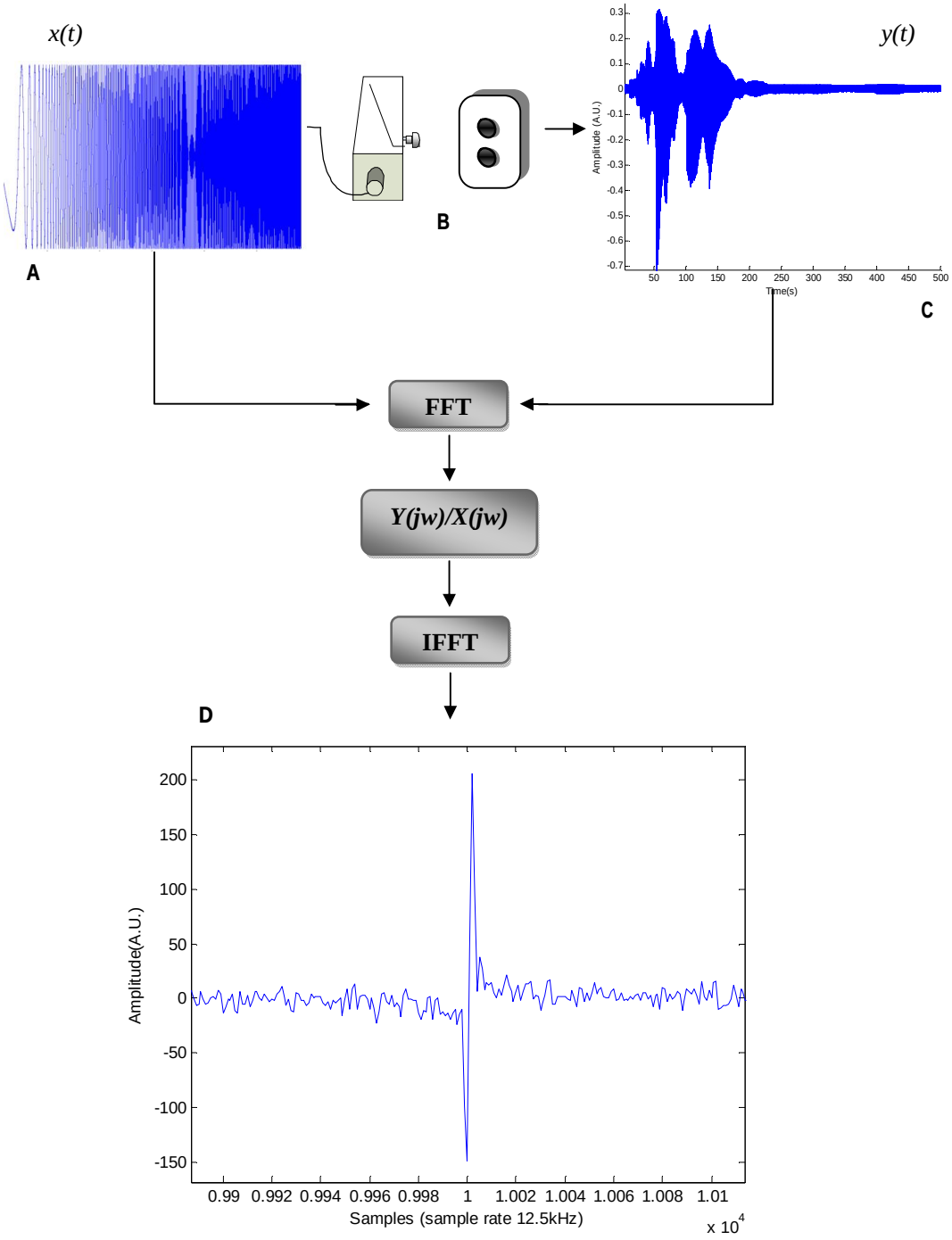

Figure 40- Scheme of the Impulse Response determination method. A - linear sweep; B - actuator exciting the sensor; C- sensor's Frequency Response; D – sensor's Impulse Response.

Both sensors were submitted to this study, and figure 41 depicts the determined Impulse Responses for each of them.

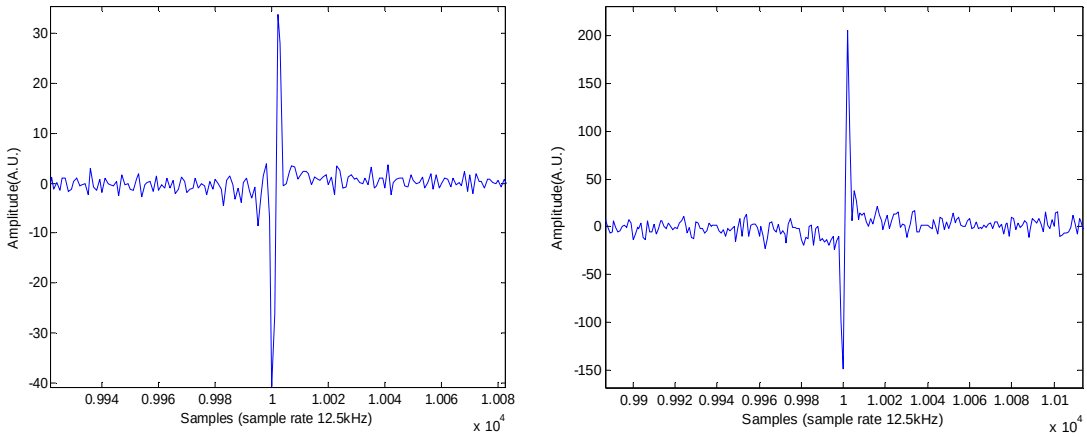

Figure 41 – Sensor 1 impulse response (on the left); sensor 2 impulse response (on the right).

The deconvolution methodology was then applied to some previously acquired signals, and the results compared with the integration method.

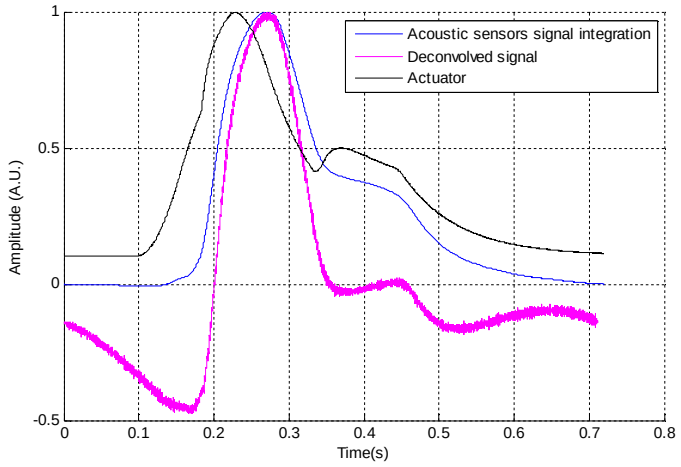

Figure 42 - Application of the deconvolution principle to the sensors signal response to a type A cardiac-like waveform.

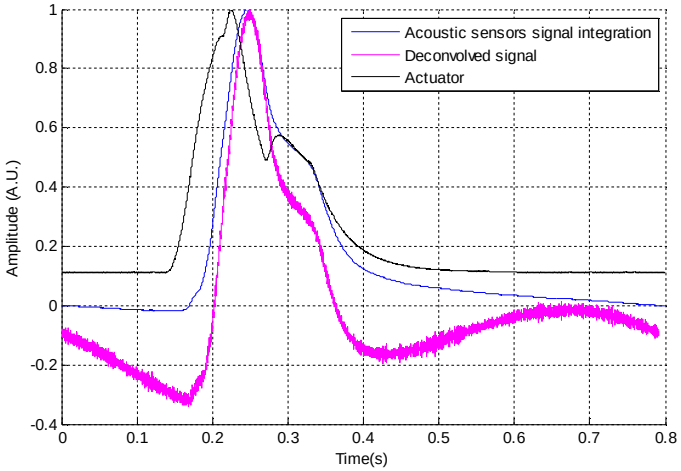

Figure 43 - Application of the deconvolution principle to the sensors signal response to a type B cardiac-like waveform.

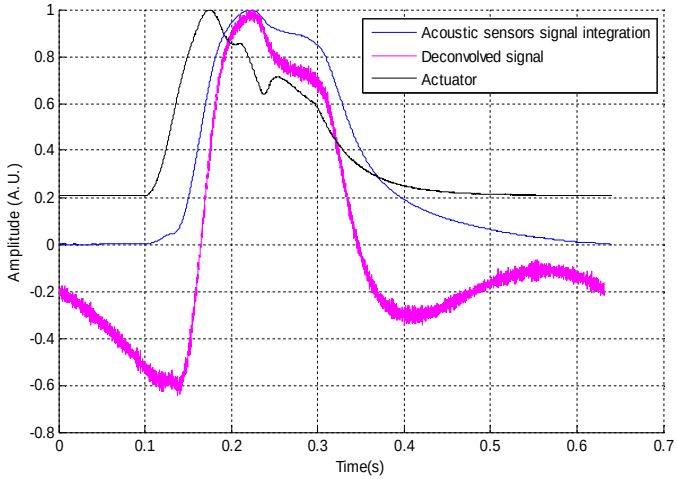

Figure 44 - Application of the deconvolution principle to the sensors signal response to a type C cardiac-like waveform.

It is clear that the integrated and deconvolved signals are similar and as already verified for the integration method, the waveforms resultant from deconvolution do not allow the discrimination of the reflected wave visible on the original waveform, especially on the type B and type C.

However, by the determination of the RMSE for both, signal integration and deconvolution, we can conclude that the methodology with best performance is the integration.

Table 5 - RMS errors for the resultant waveforms of integration and deconvolution algorithms for the reference signal (actuator).

Input waveform	Algorithm	RMSE(%)
Type A	Deconvolution	44.48
	Integration	17.62
Type B	Deconvolution	34.57
	Integration	16.02
Type C	Deconvolution	36.50
	Integration	21.12

4.8- Discussion

The aforementioned tests allowed the preliminary characterization of the double acoustic probe, especially to understand how it responds to some well defined waveform inputs, before acquiring data in human carotids.

Observing the acquired signals we conclude that the acoustic sensors have relatively cleaned signals but which correspond to the input signals differentiation, so an algorithm based on integration or deconvolution has to be applied to recover the original waveform. On the other hand, the comparison between both methods reveal better results for the signals integration which can be explained by inaccuracies in the sensors impulse response determination, given the filtering performed by the sensors themselves, which can exclude potentially important information (lower frequencies).

Regarding to the interface to be used between the sensors and the 'mushroom', we concluded that the best signals were acquired without any kind of interface material. In fact, the clean nature of the acquired signals constitutes a very important advantage. The sensors themselves seem to be good enough (execute some filtration), avoiding the need of more electronic complements and keeping the instrument simple and effective.

About the comparison between the acoustic and PZ sensors, we can conclude that the two signals are very correlated and that the acoustic sensor can provide similar information than the PZ sensors. However, other studies must be performed in the future in order to determine the characteristic points of the acoustic sensors signals, and prove, in an effective way, if the acoustic probe gives at least the same information as the PZ probe.

5. Test Bench System

5.1- Experimental Setup and Methodologies

To accomplish a complete characterization of DAP, it was necessary to perform another set of tests, in a new experiment setup, for the probe's Time Resolution evaluation.

Aiming the emulation of the main arterial pressure wave propagation characteristics in Cardiovascular System, it was implemented a new version of a test bench system previously developed and which has allowed the characterization of other probes and algorithms [27].

Although using a similar experimental setup, the new version used a latex tube instead of the silicon tube, since the last experiments showed a reduced distensibility [27]. The used setup is depicted in Figure 45.

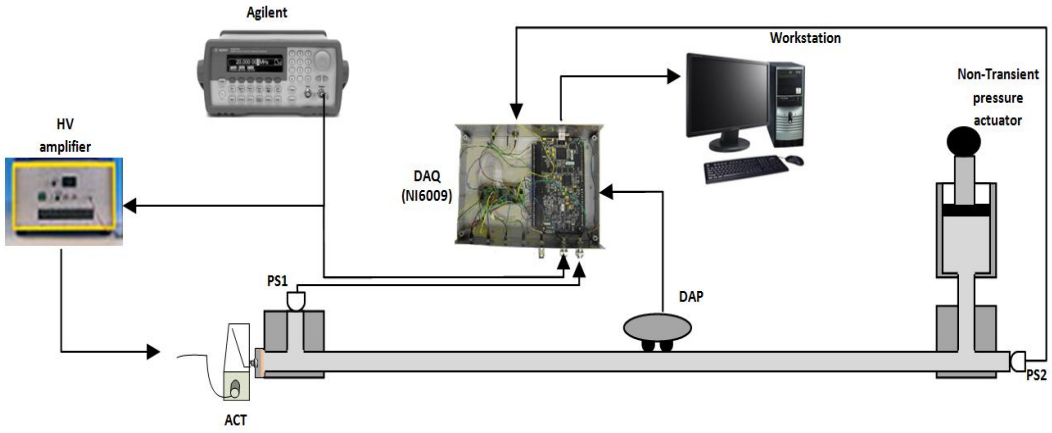

Figure 45 - Test bench system (adapted from [27]).

A 2m latex tube, filled with water was kept under a DC pressure level by a piston on one of its extremities. The opposite extremity ends with a latex membrane, which is excited by the actuator, generating a pressure waveform that propagates along the tube. At both ends of the tube are two pressure sensors (Honeywell S&C-40PC015G1A), one placed transversally (pressure sensor1), and the other longitudinally, to the tube (pressure sensor 2), both connected to two voltmeters (Digital Panel Meter 3-1/2D LCD), allowing the DC pressure monitoring.

As well as the acoustic sensor, the pressure sensors have a differentiating nature. Figure 46 and 47 depict their response to a 100ms Gaussian pressure wave.

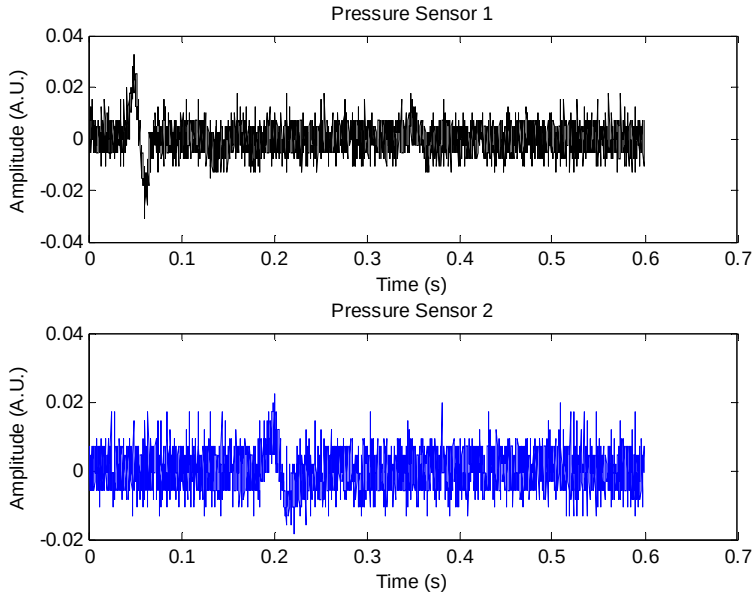

Figure 46 - Pressures sensors signals as response to a Gaussian wave pressure generated by the ACT.

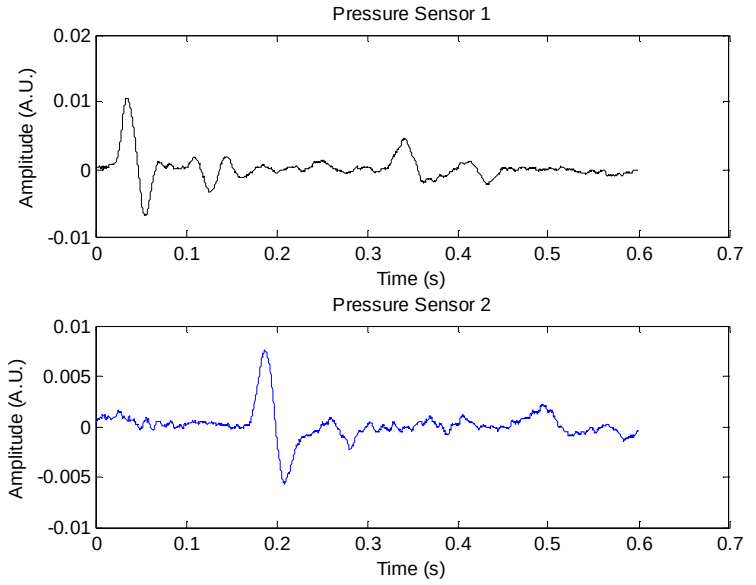

Figure 47 - Pressures sensors signals after the application of a 100 samples Moving Average filter.

5.2 – Algorithms for Time Delay estimation

For the determination of PWV in all the following described experiments, it was necessary to use specific algorithms for the time delay estimation. For this purpose, three algorithms were applied, and their performances were compared [27].

Maximum of Cross-Correlation

This algorithm is based on the determination of the of maxima values of cross-correlation between the ACT signal and the acoustic sensors signals, as well as the pressure sensors signals.

In order to obtain a similar waveform to the signals from both sensors, the ACT signal was double differentiated and then, the indexes of maxima values from the cross-correlations were determined, as time references for the time delay estimation.

Maximum amplitude detection

This approach consists of the peak detection of the acquired signals, and to ensure an accurate identification of the peaks, a 6^{th} degree polynomial fit in the maximum region was applied.

Zero-Crossing point identification

In this algorithm it was applied a linear fit for the determination of the signals indexes correspondent to the zero-crossing, which were used as time references for the time delay determination.

5.3- Test Bench Characterization

To evaluate ability of the system to reproduce the main hemodynamic properties of cardiovascular system two main studies were performed: the analysis of the wave propagation phenomenon along the tube and the relation between the PWV and the DC pressure in the tube.

5.3.1- Wave propagation along the tube

The experiment carried out to accomplish this analysis consisted of using a single acoustic sensor to sense a 100ms width (10Hz) Gaussian pressure wave (since it doesn't present any discontinuities), at every 2cm along the tube. During the execution of this experiment, DC pressure level was kept constant.

In Figure 48 it is depicted the propagation of the pressure waves, where can be easily identified the forward and the reflected waves. In fact, the pressure wave generated by the ACT suffers a first reflection on the tube's end generating a backward wave that will suffer a new reflection at the beginning of the tube, a phenomenon that keeps repeating until the pressure wave dissipation.

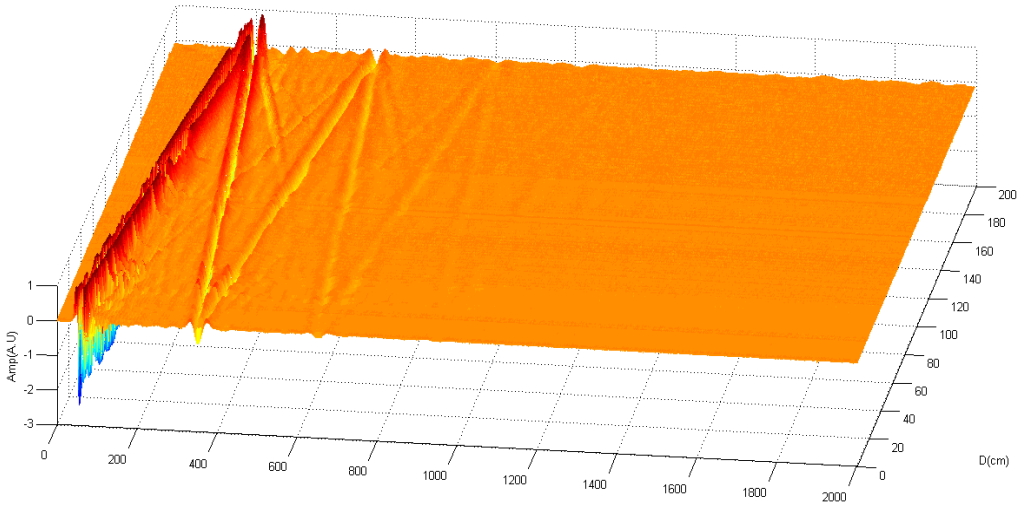

Figure 48 - Propagation of the pressure wave along the tube.

The black circles in Figure 49 result from a peck detection over all signals. Their best-straight-line-fittings (dashed lines) enhance the pattern of the propagation. The PWV was then estimated through the determination of the slopes of those lines. For the forward and backward waves (r1 and r2) the PWV was 13.9m/s. In the same figure is also possible to identify other waves (r1' and r2') with lower velocity (4.61m/s) that seem to correspond to transversal components of the main forward and backward waves.

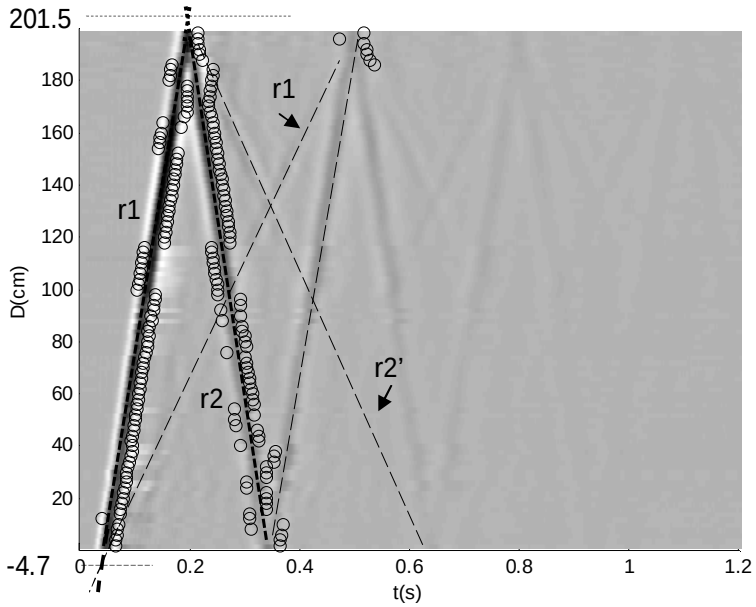

Figure 49- Propagation of the pressure wave along the tube. r1 - Forward wave; r2 - Reflected wave; A, B - Reflection sites.

Figure 50 depicts an example of a single pulse sensed at the beginning of the tube, were the forward wave, and the backward waves are clearly visible.

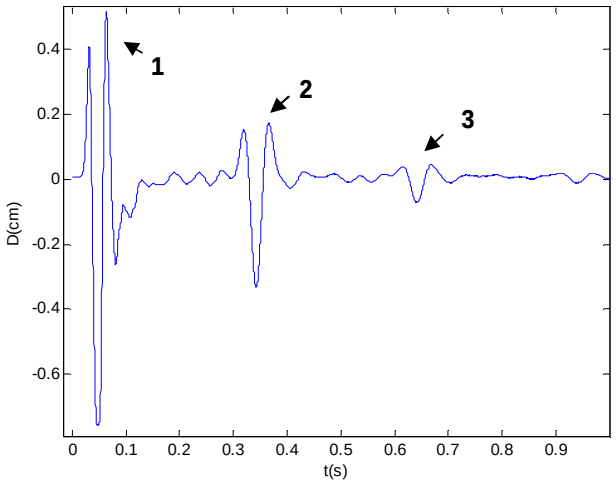

Figure 50 - Propagation of a single impulse. 1- Forward pressures wave; 2 - pressure wave due to a first reflection; 3 – pressure wave due to a second reflection.

In addition to the propagating velocity, other conclusions, particularly related to the system geometry, can be taken. With the equations determined for the straight lines found for the propagating pattern were also estimated the interception points, which coincide approximately with the physical reflection sites on the tube: 4.7 cm before the beginning of the tube and 202 cm, after its end.

For the execution of this experiment it was kept a constant DC pressure level. However, the influence of the pressure inside the tube in the values of PWV was also studied, as explained in the next section.

5.3.2 – Influence of DC pressure level on the PWV measured on the tube

For this study, PWV was estimated for several different values of DC pressure, using the general relation (velocity=distance/time). The ACT reproduced a 100ms width Gaussian pressure wave which was sensed by the two pressure sensors placed at both ends of the tube (2.108m away). The time delay between the acquired signals was estimated by the three algorithms, described in section 5.2.

It is known by the Bramwell-Hill equation [13] that PWV is higher for higher values of pressure (ρ_b- blood density, A - cross-sectional area of the artery in the diastolic phase, P-pressure):

$$PWV = \sqrt{\frac{\Delta P * A}{\rho_b \Delta A}} \quad \textit{(Eq. 7)}$$

However, the results determined with this experiment shown a different relation that was confirmed for four independent tests, and for all the three time-delay estimation algorithms. All determined PWV values can be analyzed in Appendix A and in the following figure are represented the average values obtained with all tests performed and with all algorithms.

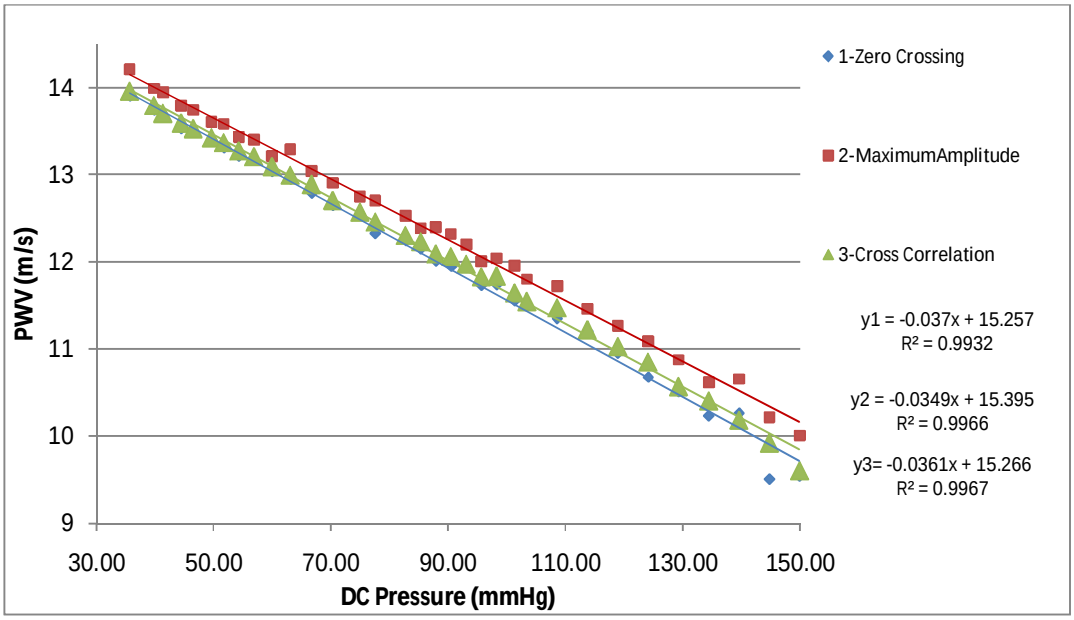

Figure 51 - PWV values for a variable DC level pressure.

Indeed, for all tests the results showed a decreased PWV with the increase in DC pressure, revealing a very good agreement with the linear trend lines.

In order to understand this phenomenon, it was studied the influence of the higher values of the latex tube distensibility and compliance[1] in the velocity values (see figure 52).

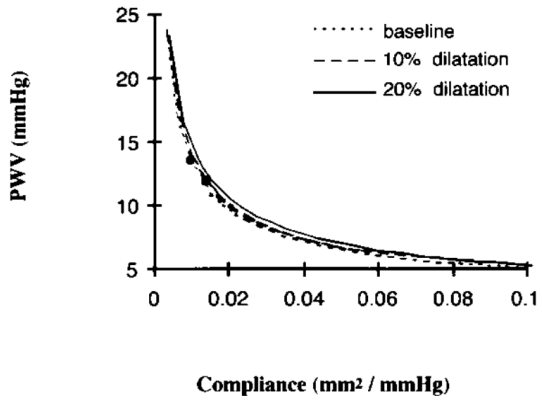

Figure 52- Theoretical curve of compliance versus PWV at 95 mm Hg pressure [54].

[1] Compliance – is an important parameter that traduces the elastic properties of the materials, corresponding to the quotient between the volume and pressure variations of the material and in this context, an important parameter for the evaluation of the arterial mechanical properties.

In fact, since the latex tube has a higher distensibility than the silicone tube, used in previous experiments, it is possible that a greater increasing of the tube's diameter can compensate the increasing pressure in the tube, leading to a decreasing in the PWV values.

In order to prove this hypothesis, were carried out three measurements of the tube's diameter, for all values of pressure used in the main procedure, using a digital paquimeter. The procedure was repeated for four times and the average values for each pressure are depicted in the following graphic:

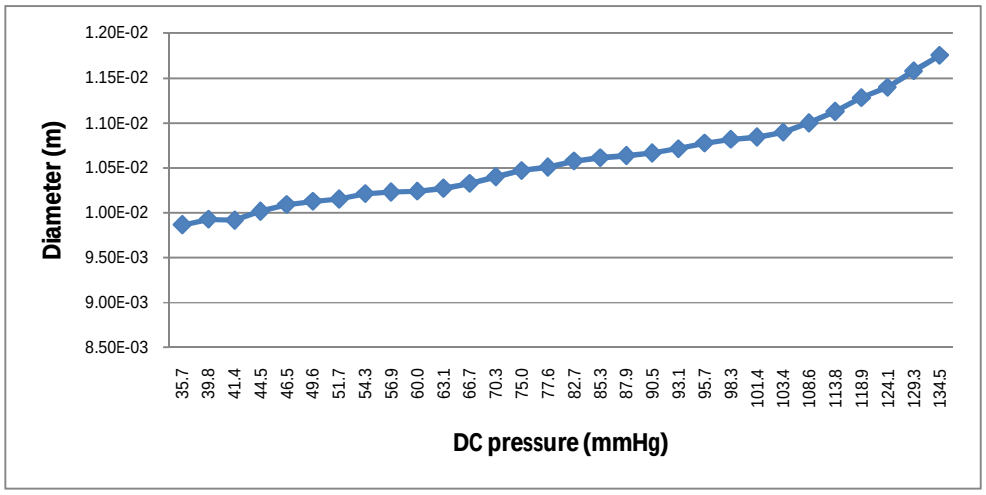

Figure 53 - tubes diameter variation with de DC pressure variation.

The increasing on the diameter with the increasing pressure is clearly visible. These values were then used to determine PWV through two different equations.

The first equation used was derived in [25] and relates PWV with distensibility:

$$PWV = \frac{1}{\sqrt{\rho D}} \qquad (Eq. 8)$$

where ρ is the density of blood (in this case, the density of water, which is $\rho = 1 g/cm^3$) and D the arterial (latex tube) distensibility. Distensibility is, in turn, given by

$$D = \frac{\Delta A}{A_d \Delta p} \qquad (Eq\ 9)$$

where ΔA is the pulse cross-sectional area corresponding to the difference between the cross-sectional area during the systole (A_s) and during diastole (A_d)ditermined through the diameter measures:

$$\Delta A = A_s - A_d \quad (Eq\ 10)$$

and Δp, the pulse pressure – the difference between pressure during systole (p_s) and during diastole (p_d):

$$\Delta p = p_s - p_d \quad (Eq\ 11)$$

As corresponding to diastole values (tube's diameter and pressure) were considered the ones measured with the minimum DC pressure, when any force was being exerted on the piston. The values corresponding to systole were the values obtained with the increase in pressure inside the tube.

The second expression used corresponds to *Eq 1* (section 2.3) and relates PWV with Young's module (*E*) where

$$E = \frac{d_d^2}{h\frac{\Delta d}{\Delta p}} \quad (Eq\ 12)$$

with d_d the tube's diameter for diastole and Δd the diameters variation between systole and diastole.

All values measured and calculated in these procedures can be analyzed in Appendix A, and the average values obtained for both methodologies, for the four testes performed are depicted in the figure 54.

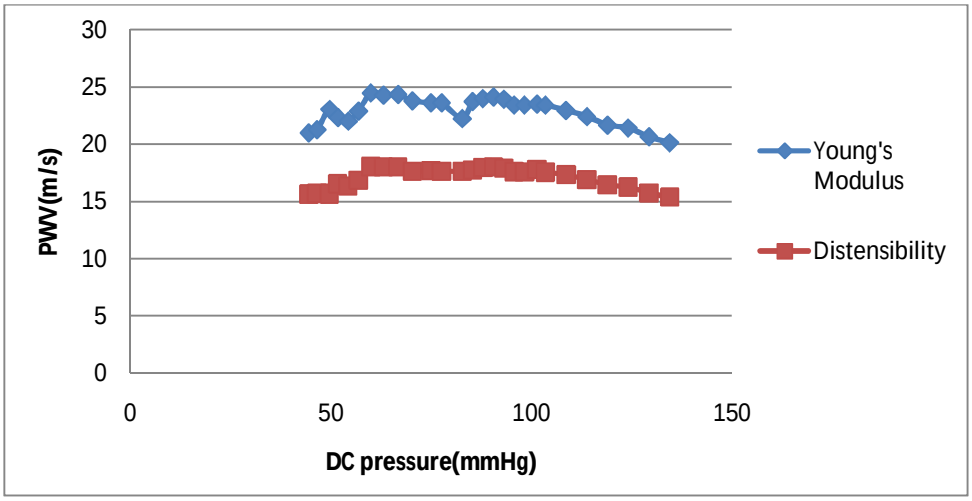

Figure 54 - PWV calculated as a function of tube's distensibility and Young's Module.

As can be seen the PWV distribution for pressure values is similar in both graphics but the velocities calculated with the Young's Module equation are higher than the values obtained with the distensibility equation.

However, even using the diameter variations of the latex tube in the PWV calculation, it does not result in an increase of its values. Despite of the small increase in the velocity for the lower pressure values, this trend is not true for higher values. In fact, despite of the lower decrease, comparing to the verified in figure 51, it is still visible.

The study is then considered inconclusive and other procedures must be carried out to better understand the phenomena that give rise to these results.

5.4 - Time Resolution Evaluation

One of the main goals of the DAP characterization was the determination of its temporal resolution, an important parameter to take into account for PWV estimation. In order to accomplish this study two main experiments were carried out: the estimation of PWV with two uncoupled sensors for successively smaller distances, and with a double probe in 24 positions along the latex tube.

Due to data processing routines, it was necessary to ensure a constant number of samples in each acquisition, so a synchronism between the beginning of the LabView recording and the Agilent's trigger was implemented.

5.4.1 – PWV for two uncoupled sensors and a variable separating distance

For this test were used two uncoupled acoustic sensors, one of which was kept fixed at 50cm position, while the other one was moving from 100cm position to 54cm position by 2cm intervals. For each position was driven a Gaussian waveform with 100ms (10Hz) width, and PWV was estimated through all the previously mentioned algorithms.

The test was repeated four times, for a constant DC pressure of 0.86 psi (44.5 mmHg).

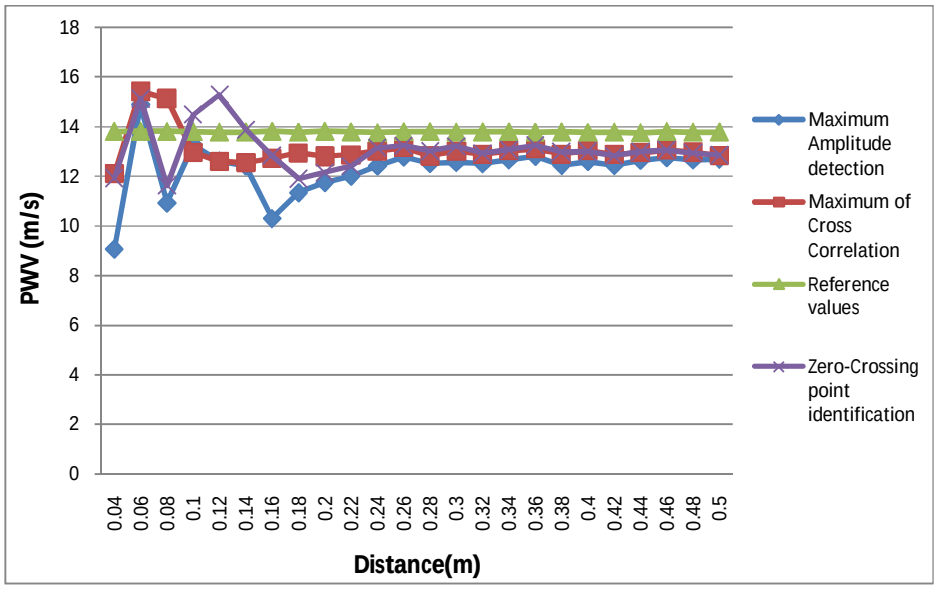

Figure 55 - Average values of the PWV obtained for three different algorithms (each value corresponds to an average value of five tests).

Graphic in figure 55 shows the average PWV values obtained with the three mentioned algorithms, for five independent tests. Reference values, on the other hand, were determined as the average values of all tests performed. All determined values, for all acquisitions performed are depicted on Appendix B.

The relative errors for each distance between the sensors (D) were also determined and can be analyzed in the graphic of figure 56.

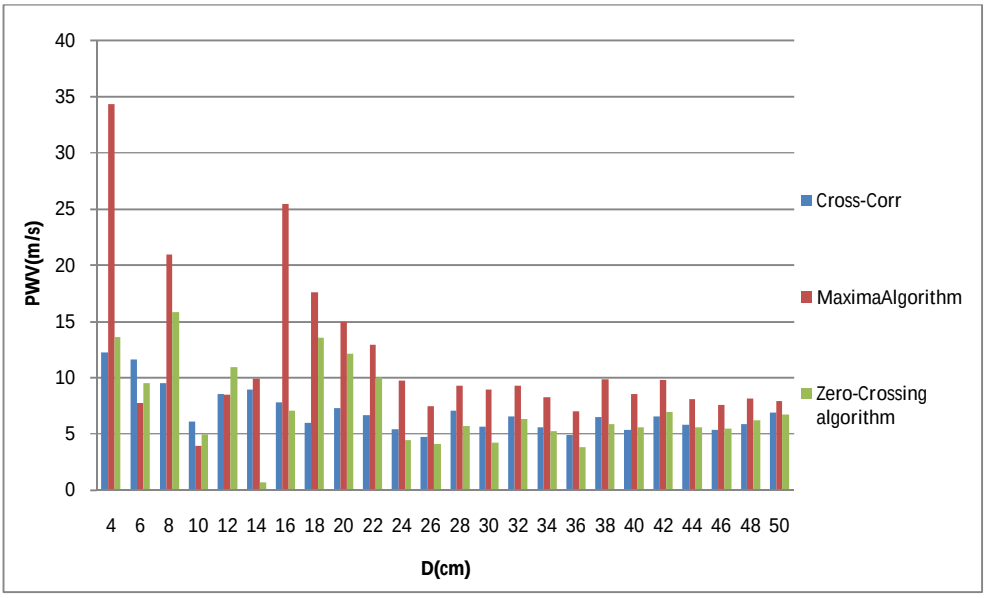

Figure 56 - Relative errors of the PWV values calculated with three different algorithms.

For this experiment, the Maximum Cross-Correlation and the Zero-Cross point identification algorithms had the lower relative errors, yet with average values of 6.9% and 7.3%, respectively. Regarding to Maximum Amplitude algorithm, the average error was 11.5%.

We can also verify that for lower distances, the relative error increases, for all algorithms and more significantly for the Maximum Amplitude approach. For the cross-correlation method the bigger increase correspond to distances lower than 8cm, but for the other two algorithms that distribution is not so clear.

5.4.2 – Dispersion of PWV measurements along the tube using a DAP

This experiment was carried out with a DAP with two sensors 2.03cm apart, for PWV estimation on 24 positions along the tube.

For this purpose, a burst of 10 Gaussian waves with 400ms width was driven (figure 57), for each position, and the correspondents PWV were estimated, with the cross-correlation algorithm since it had the best performance in the tests reported in the previous section.

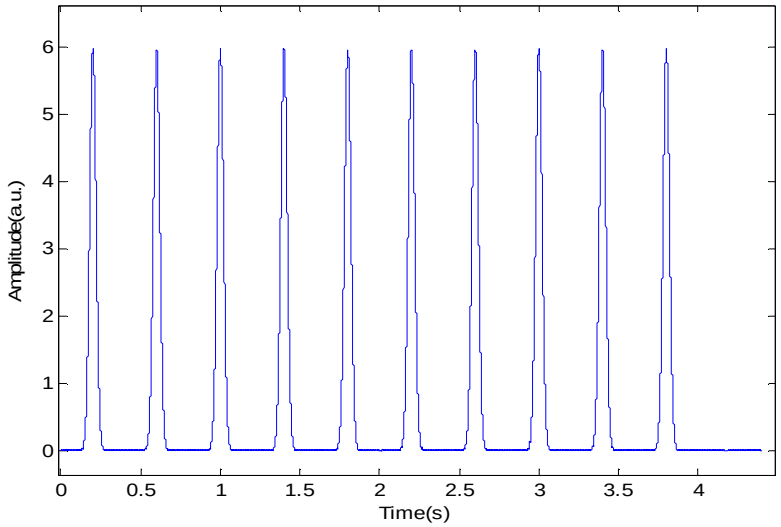

Figure 57 - Burst of 10 Gaussian pulses.

5.4.2.1 - Signal Segmentation

For the PWV determination relative to each Gaussian pulse, it was necessary the implementation of a segmentation routine.

The used method consisted on the detection of the minimum value of the second pressure sensor signal, using as 'cutting' point the correspondent to 300 points after the index of the detected minimum. The following figure depicts an example of the obtained segments.

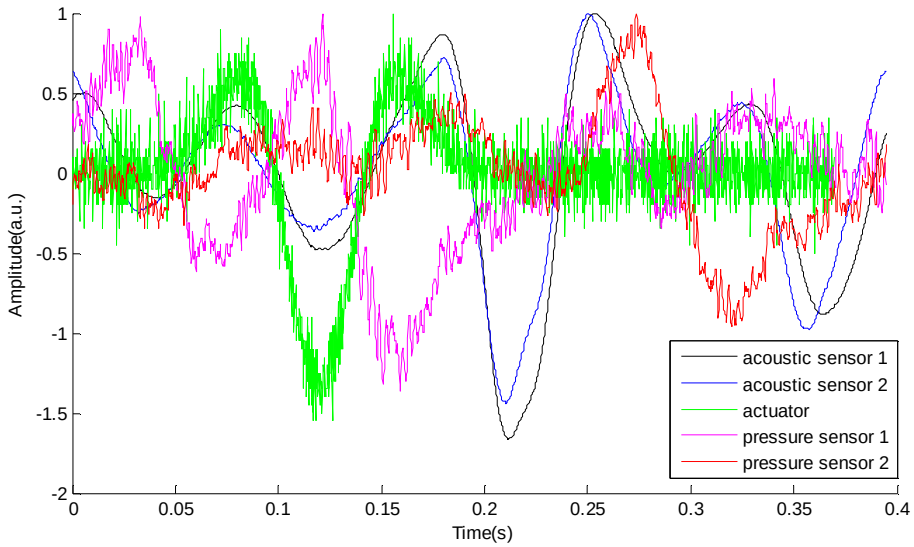

Figure 58- One of the ten segments obtained after the application of the signal segmentation routine.

In addition to the intrinsic differentiating nature of the acoustic sensors, in the acquisitions performed in this test bench, the recorded signals arise as a double differentiation of the input signal. Thus, in order to apply the cross-correlation algorithm a double differentiation of the actuator signal was computed. Despite the noisy nature of the resulted signal (in green in the previous figure), the application of more filtration origins alterations in the signals shape that would introduce significant errors in the final results.

5.4.2.2 – Results

Average values of PWV for each position were determined as well as the reference values, again determined with the pressure sensors.

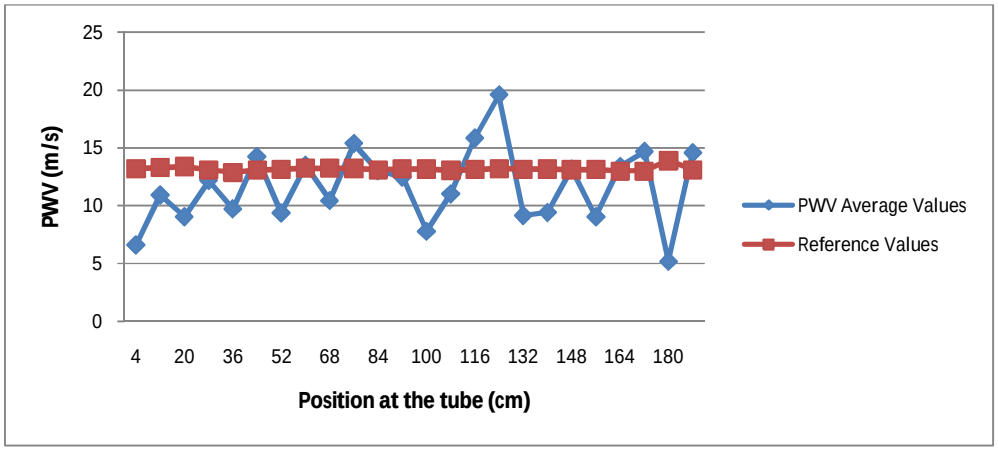

Figure 59 - Average values of the ten segments, for the four tests performed for each position.

The PWV average values for each burst of pulses were calculated with the cross-correlation algorithm since it had showed a better performance in the previous test.

The average value of the PW velocities presented in the previous graphic is 11.65m/s with a standard deviation of 3.28m/s and thus, the dispersion of the results is quite high. On the other hand, the average value of the references is 13.17±0.18m/s (low dispersion). The relative error is, then, 11.52% which is somewhat elevated.

In an attempt to improve the results, another methodology was applied in the PWV determination consisting on the determination of the segment with the best correlation between the signals of the two sensors.

The graphic presented below shows the velocity values determined for the best segment of the 10 pulses.

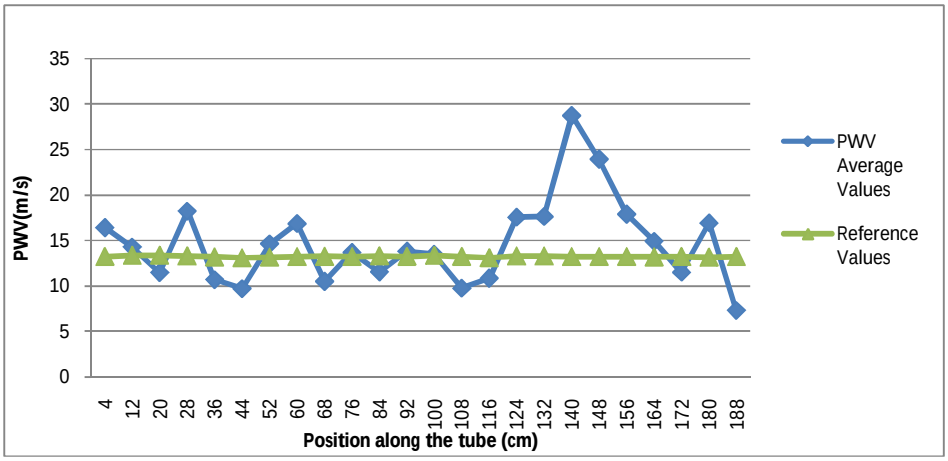

Figure 60 - Average values of the PWV correspondent to the segment with higher correlation between the signals of both sensors, for each position along the tube.

In this case, the average value of the PW velocities was 14.68±4.76m/s and for the references 13.24±0.07m/s. The relative error was 10.92%, lower than the error estimated for the previous method and for this reason, this was the PWV used for the Temporal Resolution determination, yielding a result of 0.0015 s.

5.6 - Discussion

The test bench system had allowed completing the double probe's characterization especially its temporal resolution determination. We had concluded that the velocities within the tube are of the order of 14m/s and since the sensors in the used double probe were 2cm apart, the minimum time delay to distinguish two points is approximately 2ms (0.0015 s).

The temporal resolution determination included two different tests. In the first test performed – the PWV determination for increasingly smaller distances between sensors – has proved, similarly to [27] that for lower distances, the relative errors to the reference values are higher and that the cross-correlation algorithm is the best method for the velocities determination, with a relative error of 6.9%.

The second test revealed no such positive results, with an average relative error of 10.92%. For an average value of 14.68m/s, the standard deviation (4.76m/s) is high. A possible explanation for this discrepancy on the velocities values may be related to the influence of the reflected waves on the signals shape, which can introduce errors in the time delay estimation.

6. Clinical Trials

After all the tests performed for the probe's characterization, were accomplished some acquisitions, during four weeks, in a small number of volunteers, in order to analyse the waveform and PWV variability for each subject, but also among all the subjects.

6.1 –Methodologies

Due to time limitations, only six volunteers, without any known cardiovascular disease, have participated in this study, for three weeks, once a week, and always in the afternoon.

All acquisitions were carried out with the subjects seated, while an operator acquired the signals for both, right and left carotids, one at a time. In order to analyse the influence of the operator's technique and experience on the results repeatability, the procedure was repeated for two different operators (for the two last weeks of acquisitions).

The acquisitions were performed with Audacity® at a sample rate of 44100Hz, during not less than eight to ten cardiac cycles.

6.2- Data Processing

6.2.1– Signal Segmentation

Since each acquisition includes height to ten cardiac cycles, all acquired signals were segmented with a different algorithm from the one used in section 5.4.2, given the differences between the waveforms obtained from the human carotid artery, and the ones acquired in test bench system.

The first step consists on the signal minima detection, and then the application of a threshold to select just the first minimum of each cycle, where the signal is 'cut' (Figure 61).

The threshold application intended to guarantee that the used minima were the first ones, from each cardiac cycle, when second minima were also detected in previous step.

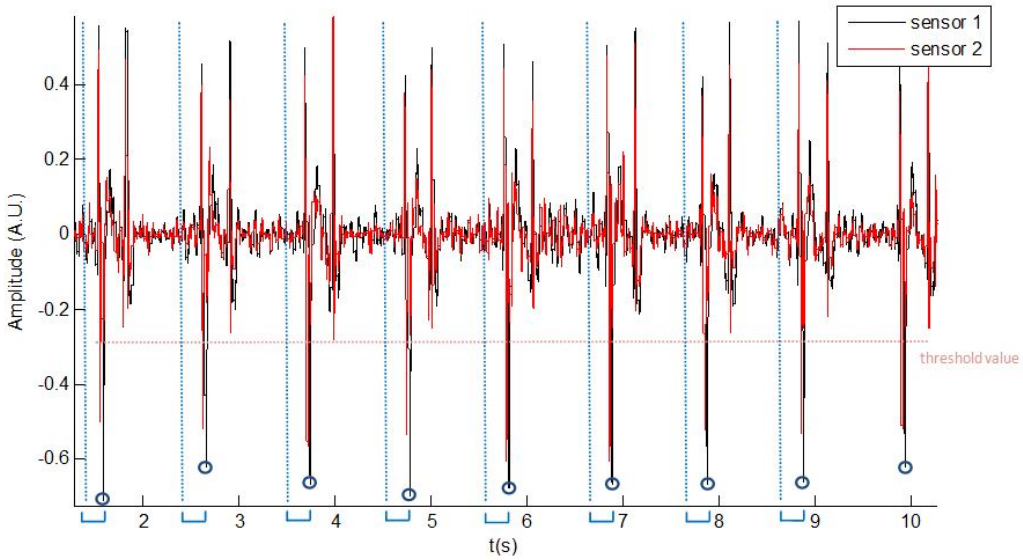

Figure 61 - Signal segmentation into the cardiac cycles, having as reference the first minimum of sensor 1; the beginning of each segment is signalized by the blue dashed lines, and the threshold value, with pink dashed line.

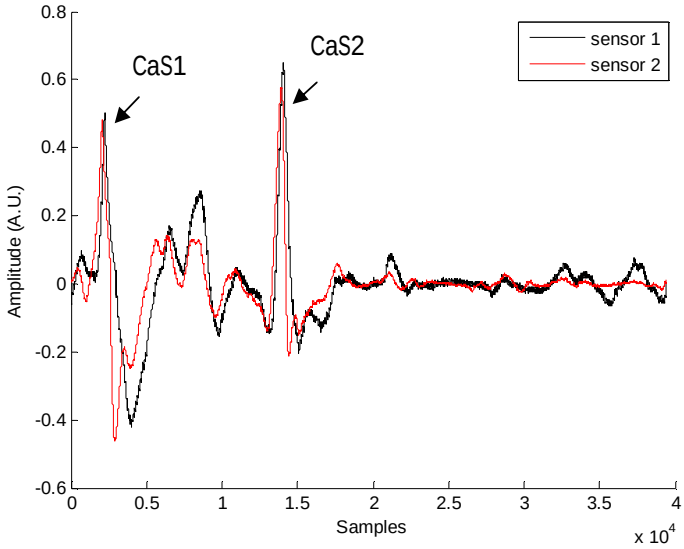

Figure 62 - Portion of the acquired signal, resulted from the signal segmentation. CaS1 - first carotid sound; CaS2 - second carotid sound.

Figure 62 corresponds to a segment resulted from the application of the signal segmentation algorithm and first and second 'cardiac' sounds are clearly visible.

6.2.2 – Algorithms for Time Delay estimation

For the determination of the PWV of each segment, were applied the algorithms with worst and best performance in the test bench system, in order to analyze their performances when applied in human carotid signals – the maximum amplitude detection and the maximum cross-correlation method.

6.2.2.1 – Maximum amplitude detection

After the application of the segmentation algorithm, all segments were filtered with a 100 samples Moving Average filter, for peak detection, this time the maximum values, which will finally be used for the time delay estimation.

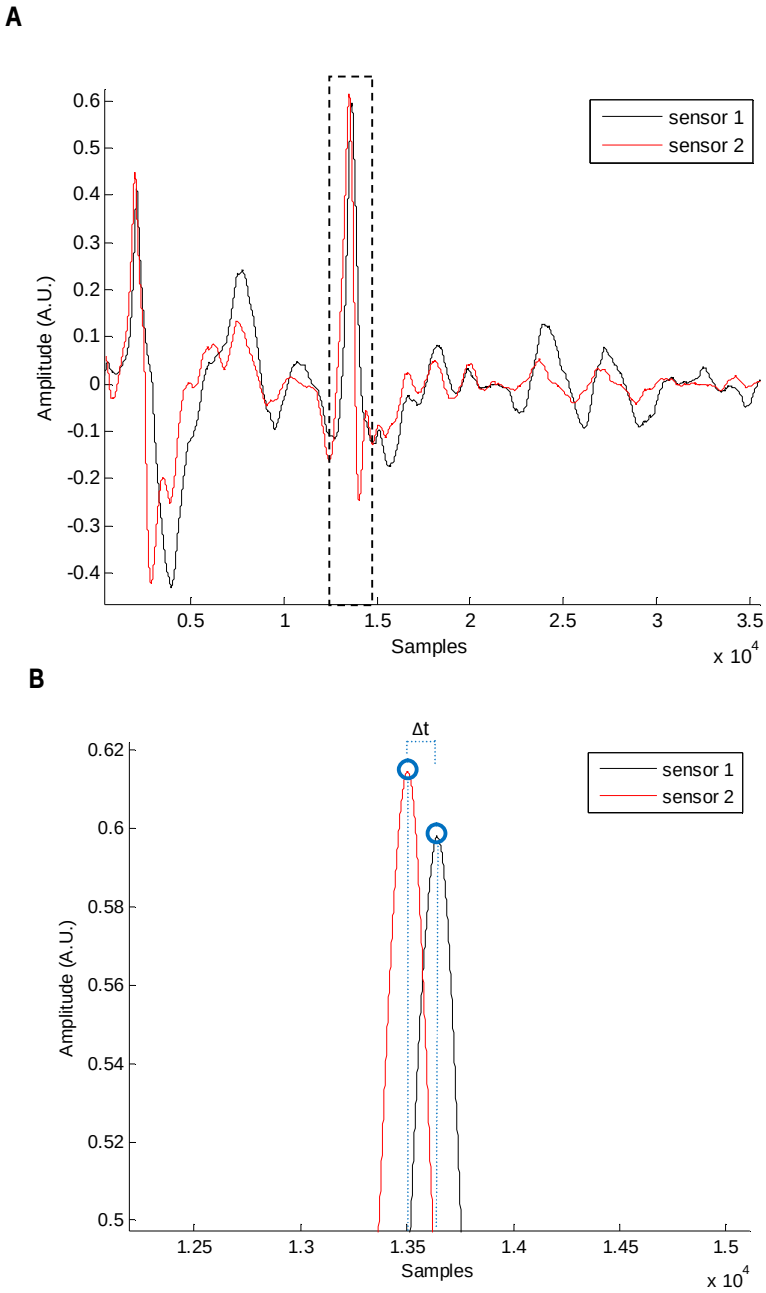

Figure 63 - Maximum amplitude detection for each segment, to estimate the time delay. A- filtered segment; B – the detected peaks and time delay between them.

Since there is the possibility of, for one sensor the peak being detected be the first, and for the other the second, after the sensor 1 peak detection, only a fragment in a defined interval around the detected peak is used for the search of the sensor 2 peak detection (Figure 63 A). This way we can avoid some mistakes on the time delay estimation.

The selected indexes are then converted to time scale and the PWV is finally determined.

6.2.2.2 – Maximum Cross-Correlation

The algorithm applied in these signals had to be changed relatively to the algorithm used in the test bench system, which used the actuator's signal as reference for the time delay estimation. In this case, the cross-correlation was computed only between the signals of the two sensors, and the index of the maximum correlation was determined, as the time delay between both signals, using the Matlab function *xcorr*.

6.2.3 – Carotid Sounds and LVET estimation

As suggested by Hasegawa *et al*. (see figure 14), the LVET was estimated through the determination of the time interval between the first and second sounds of the carotid artery. In fact, the correlation between heart and carotid sounds is confirmed by the higher amplitude of the second peak (second sound). Indeed, since the flow from the ventricles is more forceful than the flow from the atria, S2 is usually louder than S1 [34] which is verified in the majority of the recorded signals.

Therefore, the algorithm consists simply in the peak detection and the calculation of the time interval between them.

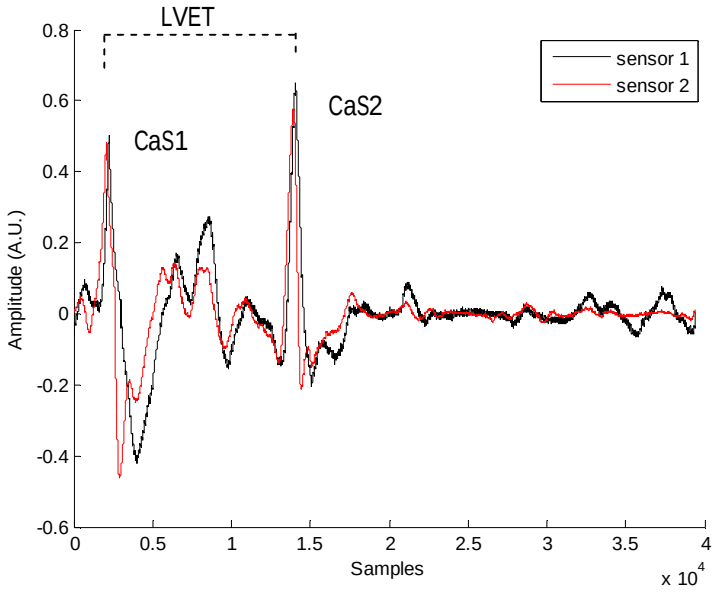

Figure 64 - Scheme of the basic principle of LVET determination.

On the other hand, since LVET varies inversely with the heart rate (the length of the cardiac cycle) [49], in addition to the ejection time it was also determined the heart rate for each acquisition, simply by counting the number of cycles (by peak detection) for the duration of the signal recorded.

6.3- Results

6.3.1 – Waveforms

Most signals recorded during the 'clinical' data collection have a similar shape to the waveform presented in the previous figure. For a more detailed waveform analyses, were computed their integration and deconvolution. Some examples of the waveforms recorded on the 'clinical' trials are depicted below.

Table 6 - Comparison between integration and deconvolution computed in carotid artery signals of 3 of the 6 individuals.

Integration	Deconvolution
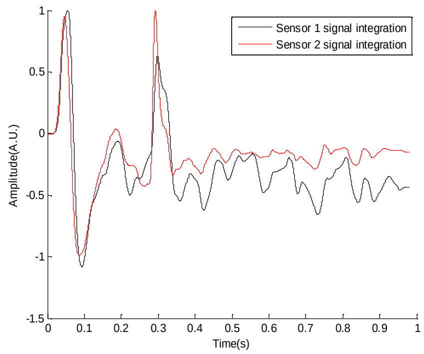	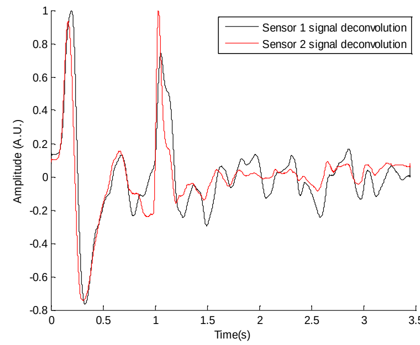
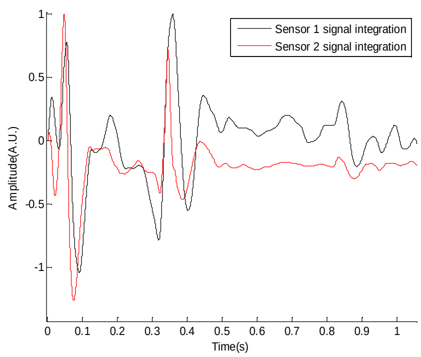	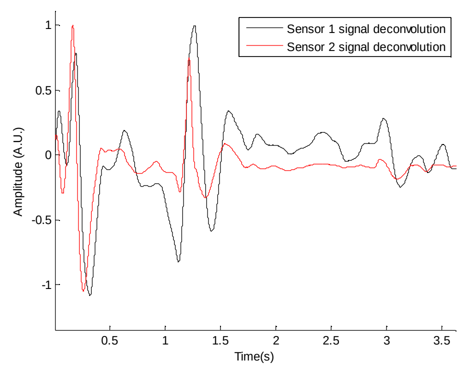
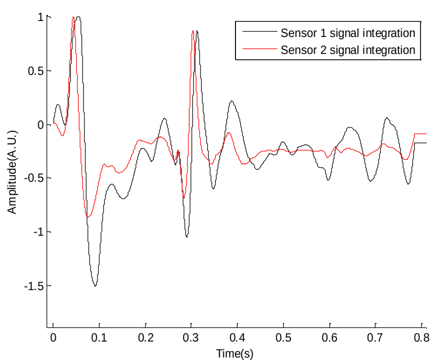	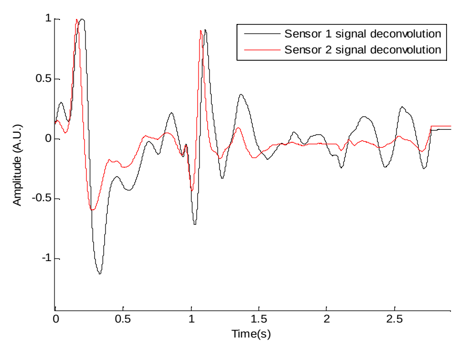

As can be verified in the examples presented in table 6, the waveforms obtained from the integration and deconvolution approaches are very similar. On the other hand, we can also verify the similarity between waveforms from different subjects, although with small differences between them.

6.3.2 – PWV

All values obtained for each acquisition are depicted in Appendix C. The following tables present the mean values obtained for each individual, and for each operator, and some comparative analysis is made.

Table 7 - Mean PWV values obtained for the acquisitions performed for Operator 1; two different algorithms were used: Maximum Amplitude Detection (MAD) and Maximum Cross-Correlation (MCC), for both left carotid (LC) and right carotid (RC).

Week	1st				2nd				3rd			
Artery	LC		RC		LC		RC		LC		RC	
Subject	MAD	MCC	MAD	MCC	MAD	MCC	MAD	MCC	MAD	MCC	MAD	MCC
1	2.50± 0.23	3.34± 0.23	3.45± 1.80	3.31± 0.62	1.75 ± 0.15	3.77± 1.06	2.57± 0.25	2.35± 0.30	3.42± 1.39	2.24± 0.14	3.84± 1.58	1.96± 0.22
2	4.98± 2.28	3.24± 0.37	2.40± 0.70	5.30± 1.24	17.74± 24.89	1.44± 0.21	4.17± 2.93	1.13± 0.13	3.26± 1.19	0.57± 0.06	3.67± 0.52	3.64± 0.84
3	9.13± 1.83	*	3.84± 0.89	1.89± 0.11	2.15± 0.32	1.23± 0.13	4.31± 0.99	0.83± 0.05	3.86± 0.77	10.65± 3.61	1.91± 0.50	1.27± 0.10
4	3.24± 1.26	2.30± 0.18	13.37± 20.85	3.54± 0.27	2.27± 0.32	1.58± 0.09	9.32± 2.88	11.89± 10.81	4.18± 3.44	2.58± 0.22	9.32± 6.43	2.86± 0.35
5	3.43± 1.56	2.28± 0.23	2.74± 0.56	2.60± 1.02	2.00± 0.18	1.64± 0.11	2.81± 0.53	1.31± 0.09	3.23± 0.85	3.04± 0.28	5.18± 1.80	3.74± 1.11
6	3.64± 0.58	1.51± 0.23	4.94± 1.25	2.76± 0.53	3.91± 1.94	0.52± 0.05	5.90± 2.61	2.46± 0.09	4.13± 1.08	2.77± 0.15	8.26± 5.50	1.18± 0.76
Variance ($\sqrt{m/s}$)	5.83	0.58	17.13	1.36	39.75	1.20	6.25	18.05	0.18	12.55	8.23	1.29

* These values were excluded of the analysis since they were not possible values in physiological conditions

Table 8 - Mean PWV values (m/s) obtained for the acquisitions performed for Operator 2; two different algorithms were used: Maximum Amplitude Detection (MAD) and Maximum Cross-Correlation (MCC), for both left carotid (LC) and right carotid (RC).

Week	2nd				3rd			
Artery	LC		RC		LC		RC	
Subject	MAD	MCC	MAD	MCC	MAD	MCC	MAD	MCC
1	2.16± 0.27	1.05 ± 0.21	2.29± 0.14	2.29± 0.28	4.09± 1.23	*	1.85± 0.10	*
2	2.11± 0.13	1.22± 0.08	5.19± 1.33	3.49± 0.64	2.97± 0.36	2.49± 0.76	3.21± 0.69	5.19± 0.38
3	7.48± 2.32	1.42± 0.11	2.55± 0.85	3.38± 1.11	5.66± 0.69	6.16± 2.33	2.17± 0.13	1.92± 0.12
6	2.42± 0.43	0.50± 0.04	2.20 ± 0.35	2.48± 0.10	*	2.78 ± 0.14	2.46± 0.15	1.38± 0.79
Variance ($\sqrt{m/s}$)	6.90	0.15	2.04	0.37	1.82	4.16	0.34	4.25

* These values were excluded of the analysis since they were not possible values in physiological conditions

By the analysis of the Tables 7 and 8 (and although no measurements were made with no reference equipment) we can verify that the mean values obtained for each subject are somewhat lower than the expected, considering the range of normal values, between 4m/s and 8m/s [3]. These deviations occur for the acquisitions of both operators and may be explained by some inaccuracies on the time delay estimations, which are very dependent on the waveform of the recorded signals.

Comparing the two algorithms used, the maximum cross-correlation algorithm revealed lower variance values than those obtained for the maximum amplitude detection. Indeed, in agreement with the already verified in section 5.4, the algorithm that reveals a higher consistency is the cross-correlation algorithm.

Inter-Operator repeatability

Table 9 - Comparison between the results obtained by the two operators on the last two weeks of acquisitions, for left carotid (all velocity values in m/s).

	Left Carotid					
	2nd week			3rd week		
Subject	Operator 1	Operator 2	Variance	Operator 1	Operator 2	Variance($\sqrt{m/s}$)
1	3.77	2.16	1.28	2.24	64.97	1967.69
2	1.44	2.11	0.22	0.57	2.49	1.85
3	1.23	7.48	19.53	10.65	6.16	10.06
6	0.52	2.42	1.81	2.77	2.78	0.00

Table 10 - Comparison between the results obtained by the two operators on the last two weeks of acquisitions, for right carotid (all velocity values in m/s).

	Right Carotid					
	2nd week			3rd week		
Subject	Operator 1	Operator 2	Variance	Operator 1	Operator 2	Variance($\sqrt{m/s}$)
1	2.35	2.29	0.00	1.96	15.92	97.48
2	1.13	3.49	2.79	3.64	5.19	1.20
3	0.83	3.38	3.25	1.27	1.92	0.22
6	2.46	2.48	0.00	1.18	1.38	0.02

Despite the limited data available, these results suggest that the operators' technique in the acquisition execution may influence the final results by being or not able to acquire a good signal. Indeed, for the same individual variance values reach in some cases very high values, reflecting perhaps the bad signals acquired by one or both operators.

In fact, some bad signals have been selected for processing by mistake. During the acquisitions, some signals appeared to show good correlation between both sensors, however, when being processed, reveal to be wrongly acquired and lead to some impossible results in PWV determinations. Due to logistical restrictions was not possible to repeat them later.

6.3.3 - LVET

Despite the simplicity of the used algorithm for their estimation, the determined LVET values turned out very consistent and close to the expected, considering the subjects heart rate.

Indeed, according to figure 16, the presented LVE times are generally lower than normal mean values, for the correspondent heart rates. Nevertheless, giving the low intra-subject variance (see Appendix C) and the lower differences for the 'expected' times, these results are considered very positive, and it is proved that this is a very relevant and pertinent parameter to take into account for future work. The average values of the obtained LVET for each cardiac cycle, of each individual (for the two operators' acquisitions) are presented in the following tables.

Table 11 - LVET values (and HR) of the acquisitions performed by Operator 1 (LC – left carotid, RC-right carotid).

	1st week				2nd week				3rd week			
	LC		RC		LC		RC		LC		RC	
Subject	LVET(s)	HR (b/min)	LVET(s)	HR(b/min)	LVET(s)	HR(b/min)	LVET(s)	HR(b/min)	LVET(s)	HR(b/min)	LVET(s)	HR(b/min)
1	0.26	64.29	0.29	62.10	0.26	79.17	0.27	71.97	0.14	78.91	0.26	76.82
2	0.29	56.50	0.45	56.68	0.28	64.39	0.30	60.34	0.29	61.33	0.27	70.46
3	0.12	81.92	0.25	82.24	0.24	88.89	0.25	89.91	0.27	82.97	0.28	73.41
4	0.28	73.01	0.23	68.03	0.28	77.20	0.30	72.07	0.28	74.78	0.28	74.82
5	0.26	67.42	0.28	66.22	0.28	74.24	0.28	71.09	0.28	80.00	0.28	71.38
6	0.24	83.80	0.24	87.94	0.25	72.14	0.26	67.03	0.26	77.33	0.26	79.14

Table 12 - LVET values (and HR) of the acquisitions performed by Operator 2.

	2nd week				3rd week			
	LC		RC		LC		RC	
Subject	LVET(s)	HR(b/min)	LVET(s)	HR(b/min)	LVET(s)	HR(b/min)	LVET(s)	HR(b/min)
1	0.25	73.33	0.27	73.37	0.28	70.67	0.27	72.46
2	0.29	53.46	0.28	53.50	0.28	60.35	0.28	62.05
3	0.26	77.37	0.23	83.18	0.27	77.64	0.27	87.20
6	0.25	76.58	0.37	75.19	0.26	80.63	0.26	80.17

6.4 – Discussion

Despite the small amount of analyzed data, it was possible to draw some conclusions regarding the acquisitions carried out.

Since the normal PWV values in the carotid artery vary from 4 to 5 m/s, it is clear that the majority of values resulted from these tests are below that range. Nevertheless, the obtained values for the PWV can be considered close to the real ones.

Two different algorithms have been applied and similarly with the results from the test bench system, the algorithm that has demonstrated a higher consistency, with lower variance values, was the cross-correlation algorithm. However, for both algorithms, was sometimes necessary to do some adjustments for the analysis of different signals. This procedure must be avoided and corrected, for the process total automation and application on larger databases.

The considerable differences and high variance values between acquisitions performed by the two operators, suggest that operator's technique should influence the acquired signals and ultimately, the final results.

Regarding to the LVET estimation, the obtained values are also below the normal range, considering the average heart rate of the volunteers. However, taking into account the simplicity of the used algorithm, the obtained values are very close to the expected and are very promising and consistent, with low variance values for all acquisitions.

About the waveforms of the acquired signals, the results suggest that integration and deconvolution algorithms lead to similar waveforms, and a considerable correlation between all subject's waveforms is verified. In this context, other studies must be carried out in the future in order to understand what kind of information can be extracted by those signals. More complex processing algorithms must be developed based, for example, on Wavelet transform, to explore the possibility of detecting wave reflections, or to distinguish other murmurs and pathological sounds in the carotid signals, applying new methodologies based on the different spectra of some characteristic pathological sounds [41].

Despite the good results obtained, to complete the study on the probes performance, more data must be collected to allow more accurate analysis regarding to the carotid sounds waveforms, as well as the improvements to be done on the used algorithms for PWV and LVET estimations, in order to make them more resistant to changes in the waveforms.

In future clinical trials, acquisitions must be carried out in clinical environment, by clinical staff, with the possibility of using simultaneously the double acoustic probe and an

equipment already established in the market as reference. In addition to a larger number of people, the selected group of volunteers must include healthy and non-healthy people (especially with cardiovascular disease) to allow a proper comparison of results.

7. Conclusions

The developed double acoustic probe is based on a very simple architecture system, making it an inexpensive equipment, which combined with its easily handling and ergonomy, could allow its use in other environments besides the clinical.

In a general way, the equipment has showed good performance in the tests carried out for its characterization.

However, in what concerns to the waveforms, the performed analysis for bench tests or the clinical data, were inconclusive regarding the information that the signals, themselves, can provide. A preliminary comparison study between DPZ and DAP signals has suggested that both sensors provide similar information, and that the determination of characteristic discontinuities of the original pressure wave, propagating along the tube, is possible with appropriate algorithms and signal processing of the DAP signals. On the other hand, possibly due to the pre-filtration executed by the acoustic sensors, the computation of integration and deconvolution algorithms didn't enable the perfect recover of the input signals on the bench tests.

Also the cross-talk analysis was not fully conclusive. Despite the undeniable presence of cross-talk in the signals obtained in the developed experimental setup, its dependency with the signal input widths, and consequently, with the noise caused by the movements of the actuator, suggests that other results could arrive from another test, this time in the bench test system, with the sensors acquiring the signals through the latex tube (more similar conditions to the real ones, on carotid arteries).

Repeatability studies yielded good results, although the determined relative errors obtained for each sensor are quite different. Nevertheless, with relative errors below 10% for both sensors, we can conclude that these results don't compromise the probes performance and the posterior signals analysis.

The test performed for the temporal resolution determination yield a very good result, near 1ms, which represents a big benefit of this instrument.

The results from 'clinical' trials were limited by the small number of volunteers available for the study. However, they allowed drawing some preliminary conclusions

regarding the waveforms of the carotid artery auscultation, as well as the main problems associated to the developed algorithms for PWV and LVET estimation.

In fact, the biggest problem of the used algorithms is related to their dependency of the signals shape, leading to the need to make some adjustments to process some specific waveforms. However, taking into account that this is a new equipment, that had never been used or tested before, the results for PWV and especially for LVET values are considered good. Indeed, the velocities estimated for the carotid signals, although lower than the normal values, are generally very close to the expected ones.

It was also possible to draw some considerations related to repeatability studies. The variance values determined show a relatively low dispersion on the PWV for each individual. On the other hand, higher variance values relative to acquisition for the same individual but with different operators suggest that the results are, indeed influenced by the 'quality' of the acquired signal and thus, by the operator's sensibility and technique to execute the acquisitions.

Regarding the LVET values, we can conclude that is actually possible to determine this parameter as the time delay between the two main peaks of the carotid signal. In fact, the estimated values are generally close to the expected, considering each subject's heart rate, and thus we conclude that the used methodology is reliable and leads to good results. However, since it is based simply in peak detection, the used algorithm is also quite sensible to changes in the waveform shape, and some improvements must be done.

8. Future Work

The obtained results are considered very promising and proved the great potential of this double probe to become a reliable and robust equipment for hemodynamic parameters assessment, with the additional advantages of being very cheap and easily to handle.

However, there is still much work to be done to achieve that goal. In next steps, many improvements and corrections must be carried out mainly regarding the data processing routines and the clinical tests.

As already mentioned, the algorithms used in this work for the time delay estimation for PWV and LVET determination, despite their differences, share the same susceptibility to the signals shape, since they are based mostly on peak detection and use of threshold values. The segmentation algorithm, used in the clinical data processing, is one of the most affected by this problem and must be modified or substituted, in order to avoid errors that inevitably will affect the final results.

On the other hand, for a more accurate determination of the proposed hemodynamic parameters, some new steps may be added to the current algorithms. The methodology used in this work consists on the signal segmentation into the cardiac cycles and the subsequent calculation of the PWV and/or LVET for each segment, following the determination of the average values. However, other methodologies related to the selection of the best segment, for instance, should be also tried. A possible method could rely on the determination of the segment with the best correlation between the signals of the two sensors (similarly to what was done in section 5.4.2).

Clinical data analysis is a key factor to complete the instrument's characterization so new trials must be carried out, with a larger number of volunteers (allowing a more reliable statistical analysis) which must include healthy and non-healthy (with CV disease) people with simultaneous acquisitions with a reference equipment (the Complior® system) for results comparison. In addition, the tests described in Chapter 6, related to repeatability studies must be repeated and the results confirmed, especially those regarding to the inter-operator and intra-operator repeatability.

Appendix A

Test Bench System Characterization

1. Relation between the DC pressure level and the PWV in the latex tube

Table 13 - Average values of the PWV (all in m/s) calculated with the three algorithms and for the three tests performed;

	ZCPI			MAD			MCC		
Pressure (mmHg)	**Test 1**	**Test 2**	**Test 3**	**Test 1**	**Test 2**	**Test 3**	**Test 1**	**Test 2**	**Test 3**
35.68	13.88	14.03	13.79	14.17	14.42	14.03	13.92	14.07	13.89
39.82	13.68	13.83	13.71	14.02	13.96	14.00	13.72	13.89	13.78
41.37	13.57	13.82	13.63	13.87	14.03	13.94	13.62	13.81	13.69
44.47	13.47	13.60	13.52	13.85	13.83	13.71	13.57	13.64	13.58
46.54	13.46	13.49	13.52	13.67	13.87	13.69	13.50	13.57	13.53
49.65	13.40	13.40	13.39	13.62	13.65	13.55	13.41	13.46	13.41
51.72	13.27	13.34	13.30	13.65	13.57	13.53	13.41	13.38	13.32
54.30	13.20	13.24	13.20	13.53	13.32	13.44	13.26	13.32	13.24
56.89	13.17	13.21	13.12	13.38	13.43	13.39	13.21	13.26	13.16
59.99	13.09	13.05	12.96	13.36	13.16	13.13	13.21	13.08	13.00
63.09	13.00	13.03	12.83	13.43	13.24	13.21	13.09	13.01	12.89
66.71	12.75	12.87	12.74	13.06	13.09	12.96	12.90	12.93	12.84
70.33	12.64	12.79	12.50	12.92	12.98	12.82	12.70	12.79	12.62
74.99	12.54	12.61	12.46	12.74	12.79	12.71	12.56	12.62	12.53
77.57	12.37	12.31	12.30	12.81	12.73	12.58	12.55	12.46	12.37
82.74	12.44	12.23	12.07	12.67	12.52	12.40	12.47	12.30	12.14
85.33	12.28	12.16	12.02	12.53	12.28	12.34	12.37	12.20	12.13
87.92	11.98	12.10	11.95	12.36	12.46	12.39	12.09	12.17	12.02
90.50	12.06	11.93	11.85	12.47	12.27	12.21	12.11	12.13	11.95
93.09	12.05	11.95	11.79	12.28	12.24	12.07	12.10	11.99	11.83
95.67	11.77	11.76	11.64	11.92	11.98	12.11	11.90	11.84	11.75
98.26	11.68	11.87	11.66	11.98	12.20	11.95	11.84	11.95	11.72
101.36	11.62	11.57	11.47	12.10	12.07	11.70	11.75	11.66	11.52
103.43	11.59	11.58	11.34	11.76	12.02	11.62	11.57	11.71	11.36
108.60	11.49	11.36	11.18	11.87	11.70	11.60	11.56	11.53	11.33
113.77	11.36	11.12	11.12	11.58	11.53	11.26	11.30	11.26	11.11
118.94	10.97	11.04	10.84	11.30	11.36	11.14	11.05	11.13	10.91
124.12	10.59	10.73	10.70	11.17	11.13	10.97	10.84	10.93	10.78
129.29	10.70	10.46	10.36	10.78	11.06	10.79	10.48	10.71	10.52
134.46	10.04	10.43	10.21	10.80	10.73	10.32	10.45	10.48	10.29
139.63	10.18	10.47	10.14	10.69	10.58	10.69	10.14	10.30	10.11
144.80	9.50	*	*	10.19	10.24	*	9.84	10.00	*
149.97	9.49	9.59	*	9.92	10.09	*	9.51	9.70	*

*due to the signals shape, the algorithm could not be applied.

2. Variation of diameter of the latex tube with the increasing DC pressure

Table 14 - Average values of the diameter variations of three measurements (presented in m) for four tests performed.

Pressure Values (mmHg)	Test 1	Test 2	Test 3	Test 4	Average Values
35.68	0.0098	0.0098	0.0099	0.0099	0.0099
39.82	0.0098	0.0100	0.0100	0.0099	0.0099
41.37	0.0098	0.0100	0.0100	0.0099	0.0099
44.47	0.0098	0.0101	0.0101	0.0100	0.0100
46.54	0.0100	0.0102	0.0101	0.0100	0.0101
49.65	0.0101	0.0101	0.0114	0.0101	0.0104
51.71	0.0101	0.0101	0.0102	0.0102	0.0102
54.30	0.0103	0.0101	0.0103	0.0102	0.0102
56.87	0.0101	0.0102	0.0104	0.0102	0.0102
59.99	0.0100	0.0103	0.0104	0.0103	0.0102
63.09	0.0102	0.0103	0.0104	0.0103	0.0103
66.71	0.0102	0.0103	0.0105	0.0103	0.0103
70.33	0.0104	0.0104	0.0105	0.0103	0.0104
74.99	0.0105	0.0105	0.0105	0.0104	0.0105
77.57	0.0104	0.0105	0.0106	0.0105	0.0105
82.74	0.0105	0.0105	0.0107	0.0116	0.0108
85.33	0.0106	0.0106	0.0107	0.0106	0.0106
87.92	0.0106	0.0106	0.0107	0.0106	0.0106
90.50	0.0106	0.0107	0.0108	0.0106	0.0107
93.09	0.0106	0.0107	0.0108	0.0107	0.0107
95.67	0.0107	0.0108	0.0108	0.0108	0.0108
98.29	0.0108	0.0108	0.0109	0.0108	0.0108
101.36	0.0109	0.0109	0.0108	0.0109	0.0108
103.43	0.0108	0.0109	0.0110	0.0108	0.0109
108.60	0.0111	0.0109	0.0110	0.0110	0.0110
113.77	0.0111	0.0111	0.0112	0.0111	0.0111
118.94	0.0113	0.0113	0.0113	0.0113	0.0113
124.11	0.0114	0.0114	0.0115	0.0114	0.0114
129.29	0.0115	0.0116	0.0116	0.0116	0.0116
134.46	0.0115	0.0119	0.0119	0.0118	0.0118

Appendix B

Temporal Resolution Determination

1.PWV determination for different distances between the sensors, for the three algorithms

Table 15 - PWV (m/s) determined with Maximum Amplitude detection algorithm.

Distance(m)	Test1	Test2	Test3	Test4	Test5	Average Values
0.04	5.26	7.69	10.00	1.18	13.33	7.49
0.06	14.29	10.00	2.29	17.64	17.64	12.37
0.08	14.29	11.11	9.75	2.81	16.66	10.92
0.10	13.89	10.20	11.90	14.70	15.62	13.26
0.12	9.23	10.90	12.00	14.28	16.66	12.61
0.14	12.07	10.76	11.29	15.90	12.06	12.42
0.16	9.64	3.30	10.95	3.68	3.70	6.25
0.18	10.23	10.58	10.71	4.00	13.84	9.87
0.20	10.20	10.41	11.23	13.69	13.15	11.74
0.22	10.48	10.89	11.34	13.58	13.75	12.01
0.24	11.32	11.42	11.76	13.79	13.79	12.42
0.26	12.38	11.81	11.71	13.97	13.97	12.77
0.28	11.38	11.66	11.96	13.46	14.14	12.52
0.30	12.19	11.90	11.53	13.27	13.88	12.56
0.32	13.01	11.59	11.76	13.67	12.50	12.51
0.34	11.89	11.56	11.64	14.91	13.28	12.66
0.36	12.86	12.08	11.76	14.75	12.58	12.81
0.38	11.80	11.44	11.72	14.17	13.01	12.43
0.40	12.05	12.05	11.76	13.986	13.15	12.60
0.42	12.57	11.79	11.79	12.88	13.13	12.44
0.44	13.02	12.29	11.95	12.79	13.17	12.65
0.46	12.78	11.98	11.97	13.60	13.45	12.76
0.48	12.57	12.06	12.18	13.87	12.63	12.66
0.50	12.76	67.57	12.43	12.88	7.06	22.54

Table 16 - PWV (m/s) determined with Maximum Cross-Correlation algorithm.

Distance(m)	Test1	Test2	Test3	Test4	Test5	Average Values
0.04	8	10.5263	10.5263	18.1818	13.3333	12.11354
0.06	16.6667	13.6364	11.5385	17.6471	17.6471	15.42716
0.08	15.3846	13.3333	12.1212	18.1818	16.6667	15.13752
0.10	12.8205	11.9048	11.9048	13.8889	14.2857	12.96094
0.12	10.3448	12	12.2449	13.0435	15.3846	12.60356
0.14	12.069	11.8644	11.8644	14.8936	12.069	12.55208
0.16	11.1111	11.5942	12.1212	14.2857	14.5455	12.73154
0.18	11.8421	12.1622	12.1622	14.2857	14.2857	12.94758
0.20	12.1951	12.0482	12.1951	14.0845	13.5135	12.80728
0.22	11.9565	12.2222	12.3596	13.9241	13.9241	12.8773
0.24	12.3711	12.6316	12.5	13.7931	13.7931	13.01778
0.26	12.8713	12.8713	12.5	13.8298	13.6842	13.15132
0.28	11.9658	12.6126	12.6126	13.2075	13.7255	12.8248
0.30	12.8205	12.8205	12.3967	13.2743	13.7615	13.0147
0.32	13.2231	12.5984	12.5984	13.3333	12.6984	12.89032
0.34	12.5	12.5926	12.5926	14.2857	13.1783	13.02984
0.36	13.0435	12.8571	12.5874	14.1732	12.8571	13.10366
0.38	12.6667	12.2581	12.5828	13.8686	13.1034	12.89592
0.40	12.7389	12.9032	12.6582	13.6054	13.245	13.03014
0.42	12.963	12.7273	12.6506	12.963	13.125	12.88578
0.44	13.0952	12.9412	12.7168	12.8655	13.1737	12.95848
0.46	12.9944	12.7778	12.6374	13.4503	13.4503	13.06204
0.48	12.8342	12.8342	12.766	13.5593	12.9032	12.97938
0.50	12.9534	12.5	12.8205	12.9534	12.9534	12.83614

Table 17 - PWV (m/s) determined with Zero Crossing point identification algorithm.

Distance (m)	Test1	Test2	Test3	Test4	Test5	Average Values
0.04	1.509657	11.1313	*	0.4902	12.7341	6.466314
0.06	17.02381	13.2491	*	20.5119	20.5119	17.82418
0.08	15.62981	13.7322	11.4203	1.4069	15.9593	11.6297
0.1	13.5621	12.6297	14.3062	15.8788	16.0837	14.4921
0.12	*	13.7117	13.8427	15.0531	18.5541	15.2904
0.14	12.06973	13.0505	13.3572	17.844	13.122	13.88869
0.16	*	*	12.8382	2.9282	2.9081	6.224833
0.18	8.065981	12.362	12.2799	*	14.9237	11.9079
0.2	7.429956	11.9515	12.4077	15.0965	13.8199	12.14111
0.22	8.500999	12.211	12.5151	14.4122	14.4123	12.41032
0.24	11.86549	12.6982	12.8029	14.2403	14.1549	13.15236
0.26	12.56135	12.8346	12.5663	14.0669	14.1409	13.23401
0.28	11.67223	12.8115	12.8196	13.5051	14.2767	13.01703
0.3	12.50596	12.9221	12.6151	13.7597	14.247	13.20997
0.32	13.02926	12.6668	12.6677	13.5332	12.6922	12.91783
0.34	12.18237	12.6177	12.6261	14.5625	13.3729	13.07231
0.36	12.848430	13.0397	12.7113	14.5104	12.7424	13.25095
0.38		12.2659	12.5786	13.8805	13.225	12.9875
0.4	12.40895	12.9114	12.6218	13.7254	13.3388	13.00127
0.42	12.72484	12.6918	12.5315	12.7761	13.3885	12.82255
0.44	12.98117	13.1075	12.658	12.8339	13.3678	12.98967
0.46	12.82982	12.7604	12.6588	13.2539	13.7463	13.04984
0.48	12.58497	12.8211	12.8513	13.5814	12.818	12.93135
0.5	12.75639	*	12.9311	12.8756	*	12.85436

*due to the signals shape, the algorithm could not be applied.

Table 18 - Reference PWV values (m/s) determined with the Maximum Amplitude Detection (MAD), the Cross-Correlation algorithm (CC) and the Zero-Crossing algorithm (CC).

Reference Values															
Test1			Test2			Test3			Test4			Test5			Average Values
MAD	CC	ZC	MAD	CC	ZC	MAD	CC	ZC	MAD	CC	ZC	MAD	CC	ZC	
13.85	13.87	13.89	13.94	13.87	14.02	13.85	13.76	13.98	13.81	13.74		13.78	13.67		13.85
13.91	13.72	13.84	13.91	13.78	13.86	13.85	13.74	*	13.80	13.72	13.89	13.78	13.65	13.90	13.81
13.87	13.85	13.86	13.64	13.69	13.88	13.69	13.64	*	13.89	13.80	14.01	13.89	13.80	14.01	13.82
14.03	13.94	13.94	13.72	13.72	13.93	13.78	13.69	13.89	13.78	13.64	13.86	13.76	13.74	13.86	13.82
13.94	13.83	13.95	13.62	13.74	13.92	13.76	13.71	13.87	13.80	13.72	13.96	13.71	13.72	13.88	13.81
13.98	13.83	13.88	13.71	13.64	13.85	13.78	13.65	13.84	13.74	13.71	13.88	13.71	13.67	13.90	13.78
13.92	13.85	13.84	13.74	13.69	13.86	13.71	13.64	13.82	13.78	13.80	13.96	13.65	13.65	13.92	13.79
13.89	13.80	13.94	13.80	13.62	*	13.76	13.67	13.84	14.00	13.78	13.99	13.71	13.72	13.91	13.81
13.92	13.83	13.83	13.72	13.67	13.89	13.65	13.64	13.85	13.83	13.78		13.74	13.67	13.83	13.78
13.91	13.83	13.89	13.85	13.67	13.83	13.72	13.69	13.84	13.98	13.80	14.03	13.80	13.65	13.81	13.82
14.02	13.83	13.86	13.64	13.60	13.78	13.76	13.69	13.81	13.83	13.74	14.01	13.81	13.65	13.86	13.79
13.72	13.80	13.89	13.76	13.65	13.84	13.74	13.67	13.85	13.74	13.76	13.88	13.67	13.67	13.85	13.77
13.92	13.80	13.94	13.65	13.74	13.86	13.76	13.64	13.80	13.81	13.83	13.99	13.71	13.71	13.90	13.80
13.87	13.81	13.91	13.76	13.67	13.87	13.78	13.67	13.81	13.81	13.74	13.99	13.78	13.71	13.85	13.80
13.87	13.81	13.91	13.83	13.76	13.86	13.76	13.64	13.86	13.74	13.74	13.94	13.67	13.67	13.84	13.79
13.83	13.89	13.94	13.76	13.65	13.81	13.85	13.69	13.84	13.78	13.69	13.85	13.74	13.67	13.88	13.79
14.07	13.92	13.90	13.69	13.62	13.73	13.81	13.69	13.82	13.81	13.65	13.89	13.72	13.69	13.94	13.80
13.96	13.89	13.92	13.74	13.69	13.78	13.65	13.65	13.81	13.74	13.64	13.89	13.69	13.67	13.89	13.77
13.76	13.83	13.92	13.71	13.72	13.82	13.78	13.69	13.86	13.80	13.64	13.86	13.87	13.76	13.86	13.79
13.81	13.85	13.90	13.71	13.72	13.82	13.62	13.64	13.79	13.83	13.69	13.85	13.76	13.74	13.86	13.77
13.91	13.81	13.88	13.87	13.65	13.83	13.83	13.67	13.89	13.74	13.60	13.83	13.72	13.67	13.87	13.79
13.89	13.94	13.95	13.69	13.74	13.89	13.72	13.69	13.86	13.55	13.58	13.82	13.62	13.65	13.77	13.76
13.89	13.87	13.87	13.76	13.65	13.89	13.81	13.71	13.81	13.80	13.67	13.86	13.89	13.71	13.93	13.81
13.96	13.92	13.88	13.78	13.69	13.83	13.85	13.74	13.89	13.64	13.62	13.85	13.71	13.65	13.81	13.79
13.98	13.91	14.00	13.60	13.67	*	13.87	13.67	13.78	13.78	13.72	13.87	13.69	13.71	*	13.79

*due to the signals shape, the algorithm could not be applied.

Appendix C

'Clinical' Trials

1. PWV for Operator 1

Table 19 - PWV values (m/s) for Subject 1 determined with maximum amplitude detection (MAD) and cross-correlation algorithm (MCC); values for left carotid (LC) and right carotid (RC);

	Subject 1											
	1st week				2nd week				3rd week			
	LC		RC		LC		RC		LC		RC	
	MAD	MCC	MAD	MCC	MAD	MCC	MAD	MCC	MAD	MCC	MAD	MCC
	2.33	3.52	2.51	2.73	1.69	5.28	2.53	2.78	6.79	2.34	3.42	2.08
	2.32	4.85	2.47	3.01	1.61	3.42	2.51	2.09	2.75	2.16	3.71	1.81
	2.47	3.86	2.34	2.83	1.64	3.39	2.32	2.45	2.50	2.36	3.60	1.88
	2.39	2.35	2.67	2.75	1.65	2.17	2.71	2.78	2.90	2.23	3.42	2.05
	2.53	3.06	2.35	3.77	1.88	3.21	2.73	2.31	2.83	2.02	2.84	1.79
	2.44	2.79	6.69	4.17	1.81	5.00	2.91	2.28	2.84	2.31	7.66	1.95
	2.49	3.63	6.01	4.17	1.65	3.15	2.13	2.13	3.25	2.42	2.70	1.70
	3.03	2.68	2.53	3.10	2.05	4.52	2.70	1.98	3.52	2.08	3.34	2.40
Average value	2.50	3.34	3.45	3.31	1.75	3.77	2.57	2.35	3.42	2.24	3.84	1.96
Standard Deviation	0.23	0.23	1.80	0.62	0.15	1.06	0.25	0.30	1.39	0.14	1.58	0.22
Variance ($\sqrt{m/s}$)	0.05	0.63	3.26	0.39	0.02	1.13	0.06	0.09	1.95	0.02	2.51	0.05

Table 20 - PWV values (m/s) for Subject 2 determined with maximum amplitude detection (MAD) and cross-correlation algorithm (MCC); values for left carotid (LC) and right carotid (RC);

	Subject 2											
	1st week				2nd week				3rd week			
	LC		RC		LC		RC		LC		RC	
	MAD	MCC	MAD	MCC	MAD	MCC	MAD	MCC	MAD	MCC	MAD	MCC
	5.72	3.12	2.55	4.17	5.46	1.74	2.18	0.98	2.20	0.50	3.93	5.11
	2.24	2.97	1.21	7.31	8.64	1.55	3.63	1.35	2.97	0.55	3.93	3.77
	5.94	3.68	2.06	4.85	3.86	1.15	6.17	1.04	4.85	0.63	4.40	3.77
	8.33	3.34	3.28	5.72	15.32	1.26	1.48	1.09	4.66	0.65	3.10	3.17
	5.11	2.71	2.70	5.79	5.34	1.52	9.13	1.11	2.32	0.51	3.06	3.39
	2.57	3.60	2.58	3.96	67.85	1.42	2.46	1.18	2.58	0.56	3.63	2.61
Average value	4.98	3.24	2.40	5.30	17.74	1.44	4.17	1.13	3.26	0.57	3.67	3.64
Standard Deviation	2.28	0.37	0.70	1.24	24.89	0.21	2.93	0.13	1.19	0.06	0.52	0.84
Variance ($\sqrt{m/s}$)	5.21	0.14	0.49	1.55	619.43	0.05	8.61	0.02	1.41	0.00	0.27	0.71

Table 21 - PWV values (m/s) for Subject 3 determined with maximum amplitude detection (MAD) and cross-correlation algorithm (MCC); values for left carotid (LC) and right carotid (RC);

	Subject 3											
	1st week				2nd week				3rd week			
	LC		RC		LC		RC		LC		RC	
	MAD	MCC	MAD	MCC	MAD	MCC	MAD	MCC	MAD	MCC	MAD	MCC
	8.80		5.00	1.86	1.71	1.35	3.54	0.78	4.48	14.84	2.90	1.18
	10.11		4.57	1.81	2.22	1.05	4.70	0.80	3.04	5.86	2.10	1.25
	12.50		4.09	1.98	2.49	1.32	3.83	0.88	5.22	15.83	1.95	1.22
	7.31		4.20	1.79	1.80	1.29	6.17	0.79	4.03	11.05	1.89	1.26
	9.31		2.39	1.95	2.16	1.09	3.25	0.88	3.44	10.11	1.42	1.23
	7.09		3.39	2.07	2.09	1.15	4.75	0.80	3.30	8.80	1.71	1.24
	8.80		3.21	1.76	2.55	1.34	3.89	0.88	3.49	8.05	1.43	1.48
Average value	9.13		3.84	1.89	2.15	1.23	4.31	0.83	3.86	10.65	1.91	1.27
Standard Deviation	1.83		0.89	0.11	0.32	0.13	0.99	0.05	0.77	3.61	0.50	0.10
Variance ($\sqrt{m/s}$)	3.34		0.80	0.01	0.10	0.02	0.98	0.00	0.59	13.00	0.25	0.01

Table 22 - PWV values (m/s) for Subject 4 determined with maximum amplitude detection (MAD) and cross-correlation algorithm (MCC); values for left carotid (LC) and right carotid (RC);

	Subject 4											
	1st week				2nd week				3rd week			
	LC		RC		LC		RC		LC		RC	
	MAD	MCC	MAD	MCC	MAD	MCC	MAD	MCC	MAD	MCC	MAD	MCC
	2.32	2.45	16.38	4.03	2.35	1.57	9.50	3.28	2.22	2.35	17.59	2.78
	2.39	2.49	3.17	3.49	2.62	1.66	11.05	5.94	7.54	2.99	7.42	2.68
	5.22	2.17	3.19	3.30	1.99	1.51	13.19	6.79	2.32	2.58	3.15	2.53
	4.80	2.51	59.37	3.52	2.32	1.60	11.05	6.88	2.12	2.39	10.55	3.60
	3.23	2.19	2.97	3.71	2.71	1.52	4.44	8.19	2.32	2.49	2.93	2.86
	2.54	2.20	3.08	3.54	1.84	1.47	8.96	33.93	10.55	2.50	18.27	2.84
	2.20	2.08	5.46	3.21	2.08	1.71	7.09	18.27	2.19	2.75	5.34	2.71
Average value	3.24	2.30	13.37	3.54	2.27	1.58	9.32	11.89	4.18	2.58	9.32	2.86
Standard Deviation	1.26	0.18	20.85	0.27	0.32	0.09	2.88	10.81	3.44	0.22	6.43	0.35
Variance ($\sqrt{m/s}$)	1.58	0.03	434.90	0.07	0.11	0.01	8.32	116.78	11.82	0.05	41.40	0.12

Table 23 - PWV values (m/s) for Subject 5 determined with maximum amplitude detection (MAD) and cross-correlation algorithm (MCC); values for left carotid (LC) and right carotid (RC);

	Subject 5											
	1st week				2nd week				3rd week			
	LC		RC		LC		RC		LC		RC	
	MAD	MCC	MAD	MCC	MAD	MCC	MAD	MCC	MAD	MCC	MAD	MCC
	2.37	2.20	3.71	2.19	2.13	1.52	3.03	1.45	3.10	3.15	4.24	6.25
	3.77	2.29	3.15	2.23	1.81	1.86	3.01	1.43	4.17	2.83	7.20	3.86
	2.36	2.32	3.03	2.19	2.23	1.70	2.47	1.35	2.78	3.15	3.19	3.60
	3.01	2.32	1.93	5.11	1.95	1.57	2.17	1.26	2.50	2.54	8.19	3.89
	2.32	2.25	2.91	2.47	2.03	1.57	3.60	1.27	4.70	3.49	3.93	2.64
	2.55	2.35	2.44	2.15	2.17	1.58	2.61	1.20	3.63	3.17	4.80	3.12
	4.17	2.15	2.51	2.14	1.71	1.63	3.39	1.23	2.49	2.95	6.17	2.99
	6.88	2.35	2.28	2.28	1.96	1.73	2.19	1.30	2.51	3.04	3.74	3.54
Average value	3.43	2.28	2.74	2.60	2.00	1.64	2.81	1.31	3.23	3.04	5.18	3.74
Standard Deviation	1.56	0.23	0.56	1.02	0.18	0.11	0.53	0.09	0.85	0.28	1.80	1.11
Variance ($\sqrt{m/s}$)	2.43	0.01	0.32	1.04	0.03	0.01	0.29	0.01	0.72	0.08	3.25	1.22

Table 24 - PWV values (m/s) for Subject 6 determined with maximum amplitude detection (MAD) and cross-correlation algorithm (MCC); values for left carotid (LC) and right carotid (RC);

	Subject 6											
	1st week				2nd week				3rd week			
	LC		RC		LC		RC		LC		RC	
	MAD	MCC	MAD	MCC	MAD	MCC	MAD	MCC	MAD	MCC	MAD	MCC
	4.75	1.34	5.28	2.15	3.39	0.46	6.33	2.60	3.80	2.84	8.64	0.68
	3.23	1.56	3.19	3.03	2.70	0.45	8.33	2.45	4.57	2.78	12.50	0.61
	3.89	1.71	4.52	2.57	2.58	0.51	4.06	2.40	3.52	2.62	3.65	2.14
	3.49	1.40	5.72	2.34	4.36	0.51	2.93	2.62	3.93	2.76	6.09	0.61
	3.60	1.41	5.05	3.47	3.65	0.52	6.17	2.42	3.23	2.55	19.79	0.61
	2.73	1.64	5.72	2.53	8.48	0.56	4.52	2.41	3.01	2.67	5.22	2.15
	3.74	1.53	3.23	2.44	3.42	0.56	4.03	2.41	6.42	3.03	3.49	2.01
	3.68	1.51	6.79	3.57	2.71	0.57	10.79	2.39	4.57	2.90	6.69	0.66
Average value	3.64	1.51	4.94	2.76	3.91	0.52	5.90	2.46	4.13	2.77	8.26	1.18
Standard Deviation	0.58	0.23	1.25	0.53	1.94	0.05	2.61	0.09	1.08	0.15	5.50	0.76
Variance ($\sqrt{m/s}$)	0.33	0.02	1.56	0.28	3.76	0.00	6.82	0.01	1.17	0.02	30.20	0.58

2.PWV for Operator 2

Table 25 - PWV values (m/s) for Subject 1 determined with maximum amplitude detection (MAD) and cross-correlation algorithm (MCC); values for left carotid (LC) and right carotid (RC);

	Subject 1							
	2nd week				3rd week			
	LC		RC		LC		RC	
	MAD	MCC	MAD	MCC	MAD	MCC	MAD	MCC
	2.55	0.93	2.44	2.54	4.70		1.83	19.00
	2.39	1.26	2.37	2.27	4.70		1.87	0.01
	1.96	1.11	2.39	2.47	5.86		1.86	26.39
	1.79	1.03	2.11	2.42	1.88		1.90	10.79
	2.27	0.78	2.20	2.24	3.68		1.64	2.49
	1.99	0.85	2.11	2.37	3.89	*	1.89	26.39
	2.20	1.35	2.40	1.71	3.93		1.96	26.39
Average value	2.16	1.05	2.29	2.29	4.09		1.85	15.92
Standard Deviation	0.27	0.21	0.14	0.28	1.23		0.10	11.53
Variance ($\sqrt{m/s}$)	0.07	0.04	0.02	0.08	1.50		0.01	133.02

* bad acquisition, leading to impossible PWV in physiological conditions

Table 26 - PWV values (m/s) for Subject 2 determined with maximum amplitude detection (MAD) and cross-correlation algorithm (MCC); values for left carotid (LC) and right carotid (RC);

	Subject 2							
	2nd week				3rd week			
	LC		RC		LC		RC	
	MAD	MCC	MAD	MCC	MAD	MCC	MAD	MCC
	2.11	1.29	4.20	4.57	3.10	1.71	3.77	5.11
	1.98	1.28	7.31	3.47	3.54	2.31	2.46	5.05
	2.28	1.28	4.09	3.08	2.58	1.97	2.34	5.52
	2.24	1.08	6.01	3.89	2.58	2.07	3.19	5.22
	2.02	1.24	5.52	2.95	2.93	3.37	4.06	5.65
	2.00	1.16	3.99	2.99	3.06	3.52	3.44	4.57
Average value	2.11	1.22	5.19	3.49	2.97	2.49	3.21	5.19
Standard Deviation	0.13	0.08	1.33	0.64	0.36	0.76	0.69	0.38
Variance ($\sqrt{m/s}$)	0.02	0.01	1.78	0.41	0.13	0.58	0.48	0.15

Table 27 - PWV values (m/s) for Subject 3 determined with maximum amplitude detection (MAD) and cross-correlation algorithm (MCC); values for left carotid (LC) and right carotid (RC);

	Subject 3							
	2nd week				3rd week			
	LC		RC		LC		RC	
	MAD	MCC	MAD	MCC	MAD	MCC	MAD	MCC
	9.69	1.42	2.49	4.20	5.79	10.11	2.12	1.88
	5.65	1.37	3.80	3.65	6.09	6.42	2.21	2.02
	8.48	1.48	2.36	2.71	4.44	3.93	2.45	2.15
	10.79	1.20	2.62	2.58	5.22	7.79	2.04	1.85
	5.94	1.41	0.95	5.40	6.33	6.51	2.13	1.87
	7.42	1.47	2.95	2.36	6.33	3.34	2.12	1.79
	4.36	1.57	2.67	2.75	5.40	5.05	2.12	1.92
Average value	7.48	1.42	2.55	3.38	5.66	6.16	2.17	1.92
Standard Deviation	2.32	0.11	0.85	1.11	0.69	2.33	0.13	0.12
Variance ($\sqrt{m/s}$)	5.39	0.01	0.72	1.22	0.48	5.42	0.02	0.02

Table 28 - PWV values (m/s) for Subject 6 determined with maximum amplitude detection (MAD) and cross-correlation algorithm (MCC); values for left carotid (LC) and right carotid (RC);

	Subject 6							
	2nd week				3rd week			
	LC		RC		LC		RC	
	MAD	MCC	MAD	MCC	MAD	MCC	MAD	MCC
	3.15	0.46	1.89	2.60	8.96	2.84	2.27	0.68
	2.33	0.45	2.73	2.45	20.65	2.78	2.28	2.01
	2.31	0.51	2.07	2.40	16.38	2.62	2.44	2.14
	1.96	0.51	2.49	2.62	47.50	2.76	2.62	0.61
	2.11	0.52	1.83	2.42	7.66	3.03	2.53	0.66
	2.65	0.56	2.20	2.41	13.19	2.67	2.60	2.15
Average value	2.42	0.50	2.20	2.48	19.06	2.78	2.46	1.38
Standard Deviation	0.43	0.04	0.35	0.10	14.73	0.14	0.15	0.80
Variance ($\sqrt{m/s}$)	0.18	0.00	0.12	0.01	216.93	0.02	0.02	0.63

3. LVET values for Operator 1

Table 29 - LVET values (s) for Subject 1 determined with maximum amplitude detection (MAD) and cross-correlation algorithm (MCC); values for left carotid (LC) and right carotid (RC);

	Subject 1											
	RC						LC					
	1st week		2nd week		3th week		1st week		2nd week		3th week	
	LVET(s)	HR (b/min)	LVET(s)	HR (b/min)	LVET(s)	HR (b/min)	LVET(s)	HR (b/min)	LVET(s)	HR (b/min)	LVET(s)	HR (b/min)
	0.28	62.10	0.28	71.97	0.25	76.82	0.15	64.29	0.26	79.17	0.15	78.91
	0.29		0.26		0.26		0.27		0.26		0.13	
	0.30		0.28		0.27		0.29		0.27		0.13	
	0.29		0.28		0.26		0.29		0.27		0.14	
	0.28		0.26		0.25		0.27		0.25		0.14	
	0.30		0.28		0.26		0.29		0.26		0.13	
Average value	0.29		0.27		0.26		0.26		0.26		0.14	
Standar Deviation	0.01		0.01		0.01		0.06		0.01		0.01	
Variance ($\sqrt{s}$)	0.00		0.00		0.00		0.00		0.00		0.00	

Table 30 - LVET values (s) for Subject 2 determined with maximum amplitude detection (MAD) and cross-correlation algorithm (MCC); values for left carotid (LC) and right carotid (RC);

	Subject 2											
	RC						LC					
	1st week		2nd week		3th week		1st week		2nd week		3th week	
	LVET(s)	HR (b/min)	LVET(s)	HR (b/min)	LVET(s)	HR (b/min)	LVET(s)	HR (b/min)	LVET(s)	HR (b/min)	LVET(s)	HR (b/min)
	1.21	56.68	0.28	60.34	0.27	70.46	0.30	56.50	0.29	64.39	0.27	61.33
	0.29		0.33		0.28		0.30		0.28		0.29	
	0.30		0.29		0.28		0.27		0.28		0.30	
	0.29		0.29		0.26		0.29		0.27		0.30	
	0.30				0.27		0.31		0.28		0.31	
	0.29				0.29		0.30		0.28		0.29	
Average value	0.45		0.30		0.27		0.29		0.28		0.29	
Standar Deviation	0.37		0.02		0.01		0.01		0.01		0.01	
Variance ($\sqrt{s}$)	0.14		0.00		0.00		0.00		0.00		0.00	

Table 31 - LVET values (s) for Subject 3 determined with maximum amplitude detection (MAD) and cross-correlation algorithm (MCC); values for left carotid (LC) and right carotid (RC);

	Subject 3											
	RC						LC					
	1st week		2nd week		3th week		1st week		2nd week		3th week	
	LVET(s)	HR(b/min)	LVET(s)	HR(b/min)	LVET(s)	HR(b/min)	LVET(s)	HR(b/min)	LVET(s)	HR(b/min)	LVET(s)	HR(b/min)
	0.24		0.25		0.29		0.13		0.24		0.27	
	0.26		0.25		0.28		0.12		0.25		0.27	
	0.26		0.23		0.27		0.12		0.25		0.26	
	0.26	82.24	0.24	89.91	0.28	73.41	0.10	81.92	0.24	88.89	0.27	82.97
	0.25		0.25		0.28		0.13		0.23		0.27	
	0.24		0.24		0.26		0.13		0.25		0.27	
	0.25		0.25		0.28		0.13		0.25		0.26	
Average value	0.25		0.25		0.28		0.12		0.24		0.27	
Standar Deviation	0.01		0.01		0.01		0.01		0.01		0.01	
Variance ($\sqrt{s}$)	0.00		0.00		0.00		0.00		0.00		0.00	

Table 32 - LVET values (s) for Subject 4 determined with maximum amplitude detection (MAD) and cross-correlation algorithm (MCC); values for left carotid (LC) and right carotid (RC);

	Subject 4											
	RC						LC					
	1st week		2nd week		3th week		1st week		2nd week		3th week	
	LVET(s)	HR (b/min)	LVET(s)	HR (b/min)	LVET(s)	HR (b/min)	LVET(s)	HR (b/min)	LVET(s)	HR (b/min)	LVET(s)	HR (b/min)
	0.29		0.39		0.28		0.28		0.28		0.28	
	0.28		0.26		0.27		0.27		0.28		0.28	
	0.28	68.03	0.30	72.07	0.28	74.82	0.28	73.01	0.28	77.20	0.28	74.78
	0.28		0.28		0.29		0.27		0.27		0.27	
	0.03		0.29		0.28		0.28		0.28		0.28	
Average value	0.23		0.30		0.28		0.28		0.28		0.28	
Standar Deviation	0.114		0.05		0.00		0.00		0.00		0.00	
Variance ($\sqrt{s}$)	0.013		0.00		0.00		0.00		0.00		0.00	

Table 33 - LVET values (s) for Subject 5 determined with maximum amplitude detection (MAD) and cross-correlation algorithm (MCC); values for left carotid (LC) and right carotid (RC);

	Subject 5											
	RC						LC					
	1st week		2nd week		3th week		1st week		2nd week		3th week	
	LVET(s)	HR (b/min)	LVET(s)	HR (b/min)	LVET(s)	HR (b/min)	LVET(s)	HR (b/min)	LVET(s)	HR (b/min)	LVET(s)	HR (b/min)
	0.28		0.26		0.29		0.29		0.31		0.29	
	0.29		0.27		0.29		0.06		0.32		0.29	
	0.26		0.28		0.28		0.29		0.28		0.27	
	0.29	66.22	0.29	71.09	0.27	71.38	0.30	67.42	0.28		0.27	
	0.29		0.28		0.28		0.30		0.29	74.24	0.28	80.00
	0.26		0.27		0.29		0.29		0.29		0.28	
	0.27		0.28		0.29		0.30		0.15		0.26	
	0.29		0.29		0.26		0.30		0.29		0.27	
Average value	0.28		0.28		0.28		0.26		0.28		0.28	
Standar Deviation	0.01		0.01		0.01		0.08		0.05		0.01	
Variance ($\sqrt{s}$)	0.00		0.00		0.00		0.01		0.00		0.00	

Table 34 - LVET values (s) for Subject 6 determined with maximum amplitude detection (MAD) and cross-correlation algorithm (MCC); values for left carotid (LC) and right carotid (RC);

	Subject 6											
	RC						LC					
	1st week		2nd week		3th week		1st week		2nd week		3th week	
	LVET(s)	HR (b/min)	LVET(s)	HR (b/min)	LVET(s)	HR (b/min)	LVET(s)	HR (b/min)	LVET(s)	HR (b/min)	LVET(s)	HR (b/min)
	0.24		0.27		0.27		0.25		0.25		0.27	
	0.22		0.26		0.25		0.23		0.26		0.27	
	0.24		0.25		0.27		0.24		0.26		0.25	
	0.25	83.80	0.27	72.14	0.26	77.33	0.25	87.94	0.24	67.03	0.26	79.14
	0.24		0.26		0.26		0.23		0.27		0.27	
	0.21		0.14		0.27		0.23		0.27		0.27	
	0.24		0.27		0.26		0.24		0.25		0.25	
	0.24		0.26		0.26		0.24		0.27		0.27	
Average value	0.24		0.25		0.26		0.24		0.26		0.26	
Standar Deviation	0.01		0.04		0.01		0.01		0.01		0.01	
Variance ($\sqrt{s}$)	0.00		0.00		0.00		0.00		0.00		0.00	

4 . LVET values for Operator 2

Table 35 - LVET values (s) for Subject 1 determined with maximum amplitude detection (MAD) and cross-correlation algorithm (MCC); values for left carotid (LC) and right carotid (RC);

	Subject 1							
	RC				LC			
	2st week		3th week		2st week		3th week	
	LVET (s)	HR(b/min)	LVET (s)	HR(b/min)	LVET (s)	HR(b/min)	LVET (s)	HR(b/min)
	0.26	73.33	0.27	70.67	0.28	73.37	0.27	72.46
	0.26		0.28		0.26		0.25	
	0.27		0.29		0.27		0.27	
	0.27		0.28		0.28		0.28	
	0.25		0.26		0.26		0.26	
	0.27		0.28		0.27		0.28	
	0.27		0.28		0.28		0.26	
Average value	0.26		0.28		0.27		0.27	
Standar Deviation	0.01		0.01		0.01		0.01	
Variance ($\sqrt{s}$)	0.00		0.00		0.00		0.00	

Table 36 - LVET values (s) for Subject 2 determined with maximum amplitude detection (MAD) and cross-correlation algorithm (MCC); values for left carotid (LC) and right carotid (RC);

	Subject 2							
	RC				LC			
	2st week		3th week		2st week		3th week	
	LVET (s)	HR(b/min)	LVET (s)	HR(b/min)	LVET (s)	HR(b/min)	LVET (s)	HR(b/min)
	0.31	53.46	0.29	60.35	0.29	5.35	0.29	62.05
	0.30		0.27		0.26		0.28	
	0.28		0.29		0.28		0.27	
	0.26		0.29		0.30		0.29	
	0.29		0.26		0.29		0.29	
	0.31		0.28		0.26		0.29	
Average value	0.29		0.28		0.28		0.28	
Standar Deviation	0.02		0.01		0.02		0.01	
Variance ($\sqrt{s}$)	0.00		0.00		0.00		0.00	

Table 37 - LVET values (s) for Subject 3 determined with maximum amplitude detection (MAD) and cross-correlation algorithm (MCC); values for left carotid (LC) and right carotid (RC);

	Subject 3							
	RC				LC			
	2st week		3th week		2st week		3th week	
	LVET (s)	HR(b/min)	LVET (s)	HR(b/min)	LVET (s)	HR(b/min)	LVET (s)	HR(b/min)
	0.26		0.27		0.25		0.27	
	0.26		0.27		0.24		0.27	
	0.26	77.37	0.26	77.64	0.25	83.18	0.28	87.20
	0.26		0.26		0.26		0.27	
	0.26		0.27		0.14		0.27	
Average value	0.26		0.27		0.23		0.27	
Standar Deviation	0.00		0.01		0.05		0.01	
Variance ($\sqrt{s}$)	0.00		0.00		0.00		0.00	

Table 38 - LVET values (s) for Subject 6 determined with maximum amplitude detection (MAD) and cross-correlation algorithm (MCC); values for left carotid (LC) and right carotid (RC);

	Subject 6							
	RC				LC			
	2st week		3th week		2st week		3th week	
	LVET(s)	HR(b/min)	LVET(s)	HR(b/min)	LVET(s)	HR(b/min)	LVET(s)	HR(b/min)
	0.25		0.26		0.24		0.25	
	0.25		0.27		0.84		0.26	
	0.25	76.58	0.26	80.63	0.26	75.19	0.27	80.17
	0.26		0.26		0.24		0.27	
	0.24		0.27		0.24		0.25	
Average value	0.25		0.26		0.37		0.26	
Standar Deviation	0.01		0.01		0.26		0.01	
Variance ($\sqrt{s}$)	0.00		0.00		0.07		0.00	

References

[1] – http://www.ine.pt - (acedido em Julho de 2011)

[2] - http://www.who.int/mediacentre/factsheets/fs317/en/ - (acedido em Julho de 2011)

[3] - Laurent S., *et al*, "Expert consensus document on arterial stiffness: methodological issues and clinical applications", Special article, European Heart Journal, 27, pp. 2588-2605, Sep.2006

[4] – Laurent, S. *et al*, "Aortic Stiffness Is an Independent Predictor of All-Cause and Cardiovascular Mortality in Hypertensive Patients", Hypertension,37,pp.1236-1241, 2001.

[5] – Othmane, T. "The role of parameters of arterial stiffness to prognose cardiovascular survival in haemodialysis patients: determinants and therapeutic options.", Ph.D. thesis, Semmelweis University, School of Ph.D. Studies, Clinical Medicine.

[6] – Klabund, R. "Cardiovascular Physiology Concepts", Lippincott Williams & Wilkins, 2005.

[7]-http://health.howstuffworks.com/human-body/systems/circulatory/heart-pictures.htm (acedido em Julho de 2011)

[8]- Neto, Jorge E. "Great arteries contribution in orthostasis cardiovascular adaptation", Arquivos Brasileiros de Cardiologia, 2006.

[9] - http://www.bristol.ac.uk/medical-school/hippocrates/medsurg/vascular/ - (acedido em Agosto de 2011).

[10] - JP Murgo, N Westerhof, JP Giolma and SA Altobelli, "Aortic input impedance in normal man: relationship to pressure wave forms", Circulation, 1980.

[11] - Gary E. McVeigh, "Pulse Waveform Analysis and Arterial Wall Properties", Hypertension, 2003.

[12] – Solà J., Rimoldi S., Allemann Y., "Ambulatory monitoring of the cardiovascular systems: the role of Pulse Wave Velocity".

[13]- Bramwell J.C., Hill A.V., "The velocity of the pulse wave in man.", Proc R Soc Lond B Biol Sci. 1922; 93:298–306.

[14] – Hermeling, E. *et al*, "Measurement of Local Pulse Wave Velocity: Effects of Signal Processing on Precision",Elsevier, Ultrasound in Med. & Biol., Vol. 33, No. 5, pp. 774–781, 2007

[15] - Chiu YC, Arand PW, Shroff SG, Feldman T, Carroll JD. "Determination of pulse wave velocities with computerized algorithms", Am Heart J 1991; 121:1460–1470.

[16] – Chubachi N. *et al*, "Measurement of Local Pulse Wave Velocity in Arteriosclerosis by Ultrasonic Doppler Method" IEEE, 1994.

[17] - Murata R, et al "Measurement of Local Pulse Wave Velocity on Aorta for Noninvasive Diagnosis of Arteriosclerosis" IEEE, 1994.

[18] – Katsuda S. *et al* "Characteristic Change in Local Pulse Wave Velocity in Different Segments of the Atherosclerotic Aorta in KHC Rabbits", American Journal of Hypertension, 2004.

[19] – Sørensen G. *et al*, "Pulse Wave Velocity in the Carotid Artery" IEEE, 2004.

[20] – Tonking A., "Atherosclerosis and Heart Disease", Martin Dunitz, 2003.

[21] http://www.cvtsa.com/AL00080Cardiovascularsystemanatomy/M-444-170.html - (acedido em Agosto de 2011).

[22] - Safar, M. *et al*, "Aortic Pulse Wave Velocity: an Independent Marker of Cardiovascular Risk", 2002.

[23] – Jelinek M., Dobes J., Pousek L., "Correlation Analysis in a Pulse Wave Velocity Evaluation", Radioengineering, Vol.13, n.3, September 2004.

[24] - Tsui, Po-Hsiang *et al,* "Arterial Pulse Waveform Analysis by the Probability Distribution of Amplitude", National Taiwan University, Taipei (Taiwan), Physiological Measurement, May 2007.

[25] - Meinders JM and Hoeks AP *et al*, "Simultaneous assessment of diameter and pressure waveforms in the carotid artery", Elsevier, Ultrasound in Med. & Biol., Vol. 30, No. 2, pp. 147–154, 2004.

[26] - Hermeling E., *et al*, "The dicrotic notch as alternative time-reference point to measure local pulse wave velocity in the carotid artery by means of ultrasonography" J Hypertens. 2009 Oct; 27(10):2028-35.

[27] – Pereira H., *et al,* "Characterization of a Double Probe for Local Pulse Wave Velocity Assessment".

[28]' – Pereira T., "Optical Methods for Local Pulse Wave Velocity Assessment"

[29]' – Pereira H.C., et al, "Programmable test bench for hemodynamic studies"

[30] - http://complior.com/ - (acedido em Agosto de 2011).

[31] - http://www.atcormedical.com/sphygmocor_vx.html - (acedido em Agosto de 2011).

[32] - http://www.pulsepen.com/ - (acedido em Agosto de 2011).

[33] - http://www.arteriograph.nl/ - (acedido em Setembro de 2011).

[34] - Kumar D., *et al*, "A new algorithm for detection of S1 and S2 heart sounds", IEEE, 2004.

[35] - http://www.ed4nurses.com/heartsnd.aspx - (acedido em Março de 2011).

[36] - http://www.cvphysiology.com/Heart%20Disease/HD010.htm - (acedido em Agosto de 2011).

[37] – Kumar D., *et al*, "Third heart sound detection using Wavelet Transform-Simplicity filter", IEEE, 2007.

[38] – Faizan Javed, P.A. Venkatachalam and Ahmad Fadzil M.H., "A signal Processing Module for the Analysis of Heart Sounds and Heart Murmurs", Journal of Physics: Conference Series 34, 2006, 1098-1105.

[39] – Kumar D., *et al*, "Wavelet Transform and simplicity based heart Murmur segmentation", Computers in Cardiology 2006; 33:173-176.

[40] – Liang H, Lukkarinen, Hartimo I., "Heart sound segmentation algorithm on heart sound envelogram", Computer in Cardiology 1997, Vol 24.

[41] – Kumar D., *et al*, "A new algorithm for detection of S1 and S2 heart sounds", IEEE, 2006.

[42] – El-Asir B., *et al*, "Time-Frequency Analysis of the Heart Sounds", IEEE, 1996.

[43] – Carvalho P., *et al*, "Low complexity algorithm Algorithm for Heart Sound Segmentation using the Variance Fractal Dimension", IEEE, 2005.

[44] – Kumar D., *et al*, "Heart murmur classification with feature selection", IEEE, 2010.

[45] - Wintermantel E., *et al*, "Microvascular Auscultation. A New Technique, Using a Diplo-Microphone, for Analysis of Blood Flow at Structure Lines in Small Arteries", Acta Neurochirurgica 53, 25-37, 1980.

[46] - www.cs.tau.ac.il/~nin/.../MethodsForCarotidSoundDelayEstimation.ppt - (acedido em Março de 2011).

[47] – Lewis R.P., *et al* "A Critical Review of the Systolic Time Intervals", Circulation 1977, 56:146-158.

[48] – Paiva R.P., *et al*, "Assessing PEP and LVET from Heart Sounds: Algorithms and Evaluation", Int. Conference of the IEEE EMBS, 2009.

[49] – Willems J.L., *et al*, "The Left Ventricular Ejection Time in Elderly Subjects", Circulation 1970, 42:37-42.

[50] - Swaminathan M., *et al*, "An Assessment of Two Different Methods of Left Ventricular Ejection Time Measurement by Transesophageal Echocardiography", Anesthesia & Analgesia, 2003; 97:642–7.

[51] – Carvalho P., *et al*, "Assessing Systolic Time-Intervals from heart sound: a feasibility study", 2009.

[52] - http://www.ni.com – (acedido em Agosto de 2011).

[53] – Almeida V. *et al,* "Synthesized Cardiac Waveform in the Evaluation of the Augmentation Index Algorithms. Case study for a new wavelet based".

[54] – Bank A. J., Kaiser D.R., "Smooth Muscle Relaxation: Effects on Arterial Compliance, Distensibility, Elastic Modulus, and Pulse Wave Velocity", Hypertension, 1998.